universität wien

# DISSERTATION / DOCTORAL THESIS

Titel der Dissertation /Title of the Doctoral Thesis

„Physiological role and molecular effects of benzoxazinoids (Bx)“

verfasst von / submitted by

Daniela Ramos Cruz

angestrebter akademischer Grad / in partial fulfilment of the requirements for the degree of

Doctor of Philosophy (PhD)

Wien, 2023 / Vienna 2023

| | |
|---|---|
| Studienkennzahl lt. Studienblatt / degree programme code as it appears on the student record sheet: | UA 794 685 490 |
| Dissertationsgebiet lt. Studienblatt / field of study as it appears on the student record sheet: | Molekulare Biologie |
| Betreut von / Supervisor: | Prof. Dr. rer. nat. Claude Becker |

# ACKNOWLEDGEMENTS

First and foremost, I would like to thank my supervisor Claude Becker for giving me the opportunity to venture into this invaluable learning journey. I'm deeply appreciative of Claude's guidance, patience and unwavering support throughout these years.

I am also very thankful to Ortrun Mittelsten Scheid and Herman Bürstmayr for agreeing to be part of my thesis advisory committee. Their insights, critical advice and guidance have been instrumental in shaping my research.

Additionally, I would like to thank the EpiDiverse family for all the discussions, collaborations, technical support and friendship. I feel very fortunate and honored to be part of such an amazing network. I would especially like to extend my heartfelt thanks to Iris Sammarco, Paloma Perez, Barbara Diez, Dario Galanti and Adrian Contreras for their scientific support and invaluable friendship.

I would also like to extend my gratitude to all the present and past members of the Becker group for all their suggestions, fruitful discussions and technical help. Special thanks to Katarina Jhandrist for her technical support and to Eva Knoch, Jose Villaecija and Niklas Schnadry for their insightful scientific suggestions which have greatly enriched my work. I would also like to extend my gratitude to my GMI office mates; Judit Kovacs, Nuria Serra, Zsuzsanna Gunter and Natalie Hedelbacher for their valuable scientific input to my projects and for their emotional support and friendship which I greatly value. I'm also thankful to my LMU office mates; Santiago Priego, Reshi Shan and Jinn for being wonderful colleagues and providing a supportive and uplifting working atmosphere.

Moreover, I would like to thank Ulrich Schaffrath and Christian Kirsch for being open to collaboration and for sharing with us their technical and scientific expertise. I am also grateful to the ERC and Marie Curie for funding my research, and the VBC, the GMI and the LMU community for creating such a great working environment that fosters curiosity and scientific excellence.

Finally, I would like to thank my family and friends for their unconditional support and love. To my parents for encouraging me to follow my curiosity and support my life choices. To my siblings and friends for their support and companionship in the distance and last but not least, to my husband for motivating and inspiring me to keep learning and growing.

# ABSTRACT

As sessile organisms, plants have evolved a multitude of strategies to ensure survival in changing and competitive environments. One such strategy is allelopathy, which refers to the ability of some plant species to exudate specialized metabolites (allelochemicals) that inhibit the growth or development of other organisms in their vicinity. Although the phenomenon of allelopathy has been known for centuries, the underlying molecular principle and the molecular response of the affected target plants remain understudied. Here, I followed two different approaches to study the effects of allelochemicals belonging to benzoxazinoids (BX). First, I investigated the role of BX in the biotic interactions of a BX-producing species, wheat. To this end, I generated non-transgenic mutant lines deficient in BX biosynthesis, followed by a chemical and phenotypic characterization. Second, I studied the effects of the BX-derived allelochemical 2-amino-phenoxazin-3-one (APO) at the epigenetic and epigenomic level in the non-BX-producing target species *Thlaspi arvense*.

BX-deficient wheat mutants showed normal growth and development compared to wild-type. Contrary to our expectations, allelopathic interactions and defense response to pathogens were unaltered. These results suggest that BX are not essential for the response to these stresses in wheat. In whole-genome DNA methylation analyses, I observed that APO affected cytosine methylation, particularly in the asymmetric methylation context. I identified differentially methylated regions (DMRs), particularly in the promoters of genes related to cell growth and stress response. These results showed for the first time the effect of APO on the epigenome and pointed to potential APO target candidate genes. In summary, this work has generated relevant genetic material to comprehensively study the role of BX in wheat and provides new insights into the APO-mediated stress responses in dicotyledonous plants at the epigenomic level. Altogether, these findings improve our understanding of BX allelochemical physiology in both a producer crop species and a potential target weed.

# ZUSAMMENFASSUNG

Als sessile Organismen haben Pflanzen eine Vielzahl von Strategien entwickelt, um ihr Überleben in einer sich verändernden und konkurrenzbetonten Umwelt zu sichern. Eine dieser Strategien ist die Allelopathie, also die Fähigkeit einiger Pflanzenarten, bestimmte Sekundärmetabolite (Allelochemikalien) an die Umwelt abzugeben, die das Wachstum oder die Entwicklung anderer, benachbarter Organismen hemmen. Obwohl die Allelopathie seit Jahrhunderten bekannt ist, ist die funktionelle Charakterisierung der Biosynthese von Allelochemikalien sowie der molekularen Mechanismen, die allelopathische Stressreaktionen auf Zielpflanzenarten vermitteln, noch nicht ausreichend erforscht. Hier verfolgten wir zwei verschiedene Ansätze zur Untersuchung von Allelochemikalien aus der Familie der Benzoxazinoide (BX). Zunächst untersuchte ichr die Rolle von BX in biotischen Interaktionen in Weizen. Hierzu erzeugte ich eine Mutante mit unterbrochener BX-Biosynthese, gefolgt von einer chemischen und phänotypischen Charakterisierung. Im zweiten Teil meiner Arbeit konzentrierte ich mich auf die von BX abgeleitete Allelochemikalie 2-Amino-Phenoxazin-3-on (APO) und ihren Einfluss auf das Epigenom in einer Pflanzenart ohne BX-Biosynthese, nämlich *Thlaspi arvense*.

Die Weizen-Mutanten zeigten gegenüber dem Wildtyp unverändertes Wachstum und vergleichbare Entwicklung; entgegen meiner Erwartungen waren die allelopathischen Interaktionen und die Abwehrreaktion gegen unterschiedliche Pathogene nicht beeinträchtigt. Diese Ergebnisse deuten darauf hin, dass BX für die Reaktion von Weizen auf diese Stressfaktoren nicht wesentlich ist. Im zweiten Teil zeigte die DNA-Methylierungsanalyse, dass APO die DNA-Methylierung beeinflusst, insbesondere im asymmetrischen Sequenzkontext. Darüber hinaus detektierte ich differentiell methylierte Regionen (DMRs) v.a. in Promotoren von Genen, die mit Zellwachstum und Stressreaktionen zusammenhängen. Diese Ergebnisse zeigen zum ersten Mal die Auswirkungen von APO auf das Epigenom und weisen auf potenzielle Zielgene von APO hin. Zusammenfassend lässt sich sagen, dass diese Arbeit wichtiges genetisches Material für die breit angelegte Untersuchung der Rolle von BX in Weizen liefert und ihre Bedeutung für die Pflanzenabwehr aufzeigt.

Darüber hinaus liefer die Arbeit neue Erkenntnisse über die APO-vermittelten Stressreaktionen in *T. arvense* auf der Ebene des Epigenoms. Alles in allem verbessern diese Ergebnisse unser Verständnis der BX-anhängigen allelopathischen Physiologie in einer BX-synthetisierenden Nutzpflanzenart sowie einer zweikeimblättrigen Zielpflanze, die häufig als Unkraut auf agrarischen Flächen zu finden ist.

# SYNOPSIS

This thesis sets out to narrow the knowledge gap on the physiological role and the molecular effects of benzoxazinoid (BX) allelochemicals. I focused on the BX-producing species *Triticum aestivum*, also commonly known as bread wheat, and the often co-occurring and therefore potential target weed species *Thlaspi arvense*. In the first chapter, I aimed to facilitate the study of BX in wheat by generating a BX-loss-of-synthesis mutant and studied the role of BX in mediating plant allelopathic interactions and defense. This is the first BX-deficient mutant described in wheat and will serve as a valuable genetic resource for future studies of BX in this economically highly relevant crop. In the second chapter, I aimed to unravel the molecular effect of BX on a common weed plant species that itself cannot produce BX. Using whole-genome approaches, I studied the consequences of exposure of *T. arvense* to a potent phytotoxic BX derivative at the epigenetic level.

# PUBLICATIONS

**Genetic and environmental drivers of large-scale epigenetic variation in *Thlaspi arvense*.**
Galanti D, **Ramos-Cruz D**, Nunn A, Rodríguez-Arévalo I, Scheepens JF, Becker C, Bossdorf O. PLoS Genet. 2022 Oct 12;18(10):e1010452.
doi: 10.1371/journal.pgen.1010452.

**Chromosome-level *Thlaspi arvense* genome provides new tools for translational research and for a newly domesticated cash cover crop of the cooler climates.**
Nunn A, Rodríguez-Arévalo I, Tandukar Z, Frels K, Contreras-Garrido A, Carbonell-Bejerano P, Zhang P, **Ramos Cruz D**, Jandrasits K, Lanz C, Brusa A, Mirouze M, Dorn K, Galbraith DW, Jarvis BA, Sedbrook JC, Wyse DL, Otto C, Langenberger D, Stadler PF, Weigel D, Marks MD, Anderson JA, Becker C, Chopra R. Plant Biotechnol J. 2022 May;20(5):944-963.
doi: 10.1111/pbi.13775.

**Epigenetics in plant organismic interactions.**
**Ramos-Cruz D**, Troyee AN, Becker C. Curr Opin Plant Biol. 2021 Jun;61:102060. doi: 10.1016/j.pbi.2021.102060.

**The role of plant epigenetics in biotic interactions.**
Alonso C, **Ramos-Cruz D**, Becker C. New Phytol. 2019 Jan;221(2):731-737.
doi: 10.1111/nph.15408.

**Book chapters**

**A Critical Guide for Studies on Epigenetic Inheritance in Plants.**
**Cruz DR,** Becker C. Methods Mol Biol. 2020;2093:261-270.
doi: 10.1007/978-1-0716-0179-2_18.

**Introduction to Ecological Plant Epigenetics.**
Nunn A, Contreras-Garrido A, Troyee A, Díez-Rodríguez B, Dubay B, Peña C, **Ramos-Cruz D**, Galanti D, Sammarco I, López M, Van Antro M, Can N, Perez-Bello Gil P, Zhang P, Fatma S.
Free textbook. GitBook, https://app.gitbook.com/@epidiverse/s/project/

# CONTENTS

# INTRODUCTION

## 1. Benzoxazinoids as allelopathic compounds in grass species

### 1.1 Allelopathy and its ecological relevance

Plants have evolved a plethora of adaptive strategies to thrive in competitive and stressful environments. Among these strategies is allelopathy, which refers to the ability of certain plant species to produce and release secondary metabolites known as allelochemicals. These compounds inhibit the germination and/or growth of neighboring plants allowing the allelopathic plant to outcompete them and to increase its chance of survival and reproductive success. Allelochemicals also act as defense compounds against pests and pathogens[1]. In this way, allelopathy impacts ecological dynamics in competition, stress tolerance and plant fitness[2].

The phenomenon of allelopathy has been known for over 2000 years [3]; Molisch introduced the term allelopathy in 1937 [3,4]. It derives from the Greek words *allelon* ("of each other") and *pathos* ("to suffer") and means "the effect of one upon another" [3,4]. Today, in the context of plants, allelopathy is defined as both the inhibition and/or stimulation of the growth or development of an organism, through the biological action of allelochemicals produced by plant species [2]. Here, I will refer to allelopathy as the adverse and inhibitory effects that plant-derived allelochemicals exert on other organisms (plants, animals and microbes).

Allelochemicals are very diverse and can be classified into 14 categories based on their chemical similarities: 1) water-soluble organic acids, straight-chain alcohols, aliphatic aldehydes, and ketones; 2) simple unsaturated lactones; 3) long-chain fatty acids and polyacetylenes; 4) benzoquinone, anthraquinone and complex quinones; 5) simple phenols, benzoic acid but also its derivatives; 6) cinnamic acid and its derivatives; 7) coumarin; 8) flavonoids; 9) tannins; 10) terpenoids and steroids; 11) amino acids and peptides; 12) alkaloids and cyanohydrins; 13) sulfide and

glucosinolates; and 14) purines as well as nucleosides [5]. These phytochemicals are not essential for cell growth and development, but are preferentially allocated to tissues of great value or produced at early and vulnerable developmental stages, balancing a trade-off between growth, fecundity and defense [6]. Allelochemicals can be released into the environment via root exudation, leaching by precipitation (e.g. from leaves or stems), volatilization, or via decomposition of microbes and plant tissues [2].

As a consequence of allelochemical exudation, plants can impact the species community of their environment or invade new ecosystems. Examples of invasive species include *Alliaria petiolata,* which produces glucosinolate compounds such as allyl isothiocyanate and benzyl isothiocyanate, or *Sonchus oleraceus,* which produces several kinds of allelochemicals. It has been postulated that these species could become dominant in their new habitats because no tolerance or resistance to their so-called “novel weapons” existed in the native communities [7–9]. This opens new possibilities to study plant ecosystem dynamics and/or translate the use of allelopathy to agricultural setups.

In an agricultural context, it is of great interest to develop environmentally friendly practices that improve crop productivity through allelopathic control of weeds, insect pests, and crop diseases [5]). Its potential use has been extensively studied and special attention has been given to allelopathic crops [10,11]. Crops that have been investigated for their allelopathic properties include cucumber, rice, wheat, maize, rye, sorghum, sudan grass, tall and fine fescue, sunflower, and barley [12–14]. Examples of crop allelochemicals comprise: sorgoleone from *Sorghum* species, which is known for having weed-suppressive properties in the field [15]; momilactones A and B from rice, both allelochemicals but also phytoalexins [16,17]; and benzoxazinoids (BX), produced by many Poaceae species, including maize, wheat and rye [18]. Some of these allelopathic crops have been used in the field in rotational or combined cropping systems to provide a competitive advantage to non-producing species and to increase crop yield [11,13,19].

Allelopathic interactions are likely to be mediated by plant–plant recognition mechanisms that involve chemical signaling. However, such detailed interaction pathways are yet to be elucidated. Interestingly, growing evidence shows that

allelochemical synthesis or exudation is elevated in response to recognition of neighboring competing plant species in a species-specific manner. For instance, wheat production of the benzoxazinoid allelochemical DIMBOA (2,4-dihydroxy-7-methoxy-1,4-benzoxazin-3-one) increases and varies depending on the competing weed species [20–22]. Such observations suggest that the molecular signaling has evolved in a species-specific manner, targeting most likely plants that are expected to grow in the same community.

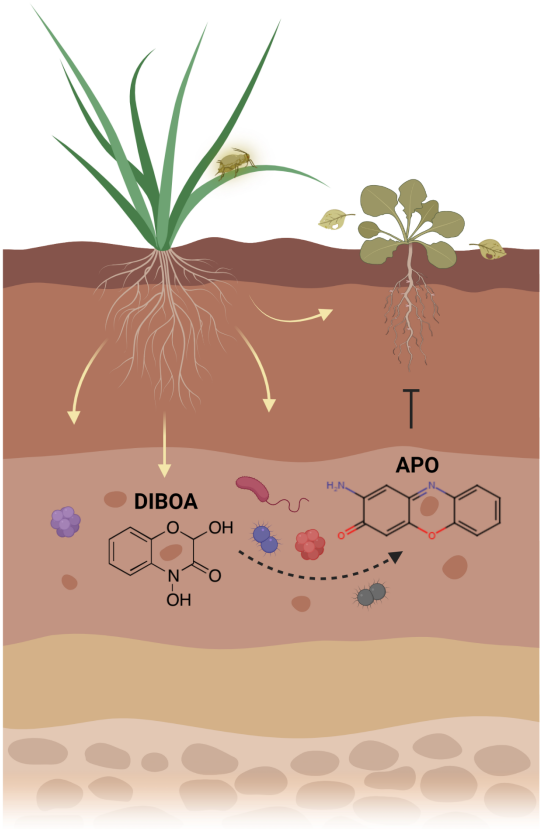


**Figure 1**. **Biotic interactions mediated by benzoxazinoids.** Upon pathogen and herbivore attack or in response to plant-plant competition, grass species release BX, such as DIBOA (2,4-dihydroxy-1,4-benzoxazin-3-one). DIBOA released into the rhizosphere (indicated by yellow arrows) is converted through microbial activity into APO (2-amino-phenoxazin-3-one). APO is a more stable and active compound with a stronger growth inhibition effect.

Another recently studied function of allelochemicals, particularly of BX, is their role in shaping the soil microbiome [23–27]. BX may promote beneficial plant-microbe interactions and provide a competitive advantage to the plant [28]. Microbes can, in turn, degrade BX and make them more stable in the soil. For example, in unsterilized

soil, microbes degrade DIBOA (2,4-dihydroxy-1,4-benzoxazin-3-one) into APO in ~43 h. APO (2-amino-phenoxazin-3-one) is a more stable and bioactive compound that can persist, depending on the environmental conditions, for more than 90 days in biologically active soil [29]. Figure 1.

In summary, allelopathy has evolved as a strategy for plants to influence their environment and as a defense mechanism against pathogens and competitors. The vast diversity of allelochemicals shows the complexity and diverse strategies that plants have used to achieve this competitive advantage. Additionally, the recent knowledge on the role of allelochemicals in structuring the soil microbiome, as well as new insights into the plant signaling mechanisms involved in allelopathic interactions will open new doors to explore allelopathic agro-ecological potential.

## 1.2 Benzoxazinoids: functions and biological interactions

Benzoxazinoids (BX) are secondary metabolites belonging to the family of cyclic hydroxamic acids that act as defense and allelopathic compounds. Their defense and allelopathic properties, but also the fact that many crops produce them, have made them one of the most agriculturally relevant metabolites. BX-producing crops include maize (*Zea mays*), wheat (*Triticum* spp.), rye (*Secale cereale*) and other cultivated Poaceae, but also wild species such as wild (but not cultivated) barley [30].

BX production has also been found in a few dicot species, such as *Acanthus mollis*, [31], *Aphelandra tetragona*, *Blepharis edulis*, *Aphelandra squarrosa* [32], *Consolida orientalis* [33],*Scoparia dulcis* [34], and *Lamium galeobdolon* [33], but their function in these species has been less explored.

The two main benzoxazinoids with allelopathic activity are DIMBOA and DIBOA [35]. In maize and wheat, DIMBOA is the main allelochemical [36], whereas in rye and wild barley, DIBOA is more prominent [18,37]. Different studies have shown that these compounds inhibit plant growth at concentrations in the range of 100-500 µm [2]. DIMBOA and DIBOA spontaneously degrade to MBOA (6-Methoxy-2-benzoxazolinone) and BOA (2-benzoxazolinone), respectively, which are further converted into AMPO (2-amino-7-methoxy-phenoxazin-3-one) and APO.

The degradation products of DIMBOA and DIBOA also exert allelopathic activities. Among them, APO is the most potent allelochemical; inhibitory effects in in vitro assays occur at concentrations as low as 3.25 µM [38]. Compared to its precursors, APO is more stable in soil and remains active for several months [29].

BX are synthesized in shoot and root tissues in both monocot and dicot species, but biosynthesis mainly occurs in above-ground tissues in dicots [39,40]. These compounds are abundant in juvenile plant growth stages and decline as the plant ages [41,42]. However, upon biotic stress induction, such as pathogen attack, BX accumulation and release occur also in older leaves [43]. It is also possible that BX are transported to the site of damage, since they have been found in phloem exudates, and accumulation of these compounds has been observed in the seeds of wheat and rye [44,45]. Furthermore, not only biotic stresses induce BX accumulation, but also some abiotic stresses such as temperature, drought, nitrogen deficiency, photoperiod, light intensity and UV radiation [43].

Within the cell, BX are stored as a glucoside in the vacuole to avoid autotoxicity. Upon disintegration of the cell, due to pathogen as well as herbivore attack, glucosidases stored in the chloroplast cleave the glucosyl group and release the toxic aglucons [18,30]. Toxicity of aglucons results from the reactivity of the open ring structure of *α*-oxo-aldehyde, which reacts with nucleophiles, particularly thiols and amines, in amino acids and proteins. Some reported effects of BX in cell function include the oxidation of cell wall peroxidases with associated production of $H_2O_2$, accumulation of lignins, disruption of lipid metabolism but also of protein synthesis, reduction of transport and/or secretory capabilities, and decreased $H^+$-ATPase activity [30,46]. Additionally, it has been observed that BX can intercalate with nucleic acids, which could modify the DNA and cause mutations [47]. Because BX can affect different conserved cell functions, they can impact several species among the different kingdoms.

Many biological interactions have been observed for benzoxazinoids with different target species, including herbivores, fungi, bacteria, and plants. Some of these interactions result in inhibitory effects on the target species, but others show the adaptive potential of some organisms to evolve resistance or the capacity to metabolize and/or use these compounds for their own benefit and growth (Table 1).

**Table 1.** Benzoxazinoids biological interactions

| Organism | Effect | References |
|---|---|---|
| **Herbivores** | | |
| *Spodoptera littoralis* | Strong BX induction in young leaves influences foraging behavior of this non-adapted species, which prefers to feed on WT plants or older leaves, where BX content is lower. | [48,49] |
| *S. littoralis* and *Ostrinia furnicalis* | Caterpillars grow more slowly on maize with prior insect damage. Such growth inhibition effects are absent in *bx1* mutants, indicating that the defense response requires BX. | [50,51] |
| *Ostrina furnicalis*, *Ostrinia nubilalis, Spodoptera frugiperda, S. exigua* and *S. littoralis* | Insect feeding induces the methylation of DIMBOA-Glc to form HDMBOA-Glc. This inducible conversion may enhance maize resistance because the HDMBOA aglucone is degraded to MBOA more rapidly than the DIMBOA aglucone. In another study, larval development of *Ostrinia nubilalis* was inhibited by DIMBOA and caused 25% mortality. | [50–55] |
| *S. frugiperda* | Detoxification of BX by re-glycosylation of activated BX, but the re-glycosylation is less effective in counteracting HDMBOA-Glc than DIMBOA-Glc in the insect. | [56] |
| *Schizaphis graminum* | Resistance of wheat to *S. graminum* correlated with the induction of DIMBOA, DIMBOA-Glc and HDMBOA-Glc. | [57] |

| | | |
|---|---|---|
| *Rhopalosiphum maidis*<br><br>*Rhopalosiphum padi* | Natural variation of different alleles of *BX12* that convert DIMBOA-Glc to HDMBOA-Glc were identified for resistance against *R. madis*. Aphids growth was affected on plants with higher DIMBOA content, presumably because of the induction of callose deposition by DIMBOA. Similarly, differences in callose-dependent aphid resistance were observed in maize B73 and Mo17 inbred lines infected with *R. padi*. Another study showed mild resistance of wheat to *R. padi* that correlated with the induction of DIMBOA and DIMBOA-Glc. | [57–60] |
| *Diabrotica virgifera* | The specialized herbivore corn rootworm (*D. virgifera*) feeds on highly nutritious tissue with high amounts of BX. The resistance of *D. virgifera* is due to the stabilization of MBOA by N-glycosylation. In turn, *D. virgifera* also employs BX for its own defense against nematodes and bacteria. | [61,62] |
| *Mythimna separata* | *M. separata* is another serious pest in rice, maize, sorghum and wheat and seems resistant to BX. *M. separata* is able to glycosylate DIMBOA and HMBOA. | [63] |
| *Diuraphis noxia* | DIBOA in wild barley species negatively impacts the development of the aphid *D. noxia.* | [64] |
| *Meloidogyne incognita* | DIBOA exuded from rye inhibits egg development of the nematode *M. incognita*. | [65] |
| **Fungi** | | |
| *Bipolaris maydis*<br><br>*Curvularia lunata*<br><br>*Alternaria alternate* | Increase of benzoxazinoids HDMBOA and MBOA caused by these phytopathogenic fungi inhibits conidia germination and tube growth. MBOA had the strongest antifungal properties. | [66] |

| | | |
|---|---|---|
| *Fusarium nivale* | Growth inhibition of Fusarium by benzoxazolinones in rye seedlings. | [67] |
| *Fusarium verticillioides* | *F. verticilliodes* can metabolize BOA into HPMA and cause disease symptoms in corn. FDB1 and FDB2 enzymes are involved in the detoxification mechanism. Another study showed that *FUG1* (*Fungal Unknown Gene 1*) gene is required for BX tolerance and successful maize kernel colonization as well as activation of the biosynthesis of fumonisins mycotoxins in *F. verticilliodes*. | [68,69] |
| *Fusarium graminearum* | Biosynthesis of toxic trichothecenes produced by *F. graminearum* is inhibited by DIMBOA in wheat, due to the suppression of the key trichothecenes biosynthetic genes *Tri6* and *Tri5*. | [70] |
| *Saccharomyces cerevisiae*<br><br>*Candida albicans* | Fungal growth inhibition by BX at a millimolar concentration. | [71–73] |
| **Bacteria** | | |
| *Pseudomonas putida* | The soil bacteria are attracted to DIMBOA in the rhizosphere, which induce defense priming, as jasmonate-induced defenses are turned on faster in colonized plants. | [28,74] |
| *Pantoea stewartii*<br><br>*Xanthomonas stewartii* | Bacterial growth inhibition caused by MBOA. | [75] |
| *Erwinia spp*<br><br>*Agrobacterium tumefaciens* | Bacterial growth inhibition caused by DIMBOA in *Erwinia* and *Agrobacterium*. | [76,77] |

| | | |
|---|---|---|
| *Escherichia coli*<br><br>*Staphylococcus aureus* | BOA, MBOA and DIMBOA antimicrobial activity. | [71,73] |
| **Algae** | | |
| *Chlorella xanthella* | Algal growth inhibition by DIBOA and DIMBOA at millimolar concentrations. | [72] |
| **Plants** | | |
| *Chenopodium album* | Rye BX growth inhibition greater than 90% in *C. album*. | [78] |
| *Sinapis alba* | DIBOA and DIMBOA produced by wheat inhibit growth of *S. alba*. | [79] |
| *Arabidopsis thaliana* | Detoxification of BOA in Arabidopsis through O-glycosylation of the intermediate BOA-6-OH. Transcriptional response also shows changes in expression of genes involved in tolerance to other xenobiotics. Moreover, expression of UGTs *BX8* or *BX9* confers DI(M)BOA tolerance to Arabidopsis. Arabidopsis is susceptible to the degradation products of DI(M)BOA, AMPO and APO, which directly inhibit histone deacetylases, inducing chromatin changes that alter gene expression and affect plant growth. | [80–82] |
| *Avena fatua, Avena ludoviciana, Descurainia sophia, Portulaca oleracea and Lolium rigidum* | A 500 µm dose of DIMBOA is sufficient to inhibit root length in *Avena fatua* by ≈70% and *Lolium rigidum* by ≈55%. In a hydroponic system, wheat produced more BX in proximity to *Avena fatua, Descurainia sophia, Lolium rigidum* and *Portulaca oleracea.* Another study showed the allelopathic potential of leaf extracts from various wheat accessions against | [83–86] |

| | | |
|---|---|---|
| | *Avena ludoviciana*. Allelopathic wheat accessions have high DIMBOA content. | |
| Various weeds | In cocultivation experiments, 9 different weeds that occur in wheat fields were inhibited by wheat. | [21] |
| *Amaranthus retroflexus* L and *Portulaca oleracea* L | These broadleaf weeds show resistance to BX mainly due to their detoxifying capacity of BOA through glycosylation. Interestingly, inhibition of seed germination and seedling growth of both weeds has been observed with rye mulches. | [19,87] |
| *Trifolium alexandrinum* | Co-cultivation of rye with berseem clover influences gene expression levels of BX biosynthesis genes and content of BX, particularly of GDIBOA and DIBOA. | [88] |

Taken together, the production of BX has evolved in some plant species as a defense and allelopathic strategy against pathogens and competitors. BX are mainly produced at vulnerable young plant stages or as a consequence of both biotic and abiotic stresses. Their role in biotic interactions has received much attention because of the capabilities of BX to interfere with many biological cell functions and affect organisms from several kingdoms of life (Table 1). Notably, crops that produce BX are of great interest because of their agricultural potential in managing plant diseases.

## 1.3 The role of benzoxazinoids in shaping the plant root microbiome

Plants interact with a multitude of microorganisms in their environment. They have co-evolved with microbes to establish close associations that can be beneficial or detrimental to plant fitness and health. Some interactions assist the plant in nutrient

absorption, pathogen resistance, abiotic stress tolerance, and growth promotion, but others cause disease and in some cases death of the host [89].

Underground, beneficial microbe-plant associations are influenced by primary and secondary metabolites released by roots into the rhizosphere. The rhizosphere is the soil zone surrounding the roots that is directly impacted by plant exudates. Besides as carbon and nitrogen sources for bacterial growth, root exudates can act as signaling molecules to attract or repel specific microbes. The rhizosphere microbiome functions as a protective layer that provides plant protection by antibiosis or serving as a niche against competing pathogens and/or by enhancing the plant immune responses. In this way, root exudates shape the plant microbiome and promote plant health [90,91].

BX and their breakdown products are important players in structuring the plant soil microbiome [23–26]. They affect the rhizobiome metabolome and favor the colonization of some bacterial and fungal taxa of the rhizosphere [24–26]. For instance, DIMBOA secreted by maize roots attracts the plant-growth promoting bacteria *Pseudomonas putida [28]* (Table 1). In contrast, BX have been shown to inhibit the growth of certain bacterial and fungal pathogens or suppress their virulence [33,92–94].

As plants can shape their soil microbiome, they can also influence the performance of other plants growing subsequently in the same soil. This phenomenon, where soil legacies affect next plant generations, is known as plant-soil-feedbacks (PSFs); and the process in which plants change soil properties is often referred to as “soil conditioning” [95]. Negative PSFs occur when the previous plant generation enriched pathogens, released allelopathic compounds, or reduced the availability of nutrients. In contrast, positive PSFs are observed when the previous plant generation promoted beneficial symbionts and enhanced nutrient availability [27]. Farmers have recognized the PSF effect for a long time and have taken advantage of beneficial crop rotations. For example, *Brassicaceae* species that produce glucosinolates have been used to biofumigate fields against fungi, oomycetes and plant-parasitic nematodes [96,97]. Recently, it was shown that maize secretion of BX conditions different types of soil, including soil from agricultural fields. PSF were observed in

maize and wheat growing on BX conditioned soils. Both plant species showed reduced growth. Interestingly, in addition to the reduced growth phenotype in maize, a herbivore growth suppression phenotype was observed in maize growth on BX conditioned soil [23,27]. These results highlight the future possibility of using BX-mediated PSF for pest control in the field.

## 1.4 Benzoxazinoids biosynthesis

BX biosynthesis has been studied in monocots, including maize [18], wheat [98], wild barley [37], and partially in rye [99], but so far not in dicots [40]. The most detailed study has been done in maize, where the whole BX biosynthetic pathway has been revealed (Figure 2) [30,100].

BX biosynthesis starts in the chloroplast. It branches off the tryptophan biosynthesis pathway with the activity of the BX1 enzyme, a homologue of the tryptophan synthase (TSA) that converts indole-3-glycerol phosphate into indole [18,101].

The indole produced by BX1 is then oxidized in the endoplasmic reticulum by a series of Cytochrome P450-dependent monooxygenases (BX2-BX5) at four different positions, to produce the simplest functional benzoxazinoid, DIBOA (2,4-dihydroxy-1,4-benzoxazin-3-one) [18,100]. DIBOA is stabilized via glucosylation by the partially redundant UDP-glucosyltransferases (UGT) BX8 and BX9 [81]. DIBOA-Glc is further oxidized by a 2-oxoglutarate-dependent dioxygenase (2-ODD, BX6) and methylated by an *O*-methyltransferase (OMT, BX7) in the cytosol to produce DIMBOA-Glc (2,4-dihydroxy-7-methoxy-1,4-benzoxazin-3-one glucoside) [102]. Glycosylated BX are stored in the vacuole, and upon cell wall disruption, specific beta-glucosidases cleave the glucosyl group and release the toxic aglucons [43].

DIMBOA-Glc can be further methylated in the cytosol by the OMTs BX10, BX11, BX12 and BX14 to produce HDMBOA-Glc (2-hydroxy-4,7-dimethoxy-1,4-benzoxazin-3-one glucoside) [58]. Both BX10 and BX11 are particularly induced by herbivory [52] Subsequently, BX13 can oxidize DIMBOA-Glc to produce TRIMBOA-Glc (2,4,7-trihydroxy-8-methoxy-1,4-benzoxazin-3-one glucoside). Interestingly, the BX7

catalyzing the OMT step in DIMBOA-Glc acts again on TRIMBOA-Glc to produce $DIM_2BOA$-Glc (2,4-dihydroxy-7,8-dimethoxy-1,4-benzoxazin-3-one glucoside), which is further methylated by BX14 to form $HDM_2BOA$-Glc (2,4-dihydroxy-7,8-dimethoxy-1,4-benzoxazin-3-one glucoside) [103,104].

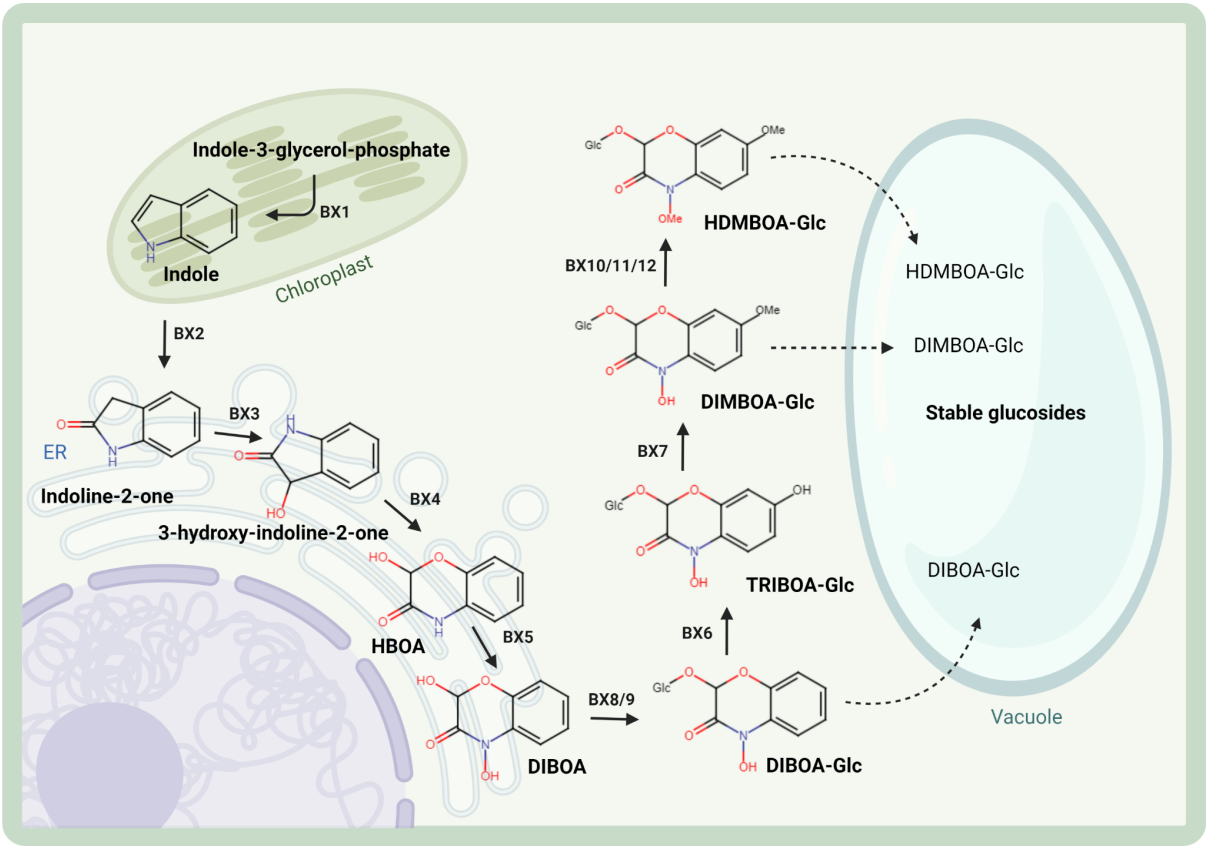


**Figure 2. Biosynthesis of benzoxazinoids.** Enzymes and intermediaries of BX biosynthesis as well as their subcellular localizations are depicted. The stable glucosides (Glc) are stored in the vacuole. In maize and wheat, the predominant benzoxazinoid is DIMBOA-Glc, while in many other plant species the final product is DIBOA-Glc.

Although BX biosynthesis has been studied for several years and resolved in detail in maize, little is known about the regulatory mechanisms that control the BX pathway. Different analyses of maize transcriptomic data have identified transcription factors (TFs) that correlate with BX abundance. However, most of those candidates have not been functionally validated [60,105,106]. Recently, two separate studies identified some transcriptional regulators of BX biosynthesis in maize and wheat. Gao et al. identified the basic helix–loop–helix ZmbHLH20 and ZmbHLH76 TFs in a protoplast system in maize, and [107,108]. found the MIB31 TF in wheat [107,108].

## 1.5 Evolution of Benzoxazinoid biosynthesis in grasses

Most of what we know about the genes involved in BX biosynthesis comes from studies in maize, but orthologs have been identified in other Poaceae species. The phylogenetic analysis suggests that BX biosynthesis has a monophyletic origin in Poaceae [30].

In contrast to other Poaceae species, the genes contributing to the BX pathway form a metabolic gene cluster in maize. Clustering is thought to facilitate co-transcription and co-inheritance of beneficial gene combinations by enabling localized changes in chromatin [109]. The core maize genes Zm*BX1* to Zm*BX5* and Zm*BX8* are located within 264 kb on the short arm of chromosome 4 [110]. Zm*BX1* expression is regulated by a distant enhancer element located in the middle of the cluster [111]. In maize, both *ZmBX1* and Zm*BX2* are tightly linked, separated only by 2.5 Kb. Such linkage is conserved in hexaploid wheat and rye, where wheat orthologs *TaBx1* and *TaBx2* localized on group 4 chromosomes (4A, 4B and 4D), while rye orthologs *ScBx1* and *ScBx2* are found in chromosome 7R. However, the rest of the cluster (*BX3* to *BX5* and *BX8*) is located on different chromosomes in these species. In hexaploid wheat, orthologues (*TaBx3*-*TaBx5*) are located in the short arm of group 5 chromosomes (5A, 5B and 5D), while in rye, they (*ScBx3*-*ScBx5*) are located on the short arm of chromosome 5R. *BX8* orthologs are localized on group 7 chromosomes in wheat and on chromosome 4R in rye [18,112,113] (Figure 3). Even though BX genes are not clustered in wheat and rye, they still seem to be coordinately expressed. Possibly, other *cis* regulatory elements as well as TFs common to all BX pathways ensure a coordinated gene transcription. [112].

Grasses are proposed to have evolved from a common ancestor with 5 proto-chromosomes [114]. According to this model, a part of chromosome 4 in maize, where *ZmBX1-ZMBX5* are located, originated from the A11 proto-chromosome. The same proto-chromosome gave origin to *TaBX1*, *TaBX2*, *TaBX3* and *TaBX5* from wheat. These observations suggest that *BX1* to *BX5* arose as a cluster that was split into two chromosomes during the evolutionary process of *Triticeae* [112,115]. Additionally, the *BX2-BX5* genes of wheat, maize, rye and wild barley share high homology, suggesting that their progenitor evolved before the

divergence of the *Triticeae* and the *Panicoideae [30].* The genes encoding glucosyl transferases and glucoside glucosidases are thought to have originated from the ancestral proto-chromosomes A8 and A4, respectively. Wheat glycosyltransferases show synteny with parts of maize chromosome 1 (where *ZmBX9* is located) and 4 (where *ZmBX8* is located), and wheat glucoside glucosidases (*Taglu*) show synteny with a part of chromosome 10 (where *Zmglu1* and *Zmglu2* genes are located). These findings imply that the *UGT* and *glu* loci had not been included in the ancestral BX-pathway gene cluster. However, the fact that one of the maize *UGT* genes, *ZmBX8*, is situated only 44 kb apart from *ZmBX1* retains the possibility of an ancestral BX-pathway gene cluster [39,112].

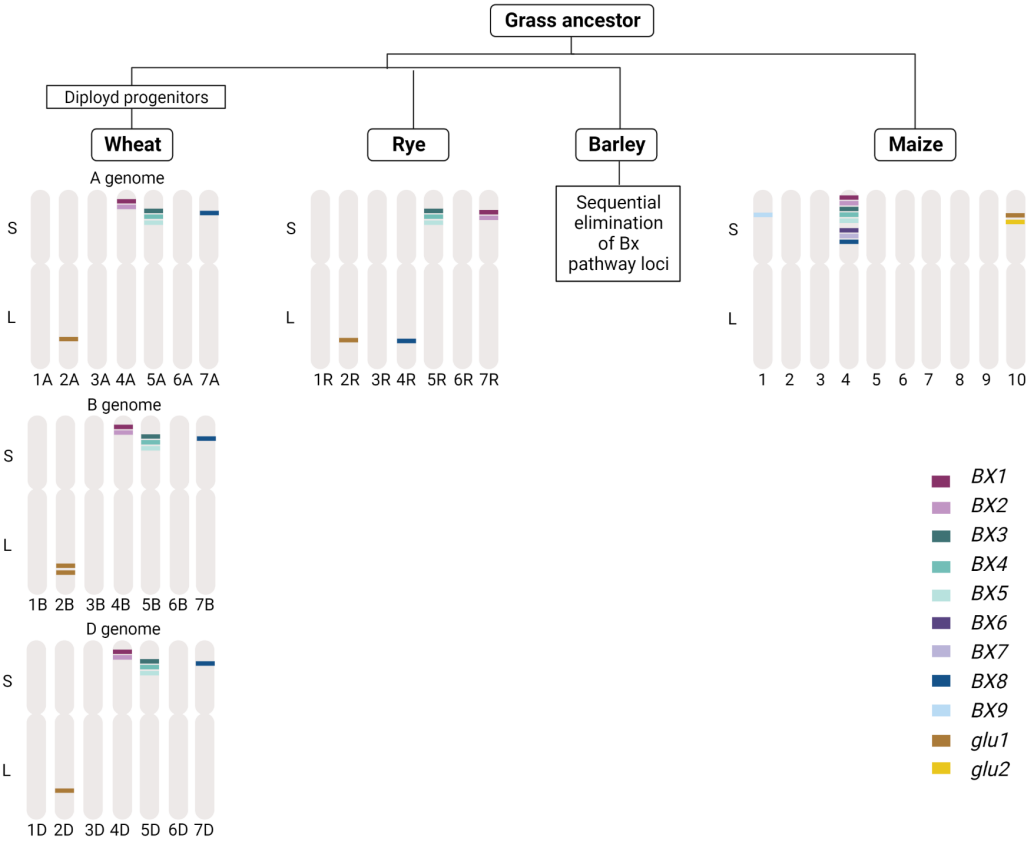


**Figure 3. Chromosomal locations of BX-pathway loci identified in Triticeae species and in maize.** *BX1-BX9* and glucosidase genes (glu) are represented as colored lines along the short (S) and long (L) chromosome arms of the three species. Note that orthologues of *BX7* haven't been determined in wheat and rye and that domesticated barley lost the BX biosynthetic cluster. Figure adapted from [112].

*BX6* and *BX7* are separated by several centimorgans from the main cluster in the short arm of chromosome 4 in maize. *BX6* is located 1.7 Mbp upstream of the cluster

and *BX7* 15 Mbp downstream [110]. In rye, an ortholog of BX6 has been identified (*ScBX6-like*) [99]. However, neither orthologs of BX6 and BX7 in wheat nor BX7 orthologs in rye have so far been identified [30,99].

The remaining maize BX biosynthetic genes are located in different chromosomes. *BX10* to *BX12* are located within 200 kb on chromosome 1. They are most probably paralogues that resulted from gene duplications [58]. *BX13* and *BX14* are both distantly located in chromosome 2. The localization of some BX biosynthetic genes on chromosome 4, but set apart from the main cluster on that chromosome, may facilitate independent regulation of steps downstream of DIMBOA-Glc, or could be the result of later evolution of these DIMBOA-Glc modification reactions. In wheat, a distantly related *TaBX10* gene has been identified. *TaBX10* is induced by caterpillar feeding and likely evolved independently [49]. All other genes have not yet been identified in other species [104].

In dicots, research on the genes and evolution of the BX pathway is scarce. Like in monocots, it has been shown that indole is generated by a homologue of TSA, and that further steps lead to BX. The *BX1* genes of the Poaceae family and the dicots *A. squarrosa*, *C. orientalis*, and *L. galeobdolon* are results of individual convergent evolution [40]. Similarly, the *UGT* gene *CoBX8* and the specific glucosidases *CoGlu* and *LgGlu1* from *C. orientalis* and *L. galeobdolon* are the result of repeated evolution. Hence, BX biosynthesis most likely evolved independently several times [116,117].

## 1.6 Wheat importance and domestication history

Wheat is one of the most important cereal grains in the world and belongs to the *Triticeae* tribe of the grasses (*Poaceae*) family. It is produced in temperate, cool, arid and semi-arid regions. Wheat grain is mainly used for a variety of bread and pasta products that contribute greatly to the health and well-being of humans. Most of the cultivated wheat, roughly 95%, is common wheat (*Triticum aestivum*) used for making bread, cookies, and pastries; while the remaining 5% is durum wheat (*Triticum durum*), used for making pasta and other semolina products. Wheat-based foods contribute to about one fifth of the total calories consumed by humans, but it is

also an important source of dietary fibers, B vitamins, minerals, and other phytochemicals [118,119]. As one of the most important staple foods of humanity, its demand and production is increasing and expected to continue to rise. In 2020 and 2021, worldwide annual wheat production reached a record of ~770 million tonnes and it is predicted to be around the same amount for 2022 (FAO, 2022). Therefore, questions regarding its origin, domestication history, development, physiology and biological interactions have fascinated scientists for years, with the hope to increase its production and nutritious value in the face of climate change and an increasing population.

Crop domestication allowed humans to change from a nomad lifestyle to a sedentary one. In the case of wheat, the domestication origin remains obscure. Archaeological samples, as well as the genetic relationships between wild species with domesticated einkorn (*T. monococcum*, genomes AA) and emmer (*T. turgidum* ssp. *dicoccon,* genomes BBAA), point to the west region of Diyarbakir in southeastern Turkey as the most likely origin for its domestication. From this area, domesticated einkorn and emmer expanded to Asia, Europe and Africa [118,120,121] .

Expansion of domesticated emmer to the southwest allowed it to mix with wild emmer or with emmer populations domesticated in the southern region. This formed a center of emmer diversity in the Southern levant and divided the populations from the north and the south [121]. Recent genetic evidence shows that a haplotype surrounding a major gene controlling spike fragility originated from wild emmer in the Southern levant region [122]. Non-fragile spikes marked the origin of domesticated wheat because this phenotype prevented the grains from being scattered by the wind and facilitated harvesting [118]. Archaeological data suggest that wheat domestication was a gradual process. Both fragile and non-fragile spikes were found in early PPNB (Pre-Pottery Neolithic B, starting ~10,000 “Calibrated years before present” Cal-Y BP) and took 2-3 milenia for non-brittleness to be dominant among cultivated wheat [123]. The non-brittleness phenotype was due to a loss of function mutation in the *brittle rachis 1* loci on chromosomes 3A and 3B (*br-A1* and *br-B1*) [124]. By the middle PPNB, ~9800 Cal-Y BP, further expansion of domesticated emmer to the northeast occurred from Armenia to the southwestern coastal area of the Caspian Sea. This allowed domesticated emmer to mix with *Aegilops tauschii*

(genomes DD) giving rise to hexaploid common wheat (*T. aestivum,* genomes BBAADD) [118]. *T. aestivum* was probably selected due to the contribution of variable alleles of high molecular weight (HMW) glutenins in the D subgenome that gave wheat a superior baking quality [125,126].

Among other traits that were selected through domestication are: loss of tough glumes that form free-threshing wheat, increased seed size, reduced number of tillers, more erect growth, and reduced seed dormancy [118]. Seeds of free-threshing wheat began to appear in archeological sites about 10,000 Cal-Y BP from an already extinct ancestor of durum [127]. This phenotype was due to the recessive mutations at the *tenacious glume* (*Tg*) loci and the gain-of-function mutation at the Q locus, which encodes an *AP2*-like transcription factor. Such mutations lead to various pleiotropic effects, changing the shape and thickness of glumes and causing a more compact spike [128,129]. One gene affecting seed size and grain nutrient content is *GPC-B1.* During domestication, a nonfunctional allele of *GPC-B1* was selected and fixed in both tetraploid and hexaploid wheat [130]. Apart from the genes mentioned above, no other genes involved in domestication have been identified so far.

## 1.7 Origin of bread hexaploid wheat

Both durum and common wheat are allopolyploid species, i.e., having subgenomes (chromosome sets) that derived from natural genome hybridization events of closely related diploid species. Here, we will focus on common wheat (*T. aestivum)* as our model organism, due to its high importance in agriculture. *T. aestivum* is a hexaploid species, composed of 21 chromosome pairs organized in three subgenomes, A, B, and D, Genome BBAADD, 2n=6x=42 [131,132]. The diploid species involved in the origin of *T. aestivum* have been identified through crossing and analysis of chromosome pairing, but only recently, a high quality genome assembly became available that corroborated these species [133].

Common wheat evolved through two main genome hybridization events. The first event led to the formation of wild emmer wheat (*T. turgidum* ssp. *dicoccon*), the wild progenitor of tetraploid wheat that contributed the A and B subgenomes of *T. aestivum*. This hybridization event occurred ~800,000 years ago between two diploid species: the male donor of the A subgenome, a species very similar to *T. urartu*, but

diverged from it ~1.3 MYA, and the female donor of the B subgenome, a species related to *Aegilops speltoides*, but diverged from it ~4.5 MYA [133–136]). The second hybridization event that led to the formation of hexaploid wheat occurred ~9000 YA and involved the hybridization of wild emmer as the female donor of the AB subgenome and *Ae. tauschii* as the male donor of the D subgenome (Figure 4).

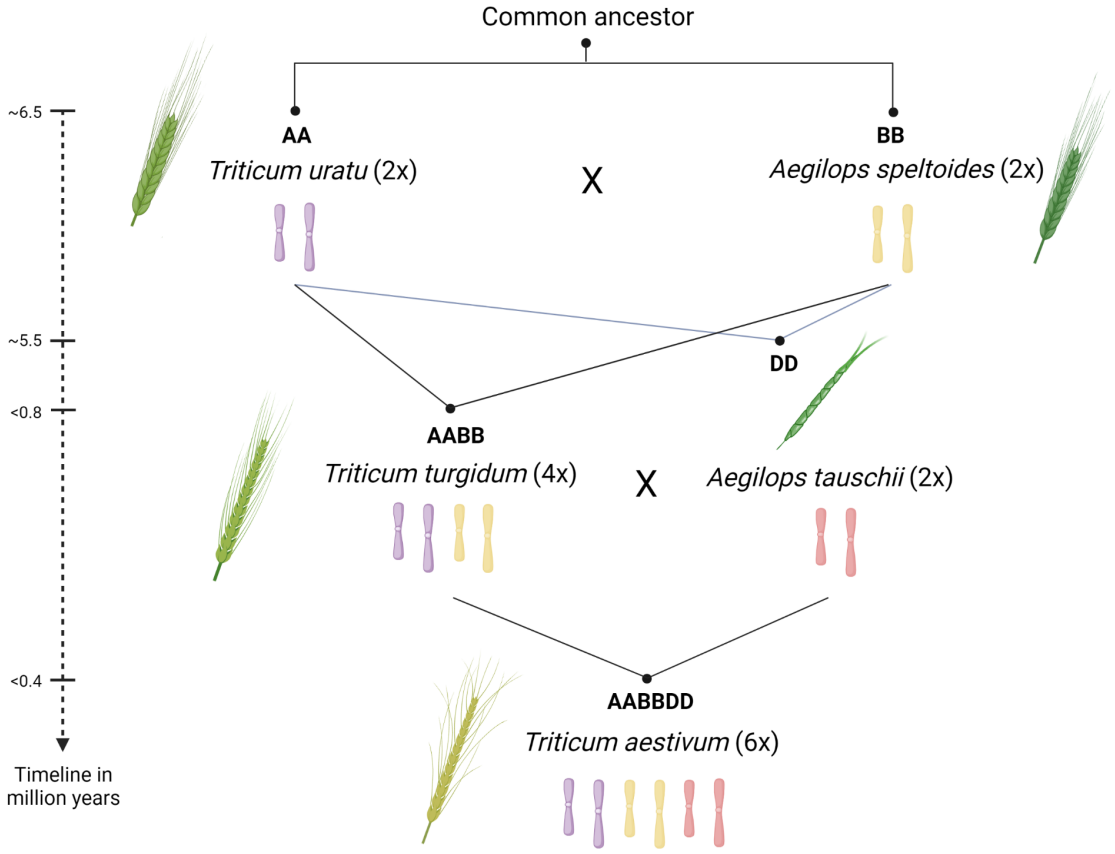


**Figure 4. Evolution of hexaploid bread wheat (*T. aestivum* AABBDD)**. Approximate dates for divergence and the three hybridization events are given in the dashed line on the left. Differentiation of the A and B genome lineages began ~6.5 Ma form a common wheat ancestor. The first hybridization occurred ~5.5 Ma between the A (*T. uratu*) and B (a close relative of *Ae. speltoides*) genomes, leading to the homoploid hybrid that originated the D genome lineage (*Ae tauschii*). The second hybridization happened <0.8 Ma by polyploidization of the A and B lineages, giving rise to the allotetraploid emmer wheat (*T. turgidum*). Hexaploid bread wheat originated by allopolyploidization from a third hybridization between the AB and D lineages.

Interestingly, the D subgenome is in itself an ancient homoploid hybrid resulting from the merge of the A and B genomes 5.5 MYA and, as mentioned before, the AB subgenome is the result of a new merge of genomes A and B, but this time to produce a tetraploid species. Additionally, a recent study highlighted the importance

of *Amblyopyrum muticum* as an ancestral contributor to both the B and D lineages. In summary, one can say that the evolution of common wheat is the result of a cycle of “diverge and merge” speciation events [133,135,136].

Through morphological, cytogenetic and genomic studies, the identity of the diploid donors for the A and D subgenomes of common wheat was determined as *T. urartu* and *Ae. tauschii,* respectively. However, no diploid species with high concordance to the B subgenome has been identified so far. This suggests that the progenitor of the cytoplasm donor of common wheat, a species closely related to *Ae. speltoides,* is either extinct or remains to be discovered [133].

Allopolyploidization leads to chromosome doubling and the generation of duplicated homeologous genes (homeologs). Consequently, the genome of hexaploid wheat has triplicated homeologs for most genes derived from the diploid progenitors. Nonetheless, homeologous genes do not always function equally, e.g. due to haplogenome-biased transcription, homeolog-specific silencing, and neofunctionalization [137–139]. For example, in wheat, the B genome contributes the largest share to BX biosynthesis [42].

The complexity of the wheat genome has limited the research on the physiological role of BX in this important crop. Further investigations and the creation of new genetic tools are needed to understand the importance of these secondary metabolites in wheat physiology and biotic interactions.

## 1.8 TILLING as a tool for functional genomics and crop improvement in wheat

Since the early 20th century, mutagenesis has become a powerful tool to achieve new genetic variation for crop improvement. Currently, more than 3,300 crop varieties obtained by mutagenesis have been registered and some of them officially released for commercialization (FAO-IAEA, Mutant Variety Database, http://mvd.iaea.org/). Historically, forward-genetic screenings of mutant phenotypes have proven to be very successful for identifying improved traits in crops. However, this approach has clear limitations, especially for polyploid species, where mutations might be masked by homeologous gene redundancy [140]. The increasing

availability of genome sequences has fostered reverse-genetic approaches and the mutation of individual target genes, allowing to link sequence variation information to traits and to investigate gene function [141,142].

TILLING (targeting induced local lesions in genomes) is a reverse-genetics approach that combines traditional random mutagenesis with high-throughput genome-wide screening to detect point mutations in desired genes. It was introduced by McCallum and collaborators in the late 1990s and uses the chemical mutagen ethyl methanesulfonate (EMS) to cause single base substitutions (G to A and C to T) [143,144]. TILLING has been used in more than 25 plant species with different ploidies [145], but it is more suitable for polyploids because the functional redundancy in their genomes makes them more tolerant to high mutation densities [146,147].

For wheat, an *in silico* TILLING resource has been developed, consisting of two mutagenised populations of tetraploid durum wheat (variety Kronos) and hexaploid bread wheat (variety Cadenza) [148]. Originally, sequence data from these mutant collections were aligned to the Chinese Spring Survey (CSS) reference genome and mutation effects were predicted based on CSS gene models. Later, the RefSeqv1.0 reference was used for alignment and mutation identification. Based on CSS gene models, deleterious mutations were predicted to occur in 90% of wheat genes, making this a powerful resource for rapidly identifying mutations in desired genes [148,149]. Currently, the updated data using RefSeqv1.0 reference is publicly available on Ensembl Plants (https://plants.ensembl.org).

When selecting a TILLING mutant line from this collection, it is important to corroborate the predicted gene mutation. Additionally, in most cases, it is necessary to combine homeologous mutations by crossing to obtain a complete null mutant. For tetraploid wheat, one cross is necessary to combine knock-out mutations in the two homoeologs, whereas in hexaploid wheat, 2 crosses are needed. Furthermore, TILLING lines harbor a lot of background mutations; typically, a mutant line has between 50 (tetraploid) and 110 (hexaploid) deleterious mutations; therefore, repeated backcrossing to wild type may be required before assessing the mutant phenotype [149].

Among the reverse-genetics approaches, TILLING has proven to be a convenient strategy for generating new genetic variation in crops. Although to date, no TILLING derived crop variety has been released for commercialization, some successful examples exist in both diploid and polyploid species [150]. Particularly in wheat, few improved varieties had been developed. These include the modified *Triticum aestivum* variety that shows an increased resistance to Powdery mildew [151] and the increased amylose content in *Triticum turgidum* subsp. *durum [152]*. In part, the complexity of the wheat genome has limited the creation of new genetic material to investigate wheat physiology and to create improved varieties. In future, it will be necessary to exploit TILLING as well as other reverse genetic approaches to overcome this limitation.

# 2. Epigenetics in plant-environment interactions

## 2.1 Defining epigenetics

In eukaryotes, the DNA is organized in a hierarchical manner as packed chromatin inside the nucleus [153]. At the base of this organization is the nucleosome. A nucleosome consists of an octamer of histone proteins, each composed of two copies of core histones (H2A, H2B, H3 and H4) and a linker histone H1, around which 147 bp of DNA are wrapped [154]. Besides DNA sequence, chromatin structure, together with epigenetic modifications on histones and DNA, affect gene expression by regulating the accessibility of the transcriptional machinery to the genes [153]. A coordinated regulation of gene expression ensures normal growth and development, as well as an optimal response to environmental stimuli [155].

The stable and inherited changes in gene expression that are independent of DNA sequence are known as epigenetic phenomena. It is important to note that not all epigenetic modifications on histones or DNA can be considered truly epigenetic phenomena. The reason for this is that many of these modifications are not stably

inherited through cell divisions; however, some, such as symmetric DNA methylation, might be [156].

## 2.2 DNA methylation and histone modifications

DNA methylation is a conserved epigenetic mark in both eukaryotes and prokaryotes [157,158]. In plant genomes, mostly two types of DNA methylation have been detected: 5-cytosine methylation and N6-adenosine methylation. Cytosine methylation occurs by the addition of a methyl group to the fifth position of the pyrimidine cytosine ring; adenosine methylation occurs at the sixth position of the adenine purine ring [155,159]. Cytosine methylation is associated with heterochromatin and silencing of transposable elements (TEs) and promoters, but also with gene expression when present in gene bodies [155]. The function of adenosine methylation has been less explored, but recent studies suggest that it is a mark enriched on gene bodies and associated with gene expression [160–162]. Because N6-adenosine methylation is very rare and has not been studied extensively, I will hereafter refer to 5-cytosine methylation as DNA-methylation (Figure 5A).

DNA methylation occurs in all three sequence contexts in plants: the symmetric CG and CHG contexts and the asymmetric CHH context (where H is any base but G) [163]. Symmetric DNA methylation is inherited through DNA replication and therefore considered truly epigenetic [156]. Apart from their heritability, these contexts also differ on their methylation levels and the genomic regions in which they occur. This is in part because they require different molecular machineries for their maintenance [155,157]. Figure 5B.

CG methylation is maintained by the DNA methyltransferase MET1, which recognizes hemi-methylated sites on the daughter strand during DNA replication [164,165]. CHG methylation is maintained by the plant-specific CHROMOMETHYLASE 3 (CMT3) and the H3K9 histone methyltransferase KRYPTONITE/SUVH4 (KYP) [166–168]. Together they establish a self-reinforcing regulatory loop. In the loop, CMT3 is recruited to CHG sites by the dimethylation of lysine 9 on histone 3 (H3K9me2), this creates binding sites for KYP and its close homologs SUVH5 and SUVH6, which in turn induce H3K9me2 to generate the

binding sites for CMT3 [157,169]. CHH methylation is established and maintained by CMT2 and is also associated with H3K9me2 [170]. Methylation in all contexts is maintained by the RNA-directed DNA methylation (RdDM) pathway, which involves guided small RNAs and the DOMAINS REARRANGED METHYLTRANSFERASE 2 (DRM2) [171]. The removal of DNA methylation occurs passively through dilution of 5mC during DNA replication, or actively through the base excision repair pathway (BER) that involves DNA glycosylases of the DEMETER family [155,172].

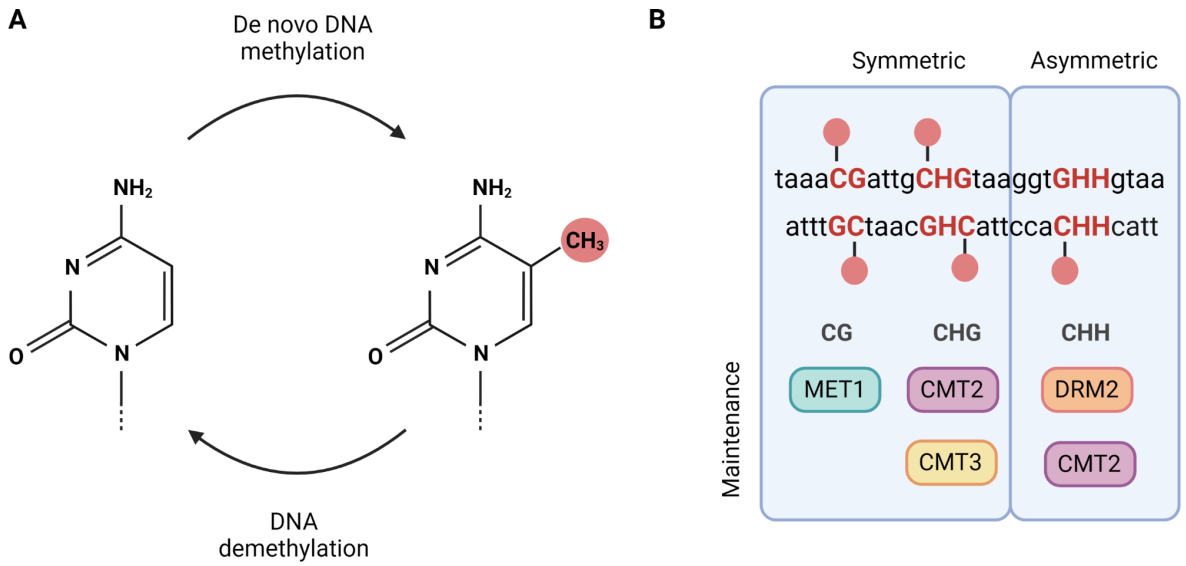


**Figure 5**. **DNA methylation in plants. A)** Schematic representation of 5-cytosine methylation. De novo DNA methylation can occur in all cytosine contexts (CG, CHG and CHH, where H is any base but G). DNA methylation can be removed by active or passive demethylation. **B)** DNA methylation maintenance in the three different contexts. After replication methylation in the symmetric CG context is maintained by MET1, whereas CHG methylation is maintained by CMT3 and CMT2 (together with a regulatory feedback loop with H3K9me2). Methylation in the asymmetric CHH context is maintained by DRM2 through RNA-directed DNA methylation (RdDM) or by CMT2.

As mentioned above, the abundance of mCs in each context varies along genomic regions. Protein coding genes are mainly methylated in CG context, while transposons (TE) and repetitive sequences are methylated in all contexts [173]. While TE methylation ensures genome integrity by maintaining TE silencing, the function of gene body methylation (gbM) is less clear. It has been observed that many constitutively expressed genes or long newly evolving genes harbor CG gbM [163,174,175]. However, mutants with decreased or increased DNA methylation in Arabidopsis do not display severely impaired phenotypes, making it more difficult to

understand the function, if any, of gbM [176]. Nevertheless, it has been hypothesized that in crop plants with larger and rich TE content genomes, which also harbor higher global DNA methylation levels, the role of DNA methylation in gene regulation might be more prominent [155,175,177]. This is supported by the observation that DNA methylation mutants in crop plants are generally either lethal or have severe growth and developmental defects [178–182].

Besides DNA methylation, histone modifications provide another set of epigenetic marks that regulate gene expression. Modifications on histones occur at the N-terminal tail, which is rich in basic amino acids that are prone to post-translational chemical modifications (PTMs). Some PTMs promote transcriptional activation, while others act as repressive marks. For instance, modifications such as acetylation and phosphorylation are generally associated with gene transcription. In contrast, sumoylation and deamination are related to repressive chromatin states. Others, such as ubiquitination and methylation, can have both activating and repressing functions [183]. However, histone regulation is much more complex, since histone PTMs can act sequentially or in combination to regulate different cellular functions. Such interplay constitutes the “histone code” that is read by downstream transcriptional regulators and the chromatin remodeling machinery [184].

## 2.3 Epigenetics and its role in biotic and abiotic stress

Plants live in constantly changing environments where they interact with a multitude of biotic and abiotic factors. Plant-environment interactions are necessary and/or beneficial for growth, development and reproduction. However, some of those interactions can cause stress and threaten plant survival [185]. To ensure an optimal response to environmental stimuli, plants have evolved high phenotypic plasticity. Phenotypic plasticity is driven by changes in gene expression that are in part regulated by epigenetic modifications. This has led to the hypothesis that epigenetic regulation of environmental responses could itself underlie selection and play a role in plant adaptation and evolution [186].

To date, several studies on different plant species have described the epigenetic contribution to different biotic and abiotic stresses. Such stresses include:

temperature (cold and heat), salinity, desiccation, nutrient deficiency, UV radiation, pathogen attack and herbivory (reviewed in [185,187,188]). Overall, such studies have approached the role of epigenetics in stress responses from two different perspectives. On the one hand, they assessed the effect of such stresses on DNA methylation either globally or at specific loci and on post-translational modifications on histones; on the other hand, they focussed on the effect of the epigenome on the plant response to the stress [189]. In other words, it has been shown that biotic/abiotic stresses can alter specific epigenetic marks or the epigenome, but also that a given specific epigenetic configuration can influence the response to the stress, making the plant either more susceptible or resistant.

Referring to the first approach, the effect of stress on the epigenome, the majority of studies have focused on abiotic stresses. In this regard and focusing on DNA methylation, many studies have shown that CHH context is often the most affected by abiotic stress [187]. For example, global CHH hypomethylation has been observed under heat, cold and drought stress in different plant species [190–194]. Additionally, CHH methylation changes at specific loci involved in the stress responses to cold and drought have been described. One example includes the drought responsive gene *ABSCISIC ACID STRESS RIPENING 2* (*SlAsr2*), which alleviates drought in tomato. *SlAsr2* has been shown to lose CHH methylation at the promoter region as well as gain CHH methylation in its coding sequence under drought conditions [195]. Another example is the gain of CHH methylation at the promoter region of *RhAG* (an *AGAMOUS* homolog), which causes decreased expression of *RhAG* and contributes to the cold-mediated phenotype in petal number in rose (*Rosa hybrida*) [196]. Additionally, DNA methylation changes have been observed in the promoter of genes involved in cold stress and acclimatation, such as *ALLANTOINASE* (*ALN*) and *MITOCHONDRIAL MALATE DEHYDROGENASE* (*BramMDH1*). Methylation in the *ALN* promoter represses *ALN* expression and promotes seed dormancy; methylation decrease in *BramMDH1* promoter causes *BramMDH1* upregulation, which might account for heat tolerance in Arabidopsis [197,198].

For biotic interactions, there are fewer studies on the impact of biotic stress on the epigenome. The few examples that exist are in the context of plant response to

pathogens and nematodes [199,200]. In the case of plant-pathogen interactions, most of what we know originated from studies of the bacterial pathogen *Pseudomonas syringae* (*Pst*). In Arabidopsis, plants infected with virulent *Pst* caused global DNA methylation changes across all sequence contexts. Such changes preferably occurred proximal to defense-related genes and correlated with their transcriptional activation upon infection, suggesting a role of DNA methylation in the plant response to pathogens [201]. In accordance with these findings, treatment with the bacterial elicitor FLG22 resulted in demethylation of transposable elements (TEs) in proximity to defense-related genes [202]. Similarly, in diploid wheat (*Aegilops tauschii*) infected with *Blumeria graminis f. sp. tritici* (*Bgt*), a reduction in AGO4 as well as in 24nt siRNAs and CHH methylation was observed in stress response genes close to TEs [203].

For plant-nematode interactions, examples include the methylome analysis of infected roots of tomato and Arabidopsis with cyst nematodes, soybean SCN *Heterodera glycines*, and beet SCN *Heterodera schachtii*, respectively. Both studies showed that cyst nematode infection causes hypomethylation in all sequence contexts [204,205]. Hypomethylation in tomato affected syncytial genes important for the establishment of the nematode-plant interaction [204]. On the other hand, hypomethylation in Arabidopsis was shown to be correlated with an abundance of 24nt siRNAs that impacted a considerable number of protein coding genes and TEs located near nematode-responsive genes [205].

In the context of histone modifications, mainly histone acetylation/deacetylation and methylation/demethylation had been analysed during abiotic stresses and pathogen attack (reviewed in [185,187]. In the context of plant-plant interactions, Venturelli et al. showed that APO and AMPO, breakdown products of the benzoxazinoids allelochemicals, inhibited histone deacetylase activity in Arabidopsis. This resulted in a hyper-acetylation of histone lysine residues, which caused misregulation of gene expression and coincided with root growth inhibition [82].

Conversely, several studies have addressed the influence of the epigenome on the plant stress response. Examples include the studies done with Arabidopsis DNA methylation maintenance mutants and on epigenetic recombinant inbred lines

(epiRILs) [189]. EpiRILs are near-isogenic lines with mosaic DNA methylation patterns that were obtained by crossing Arabidopsis wild-type Col-0 to mutants depleted in DNA methylation *met1* or *ddm1* (a loss of function mutant on the chromatin remodeler *DECREASE IN DNA METHYLATION 1*). In this way, different epigenetic patterns on epiRILs lead to different phenotypes [206,207].

For abiotic stress, it has been shown that DNA methylation is important for thermotolerance. DNA methylation maintenance mutants *nrpd2, rdr2, dcl3* and *AGO4* show hypersensitivity to acute heat stress [208]. In contrast; *cmt2* mutants and accessions with a *CMT2STOP* allele display decreased tolerance to heat stress. This suggests that DNA methylation is an important regulation of heat stress and that it can contribute to natural adaptation to variable temperatures [191]. Similarly, DNA demethylation is important to regulate cold stress tolerance in annual and perennial species [192,209–211]. For instance, *drm2* mutants show an enhanced tolerance to freezing temperatures in Arabidopsis [209].

In the case of biotic stress responses, the general trend seems to be that DNA hypomethylation enhances resistance to biotic stressors [212]. This is illustrated by the resistant phenotypes of Arabidopsis *met1-3*, *met1 nrpd2* and *drm1 drm2 cmt3* mutants infected with *Pseudomonas syringae* (*Pst*), which also showed an increased expression of defense-related genes [201,202,213]. Another example involves Arabidopsis infection with *Hyaloperonospora arabidopsidis* (*Hpa*), where hypomethylated *nrpe* mutants showed higher tolerance to pathogen infection, while the hypermethylated mutant *ros1* was more susceptible. However, the opposite effect was observed when plants were infected with the necrotrophic pathogen *Plectosphaerella cucumerina*, with *nrpe* being more susceptible [212]. This illustrates that the role of DNA methylation on biotic interactions is much more complex than a strict promotion of defense by hypomethylation. On the other hand, the studies on epiRILs showed considerable variation in their response to the defense-related hormones SA and JA, for growth under competitive pressure by weeds, and for resistance to *Pst* [214].

The studies on the epigenetic contribution of beneficial interactions are more scarce, but some examples include the role of DNA methylation in nodule formation [215–217], mycorrhizal establishment [218,219], microbiome assembly [220,221] and flower morphology to attract pollinators [222,223].

In summary, different studies have addressed the role of epigenetics in plant environment interactions following two approaches: first, by analyzing the effect of the environment on epigenetic modifications, either genome-wide or at specific loci, and secondly, by accounting for the plant genotype and phenotype on the response to environmental perturbations. From both approaches, it is clear that epigenetic factors are emerging as a new layer of regulation in plant-environment interactions. However a clear trend on the contribution of epigenetic modifications on certain biotic or abiotic stresses cannot be drawn yet, since responses may vary depending on the conditions of the stress. Further studies will help understand if there are common epigenetic modifications for certain environmental responses and if such responses are conserved among different plant species.

## 2.4 Priming and epigenetic stress memory

Exposure to the same or different stresses can occur multiple times in the course of a plant's lifetime. Priming can lead to stress memory, which optimizes the plant response to recurring stresses. The term priming was first coined in the context of plant immunity, but was later also applied to plant-abiotic interactions. Priming refers to the phenomenon by which a temporary environmental stimulus (priming stress cue) modifies a plant for future stress exposure (triggering stress cue). A plant in a primed state will respond more strongly or faster to a triggering stress compared to one in a naïve (unprimed) or reset state [156]. Priming response occurs at the transcriptional level independently of DNA sequence and is thus reversible [224,225]. Figure 6.

Memory formation after a priming event may be manifested by the activation or repression of stress response genes or a hyper-induction upon a second stimulus [226,227]. Other mechanisms, such as transcriptional feedback loops and

post-translational modifications, might also be involved in memory acquisition [228]. Plant memory may last for days to weeks (somatic memory) or even pass to the immediate progeny (intergenerational memory, also known as parental effect) or to subsequent generations (transgenerational memory) [156]. True transgenerational memory might have an epigenetic basis and potentially be important for plant adaptation. However, true transgenerational events have rarely been observed in plants [156], possibly due to the resetting mechanisms that take place during gamete formation and that prevent the inheritance of certain acquired epigenetic states [229,230]

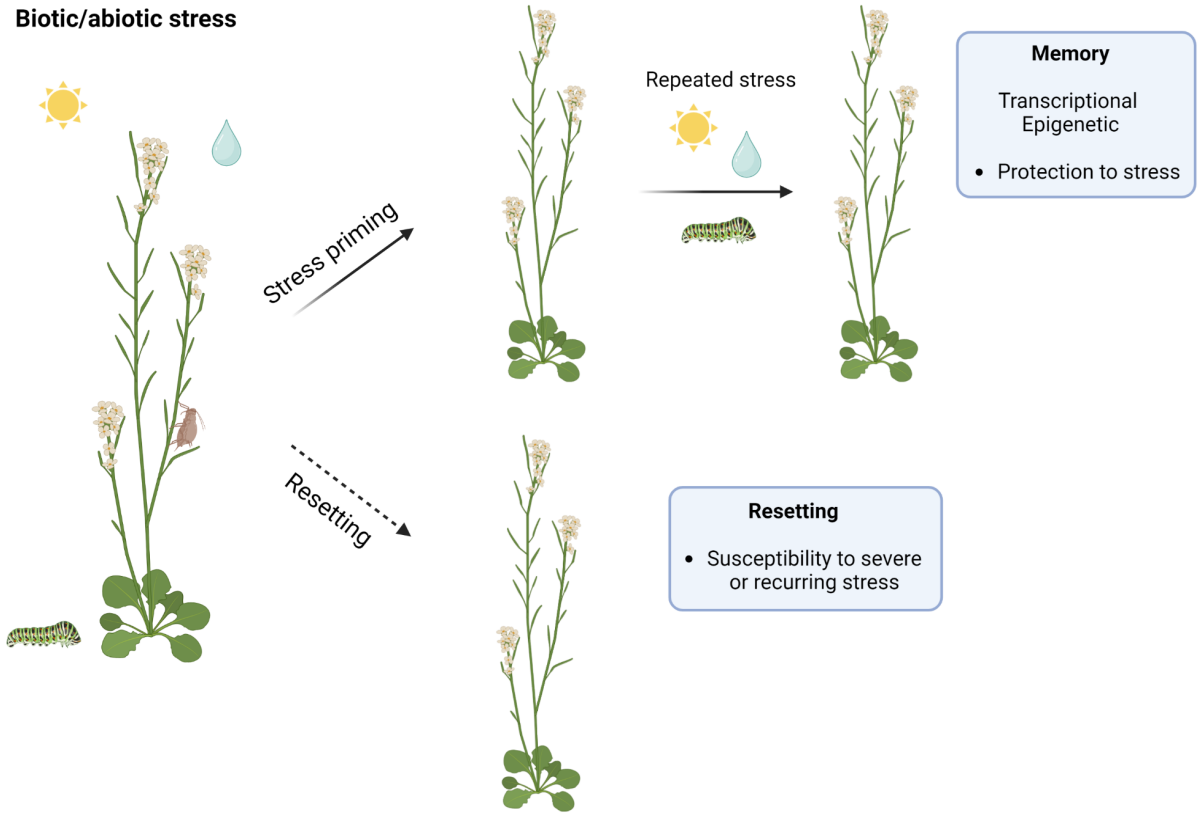


**Figure 6. Stress priming and plant memory.** Plant exposure to biotic or abiotic stress can trigger priming, which prepares the plant for future stress exposure and protects it from repeated stress via plant memory formation. Plant memory occurs at the transcriptional level and might have an epigenetic basis. Meanwhile, a plant which has not encountered or reset the response after the stress stimulus remains susceptible to future stress encounters.

Epigenetic memory has been observed for both biotic and abiotic stresses. Most examples are in the context of somatic memory formation to different abiotic stresses, including cold, heat, salinity, and drought (reviewed in [156]. For biotic stress, fewer examples exist and those include defense response to the pathogen

*Pseudomonas syringae* pv. *maculicola (Psm)* and to plant immunity elicitors [231]. Studies on somatic memory found histones as important regulators of priming and memory acquisition [156]. DNA methylation seems to be more relevant for inter- and trans-generational memory formation. Inter-generational memory related to changes in DNA methylation has been observed in response to different abiotic and biotic stresses such as salinity, iron deficiency, bacterial infection, and herbivory [232–235]. On the other hand, trans-generational memory after two stress-free generations has been observed in herbivory of caterpillars in Arabidopsis and under salt stress conditions in *Thlaspi arvense* [236,237]. In the first case, memory related to herbivory was associated with small interfering RNAs, because mutants affected in sRNA biogenesis did not exhibit inheritance resistance [236,237]. The second example In *T. arvense* used methylation-sensitive amplification polymorphism (MSAP) to determine epiloci variation under control and salt stress conditions. In this study, a heritable increase in epigenetic diversity was observed under salt stress for two stress-free generations [236,237].

In conclusion, epigenetics is emerging as a regulator of stress responses, priming and plant memory. Several studies have addressed the role of DNA and histone modifications in regulating plant environment interactions. However, a comprehensive mechanism on how different biotic or abiotic stresses shape the epigenome and how that influences stress memory is not yet well understood. Further studies on epigenetics and environmental interactions are needed to unveil such mechanisms in plants.

## 2.5 *Thlaspi arvense* as a new model organism

*T. arvense*, also known as field pennycress or stinkweed, is an annual, diploid (2n = 2x = 14), mostly selfing weed of the Brassicaceae family [238]. *T. arvense* is native to Eurasia, and is widely distributed in temperate regions of the northern hemisphere. The common habitats for *T. arvense* range from sea level to higher altitudes and include roadsides, fields, and grassy slopes [238] Recently, *T. arvense* has attracted much interest as an oilseed crop for biofuel production. The seeds contain an average of 30%-35% oil that is apt for biofuels but can also be developed into an edible oil [239–242]. Additionally, *T. arvense* is extremely winter hardy, which

makes it suitable as a winter cash cover crop. By growing *Thlaspi* in the cold months, farmers can prevent soil erosion and at the same time increase production and income [243–246].

From the research perspective, *T. arvense* is closely related to the model plant *A. thaliana* and can be used as a new dicotyledonous model for functional genetic studies. It is amenable to genetic transformation and has a short life cycle. Recently, a high-quality reference assembly of the 500 Gb genome became available, along with the methylome profile of 207 european accessions [243,247–250]. All in all, this makes *T. arvense* a new emerging crop and an accessible genetic model.

# MATERIALS AND METHODS

## 1. Plant material

Stop gain mutations on homeologous *BX3* genes were identified on the Cadenza-EMS mutant collection of the hexaploid bread wheat (*Triticum aestivum*) cv 'Cadenza' of the wheat TILLING project (www.wheat-tilling.com). Seeds were provided by the RRes-JIC Cadenza-EMS collection under the accession numbers: Cad1664, Cad0389 and Cad1491 (stop gain mutation in the *BX3* A, B and D genome, respectively) and Cad0000 as wild type (WT).

*Arabidopsis thaliana* Col-0 were obtained from the NASC collection under the accession number N1092. Arabidopsis accessions Rak-2 and Bor-4, accession numbers 8365 and 6903, respectively, were provided by the Nordborg lab at the Gregor Mendel Institute. *Thlaspi arvense* seeds of the reference accession MN106-Ref were provided by Dr. Ratan Chopra from the Department of Agronomy and Plant Genetics at the University of Minnesota, USA [248].

## 2. Growth conditions, genotyping and crosses

Wheat seeds (Cad1664, Cad0389, Cad1491, and Cad0000) were surface-sterilized with chlorine gas for 1 h and stratified on wet filter paper for 3 d at 4°C. Germinated seeds were transferred to pots containing a mixture of compost soil and 20% vermiculite and grown in a growth chamber under long-day conditions (16h light [21°C], 8-h dark [16°C], 140 $\mu E/m^2s$), with 60% relative air humidity. Plants were watered twice per week. DNA was extracted from 2-week-old frozen leaf tissue using the cetyl trimethylammonium bromide (CTAB) method [251]. Plant genotyping was performed using KASP genotyping assay following the manufacturer's protocol with the primer pairs listed in Supplemental Table 1, in individual PCR reactions for each genotype. Confirmed genotypes were used for subsequent seed propagation and crossing.

Seeds of selected genotypes were germinated in seedling starter trays on a mixture of compost and sand, following vernalization at 4°C with a 12/12h day/night light regime for 1 week. Four seedlings per line in two replicates were planted into 4 L pots (18 cm diameter, 21 cm height) filled with a mixture of potting soil (75% heat-sterilized recycled compost, 23% peat, 2% silica sand) and transferred to the greenhouse (14/10 °C day/night with 12 h photoperiod for the first 40 d). At spike emergence, greenhouse conditions were changed (22/18 °C day/night with a 16 h photoperiod at 15 000 lx) to ensure a healthy spike set.

Crosses were performed following the wheat training guidelines on 'how to cross wheat' (www.wheat-training.com). Selected genotypes of *BX3+/+/-* (aaBBDD, AAbbDD and AABBdd) were crossed in pairs to produce F1 double heterozygous genotypes AbBbDD, AABbDd and AaBBDd). Double heterozygous AbBbDD and AABbDd were crossed; in the resulting F2 population, segregant plants with the genotype AabbDd were selected for selfing and for backcrossing to the WT background (backcrossed two times). In the F3 population, two independent lines, *bx3-158* and *bx3-162*, with the triple homozygous mutant genotype *bx3* (aabbdd) were selected and used for further characterization. Both *bx3-158* and *bx3-162* were selfed for seed propagation and backcrossed to WT background twice.

To genotype crosses, leaf material of 2-week-old seedlings was collected and dried at 37°C degrees for 3-4 d. Dry tissue was ground on a tissue lyser and DNA extraction was performed with the CTAB method [251] as described previously. PCR amplification was done for 30 cycles with the primer pairs listed in Supplemental Table 1 for each genotype in individual 50 µl reactions. Amplification was performed as follows: pre-incubation at 98°C for 30 s, denaturation at 98°C for 30 s, primer annealing at 63°C for 30 s, extension at 72°C for 1 min and a final extension at 72°C for 8 min. 5 µl of PCR product was visualized on a 1% agarose gel; the remaining PCR product was purified with the MiniPEx PCR purification kit provided by the Molecular Biology Service at the Vienna Biocenter (VBC), followed by Sanger sequencing performed by the in house Molecular Biology Service at the VBC. SNP analysis of sequenced samples was done using CLC Main Workbench v7.7.3 software.

## 3. Analysis of benzoxazinoids in wheat lines

Wheat leaf tissue of two-week-old plants (WT, *bx3-158*, *bx3-162*, *BX3bd-154, BX3bd-167, BX3ab-155* and *BX3ab-189*) were harvested individually in 4 replicates and immediately frozen in liquid nitrogen. Sample preparation and liquid chromatography-high resolution mass spectrometry (LC-HRMS) measurements were carried out as described in [252]. Briefly, ~100 mg of sample were extracted with 10 x w/v of MeOH/$H_2O$ 3:1 (v/v) + 0.1% formic acid (FA), vortexed and incubated in an ultrasonic bath for 15 min. Samples were then centrifuged at 14,000 rpm for 10 min and the supernatant was recovered and diluted with $H_2O$ + 0.1% FA to a final ratio of MeOH/$H_2O$ 1:1 (v/v) + 0.1% FA. Sample measurements were carried out using an Orbitrap QExactive HF (Thermo Fischer Scientific) equipped with a heated electrospray ionization source coupled to a reverse-phase ultrahigh-performance liquid chromatography system (Vanquish UHPLC, Thermo Fischer Scientific). Samples of each genotype were analyzed in separate batches. Results were plotted in R studio version 4.2.2 using the ggplot2 package [253].

## 4. Wheat *bx3* mutants phenotyping

For root and shoot phenotyping of young plants, wheat seeds (WT, *bx3-158* and *bx3-162*) were surface-sterilized with chlorine gas for 1 h and pre-germinated in square plates on wet filter paper for 6 d in a growth chamber in long-day conditions (16 h light [21°C], 8 h dark [16°C], 140 µE/$m^2$s) with 60% relative air humidity. Ten germinated seedlings per genotype were manually transferred to our root phenotyping system (Supplemental Figure 2A) and placed in a randomized way in the greenhouse in long-day conditions (16 h light [24°C] and 8 h dark [18°C], 400 W). Briefly, our root phenotyping system consists of filter paper sheets; the area of root growth is covered with a black foil. Papers were stacked together in a rack-box filled with 5 L of half-strength Hoagland nutrient solution with 1 M phosphate [254]. Two-week-old plants were photographed using a SONY DSC-HX400V camera fixed to a tripod, and root and shoot length was measured using Fiji ImageJ software [255]. Data was plotted in R studio version 4.2.2 using the ggplot2 package and tested for statistical significance using an analysis of variance (ANOVA) test [253].

For shoot phenotyping and seed biomass measurements, sterile seeds (WT, *bx3-158* and *bx3-162*) were pre-germinated in pots (6.5 cm diameter, 7 cm height) filled with a mixture of field soil and 20% sand. Field soil was collected from an Agroscope field in Changins, Switzerland [23] and was provided by Dr. Klaus Schlaeppi (Institute of Plant Science, Bern University, Switzerland, and Agroscope, Zürich, Switzerland). Plants were grown in a greenhouse in a randomized way in long-day conditions (16 h light [24°C] and 8 h dark [18°C], 400 W) and watered twice per week. Four weeks after germination, 4 plants per genotype were transferred to 2–liter pots (17.7 cm diameter, 13.1 cm height) filled with soil substrate (Stender) in two replicates per genotype. When plants were dry and yellow (~6 months after sowing) they were harvested and dried at 37°C degrees for 7 d. Dry weight and seed biomass was measured on an analytical balance. Data was plotted in R studio version 4.2.2 using the ggplot2 package and analyzed using an ANOVA test for statistical significance [253], followed by Tukey post hoc test.

## 5. Competition assays

Wheat (WT, *bx3-158* and *bx3-162*) and Arabidopsis seeds (Col-0, rak-2 and Bor-4) were surface-sterilized with chlorine gas for 1 h. Sterile seeds were planted into pots (5 cm diameter, 5 cm height) filled with a mixture of field soil and 20% sand [23]. Plants were grown in a greenhouse in a randomized way in long-day conditions (16 h light [24°C] and 8 h dark [18°C], 400 W) and watered twice per week. Experimental design was performed in 3 independent replicates with 1 wheat plant in the center of the pot (WT, *bx3-158* or *bx3-162*), surrounded by 3 Arabidopsis plants distributed at equal distance from the wheat plant and from each other. Control conditions included wheat (one plant) and Arabidopsis (three plants) growing alone, distributed in the pot in the same way as described above.

Mature Arabidopsis (8 weeks old) and wheat plants were harvested individually and dried at 37°C degrees for 7 d. Dry weight was measured on an analytical balance. Data was plotted in R studio version 4.2.2 using the ggplot2 package and analyzed using an ANOVA test for statistical significance [253], followed by Tukey post hoc test.

## 6. Pathogen bioassays

*Magnaporthe oryzae* (*M. orizae*) isolate BR32 was kindly provided by Dr. D. Tharreau (CIRAD, Montpellier, France). Maintenance and sporulation of fungal cultures was done as described in [256]. Inoculation was performed as described in [256]. Briefly, two weeks after sporulation, conidia were harvested by rinsing the plates with water and filtering through three layers of gauze. For inoculation, the conidia were suspended in a spraying solution (2 g/L gelatin, 1 ml Tween/L) at a concentration range of 160,000-180,000 conidia/ml and sprayed onto wheat primary leaves (8 day old seedlings). Plants were then incubated at 24-26°C and 100% relative humidity in the dark. Inoculated plants were covered with a plastic hood and kept in a growth chamber in long day conditions (16 h light [26°C], 8 h dark [23°C], 200-250 μmol/$m^2$s). Leaf damage was analyzed six days post infection (dpi). *Puccinia graminis* f.sp. *tritici* (*P. graminis* f.sp. *tritici*) cultures were grown for 10 days as described in [257]. Inoculation was performed according to [258]. Spores were suspended in Fereon 131 and sprayed onto primary and secondary leaves at a concentration of ~50 mg spores/25 ml of Freon 131. After inoculation, plants were placed in a moist chamber for 24 h with an initial dark period of 16 h and then grown as described above. Evaluation of uredinia lesions was done 13 dpi. Data was plotted in R studio version 4.2.2 using the ggplot2 package and analyzed using an ANOVA test for statistical significance [253], followed by Tukey post hoc test.

## 7. Growth inhibition assay in *Thlaspi arvense*

*T. arvense* seeds were surface-sterilized with chlorine gas for 1 h. The growth inhibition assay was conducted as a concentration response experiment in square plates containing 0.5X Murashige and Skoog (MS) medium with 1% agar and supplemented with APO in a concentration range from 0 to 50 μM (APO was chemically synthesized by abcr Gute Chemie. Karlsruhe, Germany). Each plate contained 10 *T. arvense* seeds. Plates were kept at 4°C for 3 d and subsequently grown vertically in a growth chamber in long-day conditions (16 h light [21°C], 8 h dark [16°C], 140 μE/$m^2$s). Root length was measured after 8 d from scanned plate images using Fiji imageJ software [255]. Data was plotted in R studio version 4.2.2 using the drc package [259]. LC50 was determined at 3.3 μM.

## 8. APO stress assay

*T. arvense* seeds were surface-sterilized with chlorine gas for 1 h and stratified at 4°C for 3 d. Seeds were germinated on squared plates containing 0.5X MS with 0.8% agar and grown vertically in a randomized way in a growth chamber in long-day conditions (16 h light [21°C], 8 h dark [16°C], 140 µE/$m^2$s) for the whole experiment. To expose the seedlings to APO-induced stress, the medium was supplied with 3.5 µM of APO; as control, seedlings were exposed to the solvent DMSO in equal concentration as in the APO treatment. For recovery, seedlings were transferred to APO- and DMSO-free medium. Six days after germination (DAG), seedlings were manually transferred to 3 experimental replicates of 12 seedlings each to either of the following conditions: 1) Primed (two short APO stress for 24 h with a 24-h recovery period after each short APO stress, followed by a long APO stress of 6 d), 2) Non-primed (two short mock treatments with a 24 h recovery period after each mock treatment followed by a long APO stress of 6 d), 3) Control of priming (two short APO stress treatments for 24 h with a 24 h recovery period after each short APO stress, followed by a long mock treatment of 6 d), and 4) Control (two short mock treatments for 24 h with a 24 h recovery after each short mock treatment, followed by a long mock treatment of 6 d) (Figure 13).

## 9. Whole genome bisulfite (WGBS) library preparation and sequencing

Shoot and root tissue of 16 d old *T. arvense* plants from the APO stress assay was harvested separately using a razor blade and immediately frozen in liquid nitrogen. Genomic DNA was extracted with the DNeasy Plant Mini Kit (QIAGEN) from disrupted frozen tissues. For each sample, 100 ng of genomic DNA was sonicated (Covaris) to a mean fragment size of ~350 bp. Library preparation was done with the NEBNext Ultra II DNA Library Prep Kit for Illumina (New England Biolabs) following the manufacturer's protocol. Adapter-ligated DNA was treated with sodium bisulphite using the EpiTect Plus DNA Bisulfite Kit (QIAGEN) following the manufacturer's protocol and amplified using Kapa HiFi Uracil + ReadyMix (Roche) in 10 PCR cycles. WGBS libraries were sequenced on an Illumina HiSeq 2500 instrument at a 10x coverage with 125-bp paired-end reads. All the sequencing data can be found in the

European Nucleotide Archive (ENA, www.ebi.ac.uk/ena/), under the project PRJEB51727.

## 10. Methylation analysis

Sequencing reads were analyzed using the EpiDiverse WGBS pipeline (https://github.com/EpiDiverse/wgbs) [260]. Briefly, the pipeline performed quality control (FastQC v.0.11.9), base quality and adaptor trimming (cutadapt v.3.5), bisulfite aware mapping (erne-bs5 v.2.1.1), duplicates detection (Picard MarkDuplicates), alignment statistics, and methylation calling (Methyldackel v.0.6.1). In the mapping step we only retained uniquely-mapping reads. Because plant chloroplasts are not methylated, reads originating from those sequences were used to evaluate the bisulfite conversion rate [261]. The pipeline outputs context-specific (CG, CHG and CHH) individual-sample bedGraph files which were combined in multisample unionbed files using bedtools [262]. We retained all cytosines with a minimum coverage of 3x and used this dataset for subsequent analysis (with the exception of the general methylation patterns analysis in *T. arvense*).

For describing general patterns of methylation in *T. arvense*, the control WGBS libraries were processed using the nf-core/methylseq v1.5 pipeline, combining bwa-meth v0.2.2 as an aligner and MethylDackel v0.5.0 for the methylation calling, as described in [248].

## 11. Identification of differentially methylated regions (DMRs)

DMR calling was done using the EpiDiverse DMR pipeline [260] with default parameters and a minimum coverage of 5 independent reads. The DMR pipeline calls DMRs in all pairwise comparisons, but we retained only DMRs of control vs stress (APO treated) comparisons for our analysis. From the DMR pipeline output, we joined all DMRs that were less than 146 bp apart (consistent with the pipeline fragmentation parameters) and that had the same direction of methylation divergence (hypomethylation or hypermethylation). We then merged DMRs for all specific comparisons using bedtools [262]. Lastly, we filtered DMRs with a minimum methylation difference of 15% and 0.001 FDR to select DMRs with variability in our dataset. Filtered DMRs were then intersected with the annotated *T. arvense* genome

using bedtools [262]. The DMRs that occurred in a 2kb window upstream or downstream of genes were selected as stress-related candidate DMRs.

# RESULTS

## 1. Loss of benzoxazinoids synthesis in hexaploid wheat

### 1.1 Loss of *BX3* affects benzoxazinoids biosynthesis in wheat

Previous studies have shown that mutation in the genes encoding for BX1 and BX2 enzymes, involved in the early steps of benzoxazinoid biosynthesis, leads to loss of BX biosynthesis and an impaired defense response in maize [18,24,25,44]. To study the effect of loss of BX biosynthesis in wheat, I generated a loss of synthesis mutant in the *BX3* gene, which encodes for the third enzyme involved in BX biosynthesis (Figure 7A). To generate *bx3* mutants, we followed a reverse genetics approach using hexaploid Wheat TILLING mutant lines with stop gain mutations in *BX3* homeologous genes. I did not target BX1 because point mutation in *BX3A* gene could not be confirmed by sequencing and for the case of BX2, no mutant TILLING line for *BX2A* was available in the TILLING collection.

For *BX3,* I identified TILLING lines with point mutations in the third exon of *bx3*A, the first exon of *bx3B*, and the first exon of *bx3D* (Supplemental Figure 1A). All lines were crossed among them for two generations to obtain candidate segregant plants (Supplemental Figure 1B). In the F3 generation, I genotyped 70 plants from a segregant population of previously selected single homozygous line *bx3b-11* (genotype: *BX3* AabbDd). From this screening, two independent triple homozygous mutant lines, *bx3a bx3b bx3d-158* and *bx3a bx3b bx3d-162* (subsequently referred to as *bx3-158* and *bx3-162*), and four independent double homozygous segregant lines *bx3b bx3d-154*, *bx3b bx3d-167*, *bx3a bx3b-155* and *bx3a bx3d-189* (subsequently referred to as *BX3bd-154, BX3bd-167, BX3ab-155* and *BX3ab-189* respectively) were selected along with wild-type (WT).

We then performed liquid chromatography–high-resolution mass spectrometry (LC-HRMS) on young leaf tissue to determine DIMBOA and DIMBOA-Glu content in *bx3* mutants, double homozygous lines and WT plants. No DIMBOA or DIMBOA-Glu could be detected by LC-HRMS in *bx3-158* and *bx3-162* mutants. In contrast,

DIMBOA and DIMBOA-Glu were detected in double homozygous and WT samples (Figure 7B).

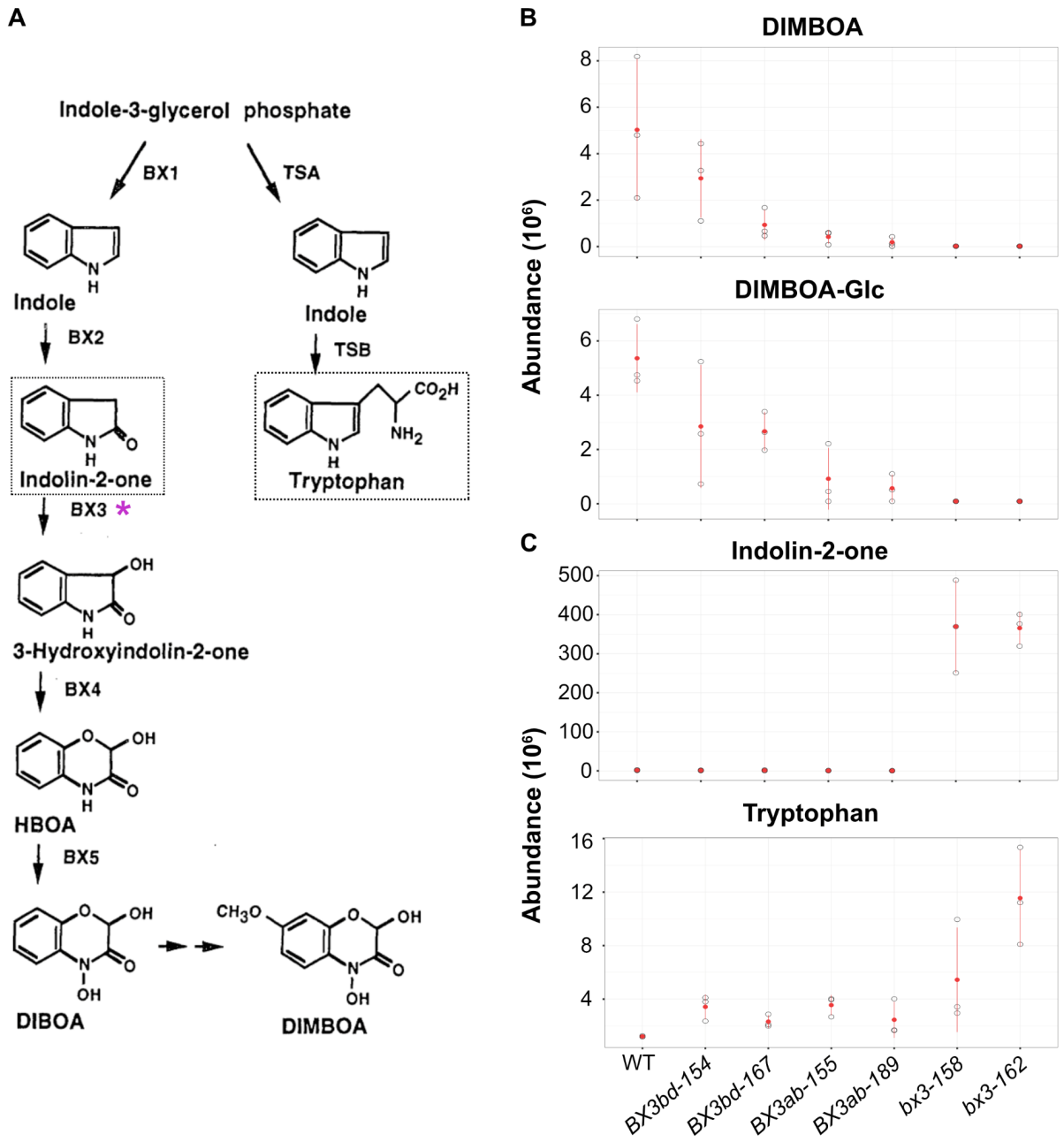


**Figure 7. Impact of wheat *BX3* homeologous mutations in BX production. A)** Benzoxazinoid biosynthetic pathway; pink asterisk indicates the position of the product mutated *BX3* gene in the biosynthesis cascade. Dashed contour indicates the intermediary compounds detected in this study in *bx3* mutants. **B)** Relative abundances of DIMBOA and DIMBOA-glucoside (Glc) detected by LC-HRMS in young leaf tissue of wheat wild type (WT) mutants. **C)** Relative abundances of intermediary compounds, indoline-2-one and tryptophan detected in young leaf tissue of wheat WT and mutants. Unfilled data points indicate biological replicates (n = 3). Mean and SD are depicted by red points and whiskers, respectively.

Interestingly, double homozygous segregants showed a decrease in DIMBOA and DIMBOA-Glu production compared to WT, indicating that all three sub-genomes contribute to BX biosynthesis. This is in accordance with previous observations that showed that all three sub-genomes were actively transcribed, albeit to different degrees and with different catalytic properties [42]. Taken together, these results demonstrate that an intact *BX3* gene is necessary for DIMBOA biosynthesis in wheat and that the triple homozygous mutant line generated here was incapable of producing either DIMBOA or its glucosinolated conjugate.

Because *BX3* mutation occurs downstream of the formation of indole in the biosynthetic pathway (Figure 7A), we checked for the accumulation of intermediary compounds in *bx3-158* and *bx3-162* mutant lines. LC-HRMS showed that the upstream intermediary compounds, indoline-2-one and tryptophan, accumulated in young leaf tissue of *bx3* mutants compared to WT (Figure 7C). The immediate substrate of BX3, indoline-2-one, was strongly accumulated in mutant plants and was not detected in WT or double homozygous mutant samples. In contrast, tryptophan, the synthesis of which branches off the BX pathway at the early TSA reaction step, was detectable at different levels in both *bx3* triple and double homozygous mutants, but not in WT (Figure 7A and 7C). These results indicate that upstream accumulation of intermediaries occurs in *bx3* mutants and suggest that precursors are redirected to tryptophan production when BX biosynthesis is impaired.

## 1.2 Growth and developmental effects on *bx3* mutants

I next sought to determine whether loss of BX biosynthesis would affect plant growth and development. Previous studies on BX deficient mutants in maize did not report any growth or developmental effect in such mutants [25]. Yet, considering the accumulation of intermediaries such as tryptophan (Figure 7C) that could affect plant phenotype, I decided to screen for any growth or developmental effect on seedlings and adult *bx3* mutant plants. For seedling phenotyping, I germinated and grew the plants on filter paper in our plant phenotyping system (Supplemental Figure 2A). Both *bx3* and WT plants germinated 3-4 d after sowing (Supplemental Figure 2B). In seedlings (two weeks old), I measured root and shoot length, as well as number of seminal roots. In adult plants (6 months old), I measured dry biomass of aerial tissue

excluding spikes, and fitness (scored as seed weight). We observed no significant difference between WT and *bx3* mutants in any of the phenotypes tested (Figure 8 and supplemental Figure 2C), indicating that, overall, *bx3* mutation does not affect plant growth, development and fitness.

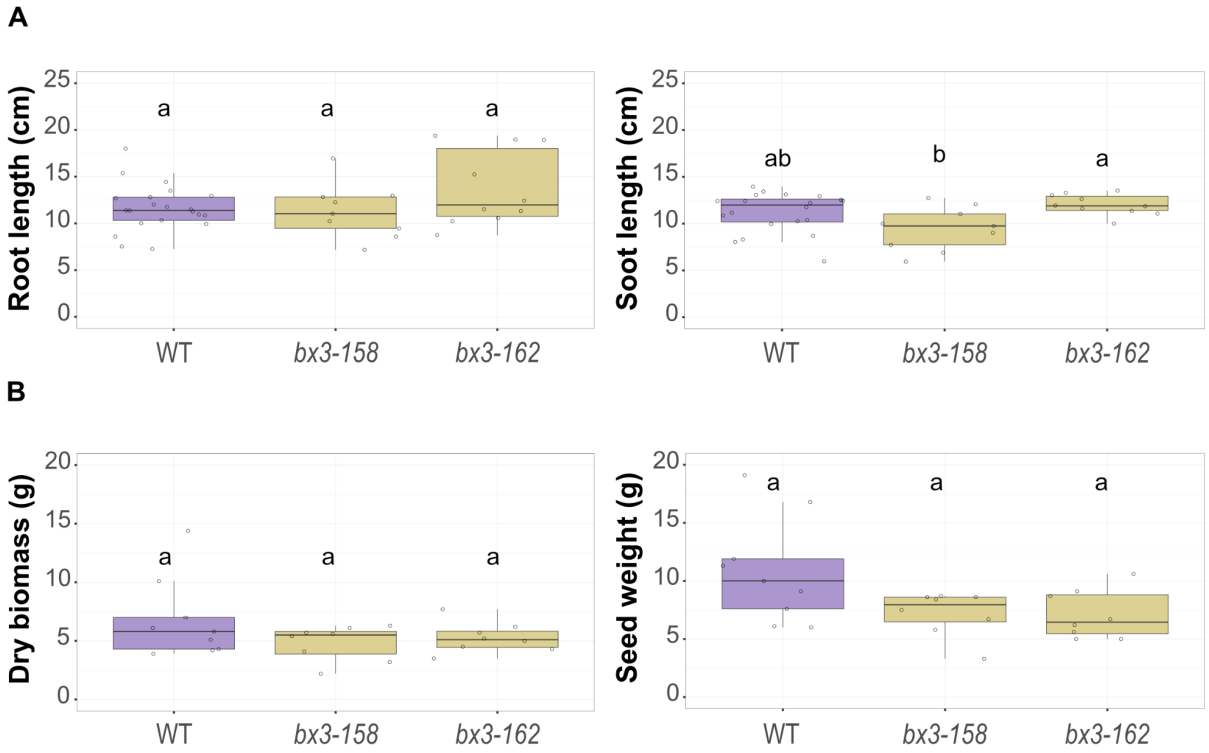


**Figure 8. Effect of *BX3* mutation on plant phenotype. A)** Root and shoot length of two week old wild type (WT) and *bx3* mutant plants (*bx3-158* and *bx3-162*). **B)** Dry biomass and seed weight of adult WT and *bx3* mutant plants. Individual data points indicate biological replicates [**A)** n = 8-20 and **B)** n = 8-9]. Different letters indicate different statistical groups (ANOVA, posthoc Tukey, $p \leq 0.05$).

## 1.3 BX effect on biotic interactions in wheat

BX compounds have been mainly recognized as defense compounds against a variety of biotic stressors in grasses (Table 1). For instance, maize *bx1* mutant plants show an impaired defense response against fungi and herbivores [44]. We hypothesized that a similar altered defense response would occur in our BX deficient mutants, *bx3-158 and bx3-162.* To test this hypothesis, we investigated the basal resistance against the pathogenic fungus *Magnaporthe oryzae* (*M. orizae*), responsible for head blast disease, and the stem rust pathogen *Puccinia graminis* f.sp. *tritici* (*P. graminis* f.sp. *tritici*); we then compared leaf area damage caused by the fungus between *BX3* WT and *bx3* mutant lines. Damage on the primary leaf was

measured six days after *M. orizae* inoculation and thirteen days after *P. graminis* f.sp. *tritici* inoculation. For *M. orizae* infection, we measured leaf area damage; for *P. graminis* f.sp. *tritici*, we measured the number of uredinia lesions per leaf. We observed no difference in the level of primary leaf damage after infection with both pathogens between *BX3* WT and *bx3* mutants (*bx3-158 and bx3-162*) (Figure 9). These results indicate that benzoxazinoids do not play an essential role in the defense response to these pathogens; possibly, other defense mechanisms compensate for the defense response in absence of BX.

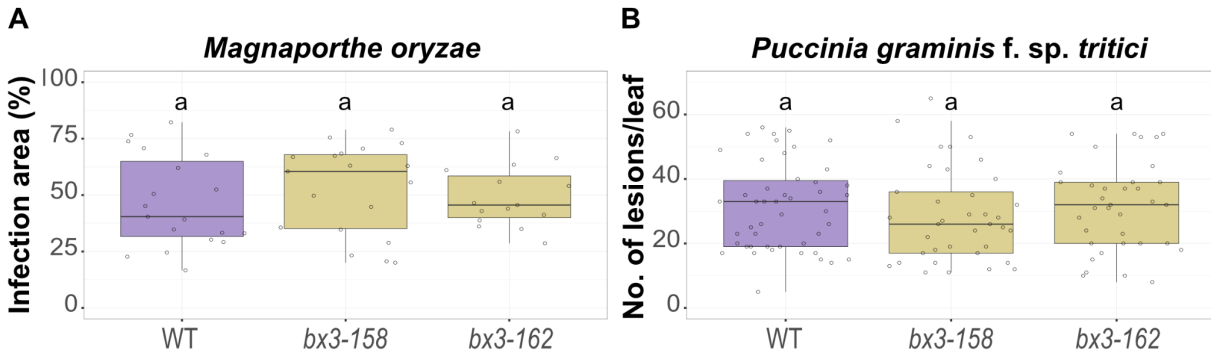


**Figure 9. Effect of *BX3* mutation on wheat basal defense response to fungal pathogens. A)** Leaf damage scored by percent of area of infection on primary leaves upon *Magnaporthe oryzae* infection in wild type (WT) and *bx3* mutants (*bx3-158* and *bx3-162*). **B)** Leaf damage scored by number of lesions per primary leaf upon *P. graminis* f.sp. *tritici* infection. Circles indicate biological replicates of two independent experiments [**A)** n = 15-19 and **B)** n = 37-47 ]. Different letters indicate different statistical groups (ANOVA, posthoc Tukey, $p \leq 0.05$).

Apart from its role on defense, BX are also known for their allelopathic properties in weed suppression [263]. We therefore sought to determine the effect of BX in wheat allelopathy. To study plant allelopathic interactions in wheat, I set up a plant-plant competition experiment in soil between Arabidopsis Col-0 and *BX3* WT or *bx3* mutant lines. I hypothesized that Arabidopsis growth would be affected when competing with WT plants due to the accumulation of BX exudates in the soil; conversely, no or moderate effect on Arabidopsis growth would be expected in plants growing together with BX deficient mutants.

Briefly, the plant-plant competition experiment involved one wheat plant from either WT or *bx3* genotype (*bx3-158* or *bx3-162*) growing in the centre of the pot, surrounded by three equidistant Arabidopsis plants (Figure 10A). Both wheat and

Arabidopsis seeds were planted at the same time and germinated between 3-4 days after sowing. Control conditions included wheat and Arabidopsis plants growing alone. At the end of the experiment (8 weeks after germination), we scored any growth effect by measuring Arabidopsis adult dry biomass. Overall, we observed a reduction of Arabidopsis dry biomass in our plant-plant competition conditions compared to the control (Figure 10B), suggesting that a space and/or nutrient competition is taking place and is affecting Arabidopsis growth. Interestingly, a more significant reduction in Arabidopsis biomass was observed in conditions when Arabidospsis grew together with WT wheat (Figure 10B). This suggests that in addition to a space/nutrient competition effect, BX synthesis and release by the wheat plant inhibited the growth of Arabidopsis.

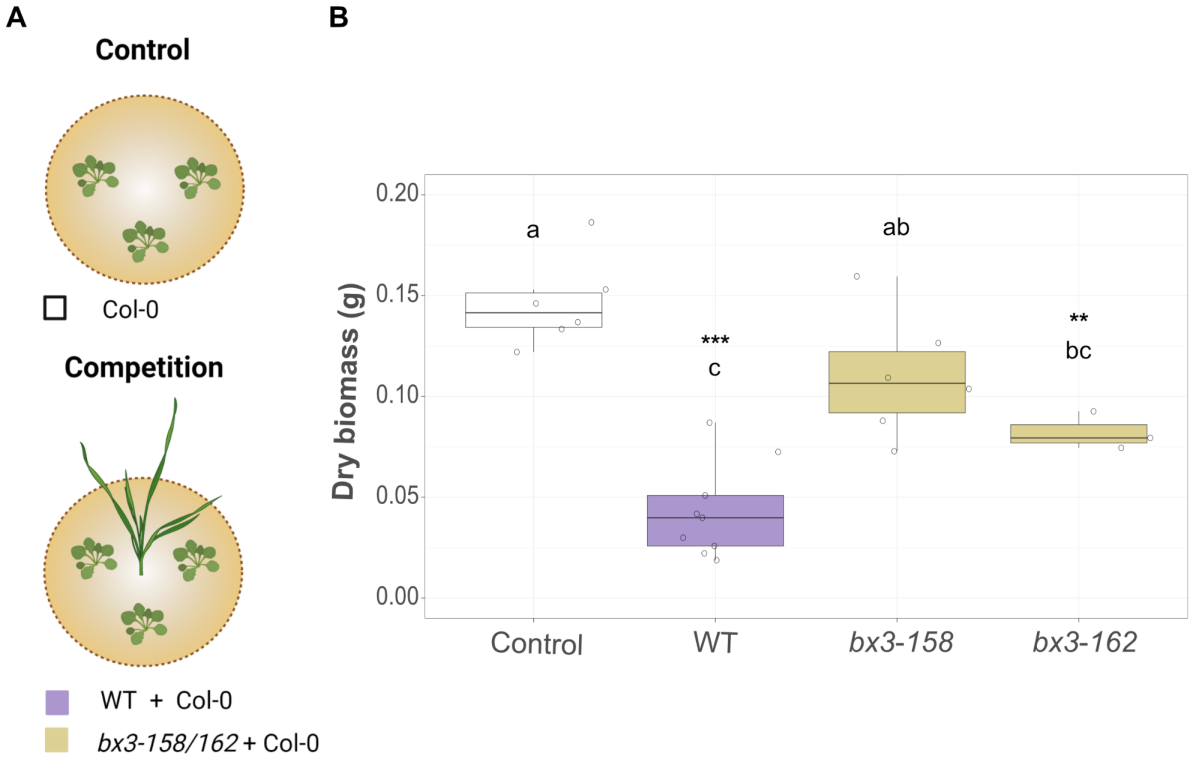


**Figure 10. Effect of *BX3* mutation on plant-plant competition. A)** Schematic representation of the plant-plant competition experiment. One wheat plant of either wild type (WT) or *bx3* mutant genotypes (*bx3-158* or *bx3-162*) was grown in the centre of the pot, surrounded by three equidistant Arabidopsis plants. The different competition scenarios are indicated by color as in B). The effect of competition on Arabidopsis was measured as dry biomass on adult Arabidopsis plants. **B)** Dry biomass of adult Arabidopsis plants after growing together with either wheat WT or *bx3* mutants (*bx3-158* or *bx3-162*) for eight weeks. Individual data points indicate biological replicates (n = 3-6). Different letters indicate different statistical groups (ANOVA, posthoc Tukey, ** $p \leq 0.01$, *** $p \leq 0.001$).

To further test the contribution of BX production/release to plant growth in the plant-plant competition experiments, I performed a competition assay including Col-0 and previously selected APO-resistant (Bor-4) and APO-susceptible (Rak-2) Arabidopsis accessions (Supplemental Figure 3); these accessions had been tested for their response to BX-conditioned soil in a separate experiment (Niklas Schandry et al., unpublished data). I performed the competition experiments in the same way as described above (Figure 10 A) and measured Arabidopsis adult dry biomass to assess any growth effects. Contrary to the expectation, dry biomass of all Arabidopsis accessions decreased compared to control in all competition conditions and independently of wheat or Arabidopsis genotypes. No significant difference was observed between Col-0 plants growing together with WT wheat vs. the ones growing with *bx3* mutants and a similar behavior was observed for both BX resistant Bor-4 and susceptible Rak-2 accessions (Figure 11), in contrast to the initial experiment with only Col-0 (Figure 10 B).

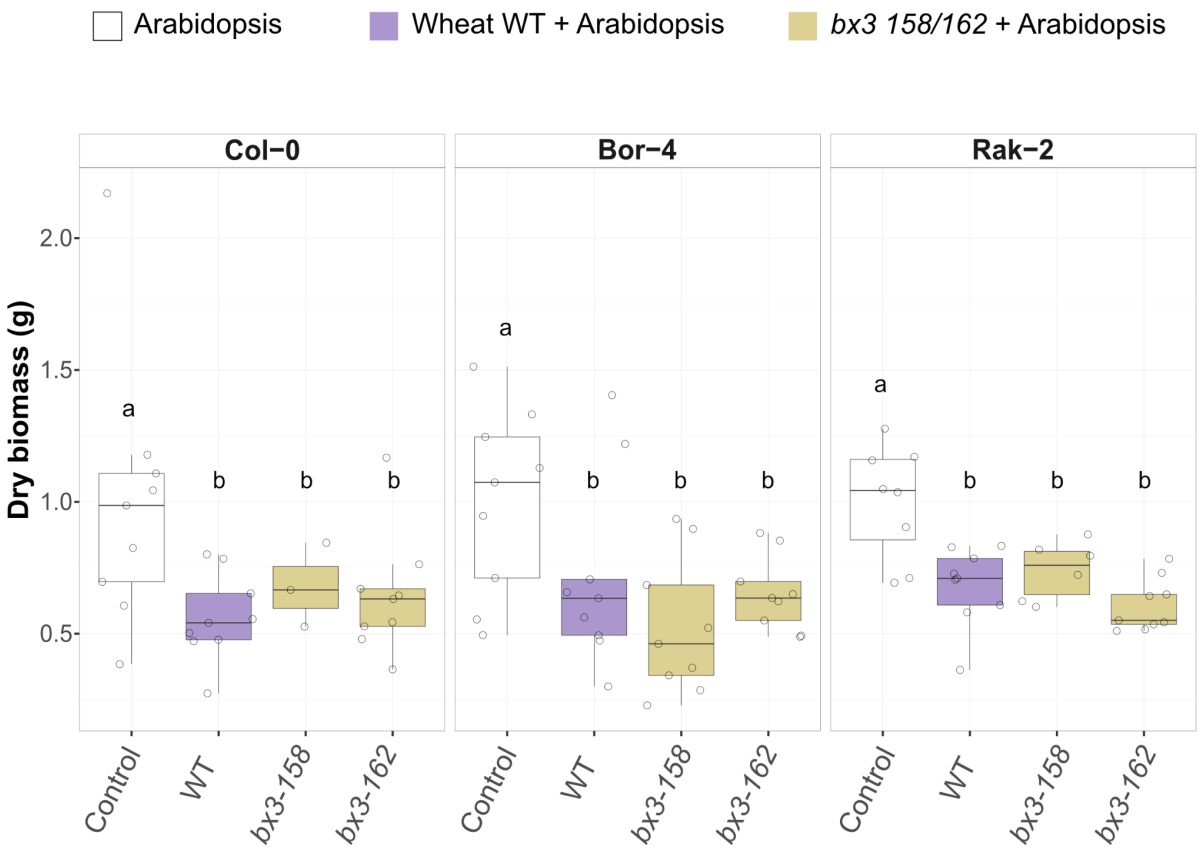


**Figure 11. Effect of *BX3* mutation on plant-plant competition with different Arabidopsis accessions.** Dry biomass of adult Arabidopsis accessions (Col-0, Bor-4 and Rak-2) after growing together for eight weeks with wheat plants of either wild type (WT) or *bx3* mutant genotypes (*bx3-158* or *bx3-162*). Dry biomass differences are represented as

relative to control of Col-0 reference accession. Individual data points indicate biological replicates (n = 3-9). Different letters indicate different statistical groups (ANOVA, posthoc Tukey, $p \leq 0.05$).

Although the previously observed competition behavior for Col-0 could not be reproduced and the results for Bor-4 and Rak-2 were unexpected, these results support our previous observations which suggested that the main driver of plant-pant competition in our biological setup is space and/or nutrient availability. Since Bor-4 and Rak-2 were selected based on their growth performance on BX conditioned soil, it is possible that the BX related phenotype previously observed on both accessions gets masked in a plant-plant interaction scenario, where wheat outcompetes Arabidopsis over a short time. Overall, we conclude that plant-plant competition is occurring in our biological setup, but it is not due to an allelopathic effect.

In conclusion, BX does not appear to play an essential role in the response to the biotic interactions tested in this study. However, further studies are required to discern if the BX effect in wheat is specific to certain pathogens, herbivores, or plants.

# 2. Epigenetic stress response to the allelochemical APO in *Thlaspi arvense*

## 2.1 APO inhibits root growth in *Thlaspi arvense*

APO can inhibit Arabidopsis root growth at lower concentrations compared to other BX or BX-derived compounds, which makes it the most phytotoxic of the BX-derived allelochemicals [38,82]. I asked whether this APO effect was reproducible in other Brassicaceae and investigated growth inhibition on the distantly related *T. arvense*. To answer this question, we performed an APO concentration-response assay (0-50 µM APO) on *T. arvense* seedlings. We found that when germinated on APO containing media, *T. arvense* seedlings showed a dose dependent root growth inhibition effect, with an EC50 determined at 3.3 µM (Figure 12). These results are in accordance with the previously observed inhibitory effect of APO in Arabidopsis root growth [38], indicating that both Brassicaceae respond similarly to APO stress treatment.

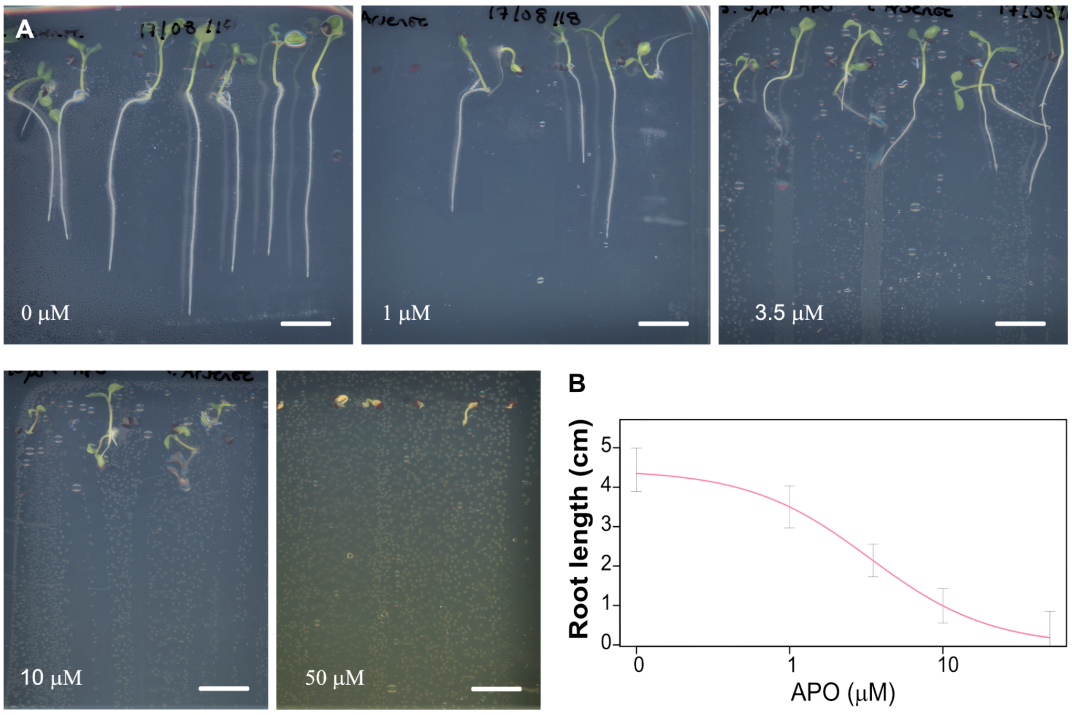


**Figure 12. APO root growth inhibition in *T. arvense*. A)** Representative seedlings (8 DAG) growing on media supplemented with increasing concentrations of APO. Scale bar = 1 cm. **B)** Dose response curve of root growth on media containing increasing concentrations of APO. The red line indicates a four-parameter log-logistic dose-response model with model-based averages and standard errors (95% confidence, n = 5-9).

## 2.2 APO stress-induced DNA methylation dynamics in *T. arvense*

Several studies have emphasized the importance of epigenetic mechanisms in regulating plant stress responses and priming [156,185,189]. In the context of allelopathy, Venturelli et al. showed that the allelochemical APO affects histone acetylation by inhibiting HDACs [82]. Additionally, a cross-talk between DNA methylation pathways and histone modifications, both methylation [264,265] and acetylation [266–268], exist to regulate gene function. However, the importance of DNA methylation in regulating allelopathic stress response has remained unexplored.

In order to investigate the role of DNA methylation in allopathic stress response, I performed an APO stress assay in *T. arvense* seedlings and prepared whole genome bisulfite sequencing (WGBS) libraries of stressed root and shoot tissues. In brief, the stress assay was done with an APO concentration of 3.5 μM and consisted of 4 experimental conditions: 1) Primed (involving 2 priming stimuli of 24 h of exposure each to APO and a subsequent long stress exposure of 6 d); 2) Non-primed (seedlings were exposed to only a long stress stimulus of 6 d in APO); 3) Control of the priming (seedlings were exposed to 2 priming stimuli of 24 h in APO, but no subsequent 6-day exposure) and 4) Control (treatment with the solvent DMSO only) (Figure 13). This experimental design was chosen to retrieve more stable and consistent changes in DNA methylation that could account for APO-related priming effects or somatic memory.

To gain insights into the genome-wide methylation profile of *T. arvense*, we first analyzed WGBS data of control samples. For this, I extracted genomic DNA from both shoot and root samples and prepared tissue-specific sequencing libraries. Genome-wide, around 70% of cytosines were methylated in the CG context, 47% in the CHG context, and 33% in the CHH context in both roots and shoots (Figure 14). This is in accordance with DNA methylation levels along the three different contexts reported for other Brassicaceae [248].

When we analyzed DNA methylation levels on different genomic features, we found that most DNA methylation colocalized with TEs and intergenic regions, specially for the CG context (Figure 15A). Conversely, DNA methylation seemed to be depleted

in gene bodies (Figure 15B). A similar pattern of lack of gbM has been reported for a close relative of *T. arvense*, *E. salsugineum*, which suggest that gbM was lost at the base of this clade [175,248,269].

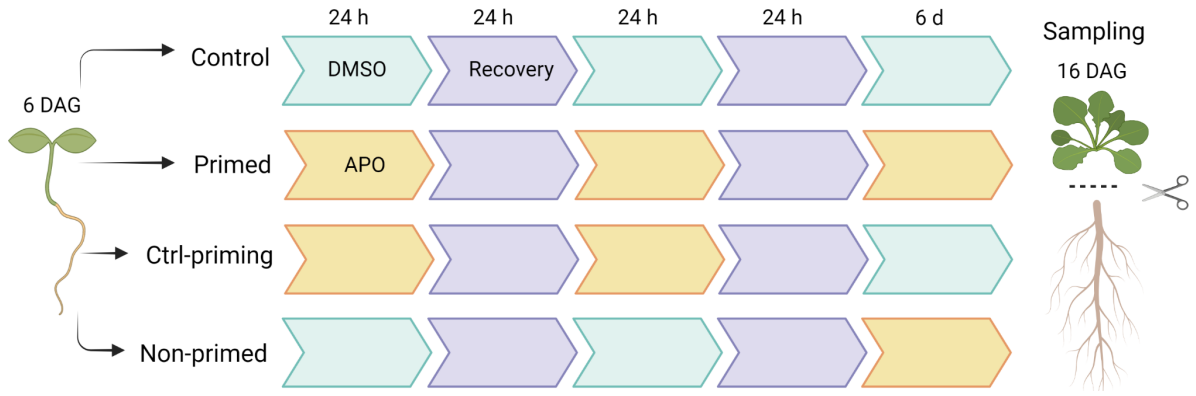


**Figure 13. Schematic representation of APO stress experimental design in *T. arvense*.** Six-d-old seedlings were sequentially transferred to any of the four experimental conditions (Control, primed, ctrl-priming and non-primed). Each treatment (represented as arrows) was performed on 1/2MS plates supplemented with 0.8% agar and a concentration of 3.5 µM of either DMSO (blue arrows) or DMSO+APO (yellow arrows). Recovery condition was done on 1/2MS media with 0.8% agar. The duration of each treatment is given on the top of each arrow. After the last treatment for 6 d, both shoot and root tissue of 16 day old plants were harvested independently.

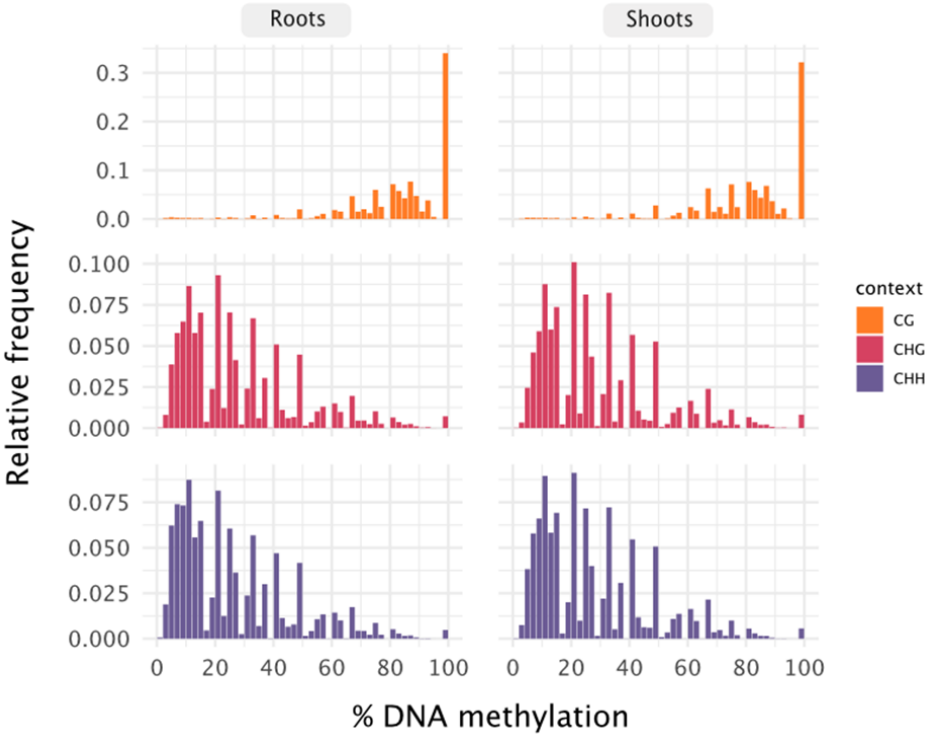


**Figure 14. Genome wide DNA methylation profile in *T. arvense*.** Methylation rate frequency distribution by sequence context in root (left) and shoot (right) tissues [248].

Interestingly, while the ortholog of the methyltransferase CMT3 seems to have been lost in *E. salsugineum*, which has been postulated as the possible cause for the lack of gbM in that species, the *CMT3* copy in the *T. arvense* genome annotation appears encode for a full-length enzyme [248,250]. However, functionality of *TaCMT3* will need to be validated in future studies.

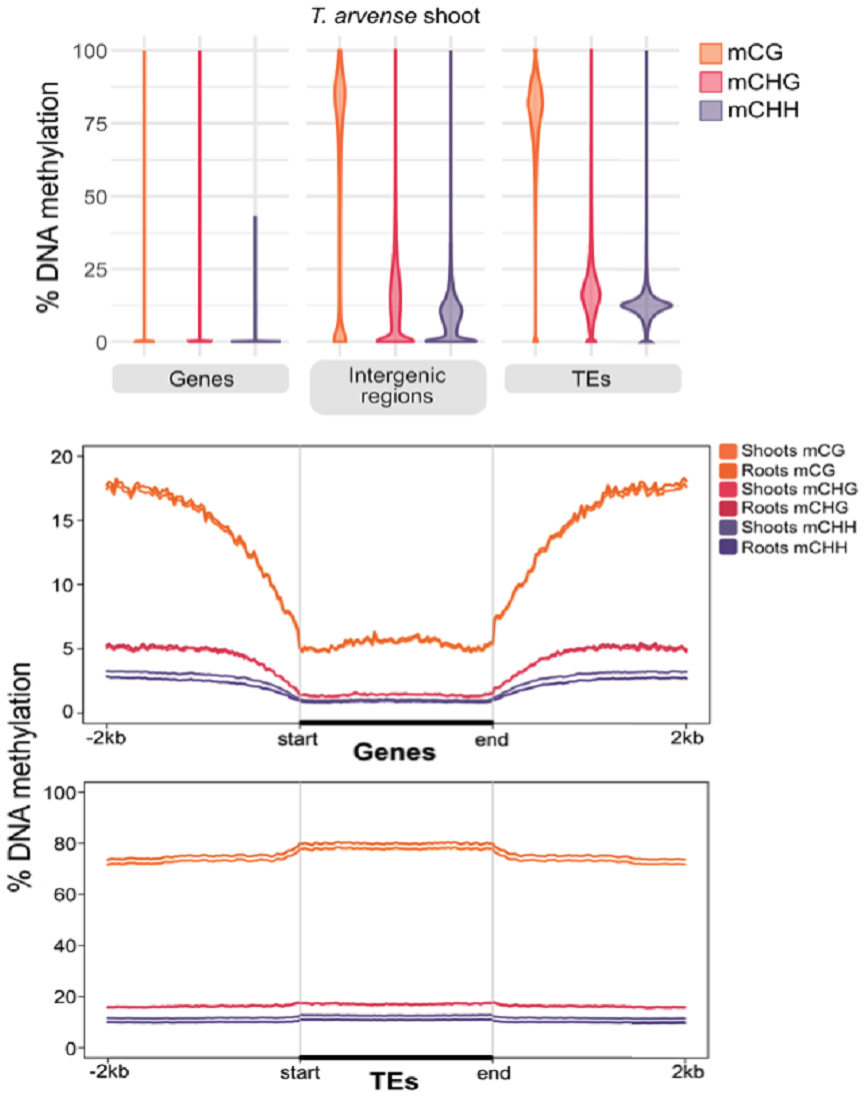


**Figure 15. DNA methylation across different genomic features in *T. arvense*. A)** Distribution of average DNA methylation by cytosine context on genes, intergenic regions and TEs. **B)** DNA methylation along genes (top) and TEs (bottom), including a 2-kb flanking sequence upstream and downstream. DNA methylation was averaged in non-overlapping 25-bp windows [248].

Next, to explore the dynamics of DNA methylation following APO stress, we analyzed WGBS libraries of stress and control samples. Principal component analysis (PCA) on global DNA methylation levels of stress and control samples

showed cluster separation according to tissue type in all the three methylation contexts (CG, CHG and CHH) (Figure 16A and supplemental figure 4), indicating that tissue type is the main driver of DNA methylation variation. In accordance with this, global DNA methylation levels of control and APO-treated root and shoot samples were more different between tissues than among treatments of the same tissue, particularly in non CG contexts. Shoot tissues showed higher DNA methylation levels in CHG and CHH contexts compared to roots (Figure 16B).

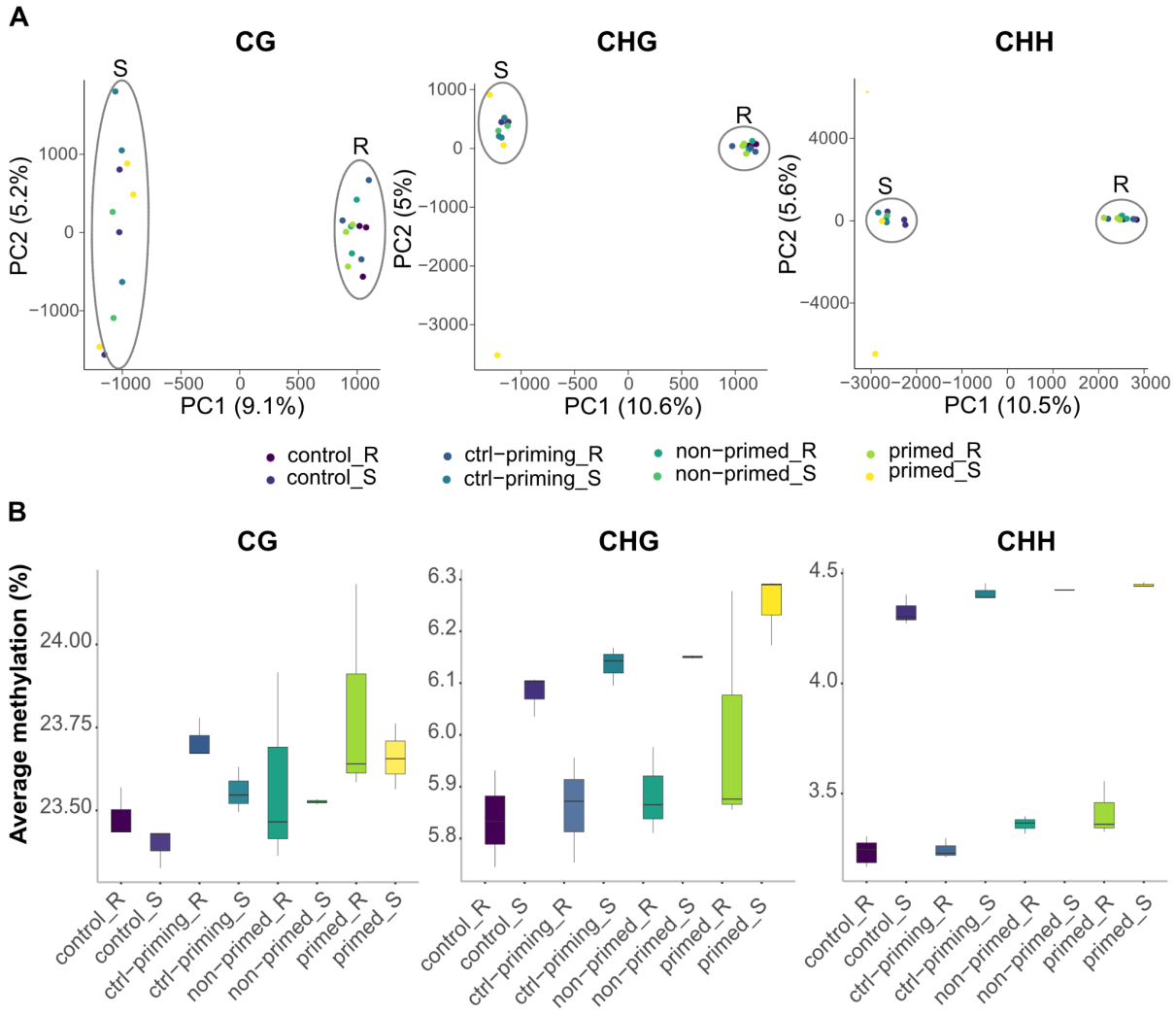


**Figure 16. Dynamics of DNA methylation after APO stress. A)** Principal component analysis (PCA) on DNA methylation levels by cytosine context (CG, CHG and CHH). Grouping of root and shoot samples are marked by R and S, respectively. **B)** Percent of average DNA methylation for each cytosine context in APO-treated root and shoot samples.

Overall, global DNA methylation level of primed, stressed and control samples of the same tissue were similar (Figure 16B). Nonetheless, there might be a small APO effect, since roots and shoots exposed to longer APO treatment (primed and

non-primed) showed a slight increase in DNA methylation in all sequence contexts. (Figure 16B).

Taken together, our results indicate that global DNA methylation is more variable by tissue type than it is upon exposure to APO, and that genome wide, there is low variation in DNA methylation across APO treated samples. Tissue-specific DNA methylation patterns have been observed in other Brassicaceae [270–272][273]. Although this epigenetic mark can be influenced by the environment, the overall tissue-specific DNA methylation signature seems to be quite stable [270,274] and changes in response to APO probably occur only in a few candidate regions.

## 2.3 APO stress-induced DMRs occur mainly in CHH context

To explore the dynamics of DNA methylation upon APO stress at specific loci, we determined differentially methylated regions (DMRs) in each sequence context (CG, CHG, and CHH, respectively). Due to the low variation in DNA methylation among samples of the same tissue type (Figure 16A), DMRs were obtained from comparisons between control and APO-treated samples for each tissue independently. In this way, we avoided selecting tissue-specific DMRs and increased the power of detection to obtain APO-dependent DMRs for each tissue, since memory related DMRs would be hard to identify in our low variation dataset.

We identified 6 CG and 4,205 CHH DMRs in shoots, and 51 CG and 2,353 CHH DMRs in roots. Hence, the majority of DMRs identified were in the asymmetric CHH context for both tissues and most of them were hypermethylated relative to the control samples (Figure 17 and Table 2). This is in line with our previous observation of an increase in global DNA methylation levels in APO-treated samples (Figure 16). Only very few DMRs were detected in the CG context and none in CHG. Overall, the longest stress treatment (primed condition) caused the most DNA methylation changes (Figure 17 and Table 2).

Because APO stress primarily affects methylation in the CHH context, we next focused on CHH DMRs. First, we selected and merged highly variable CHH DMRs filtered by a 15% methylation difference and a false discovery rate (FDR) <0.001.

This stringent filtering left us with 91 and 226 CHH DMRs in roots and shoots, respectively (Supplemental tables 2 and 3).

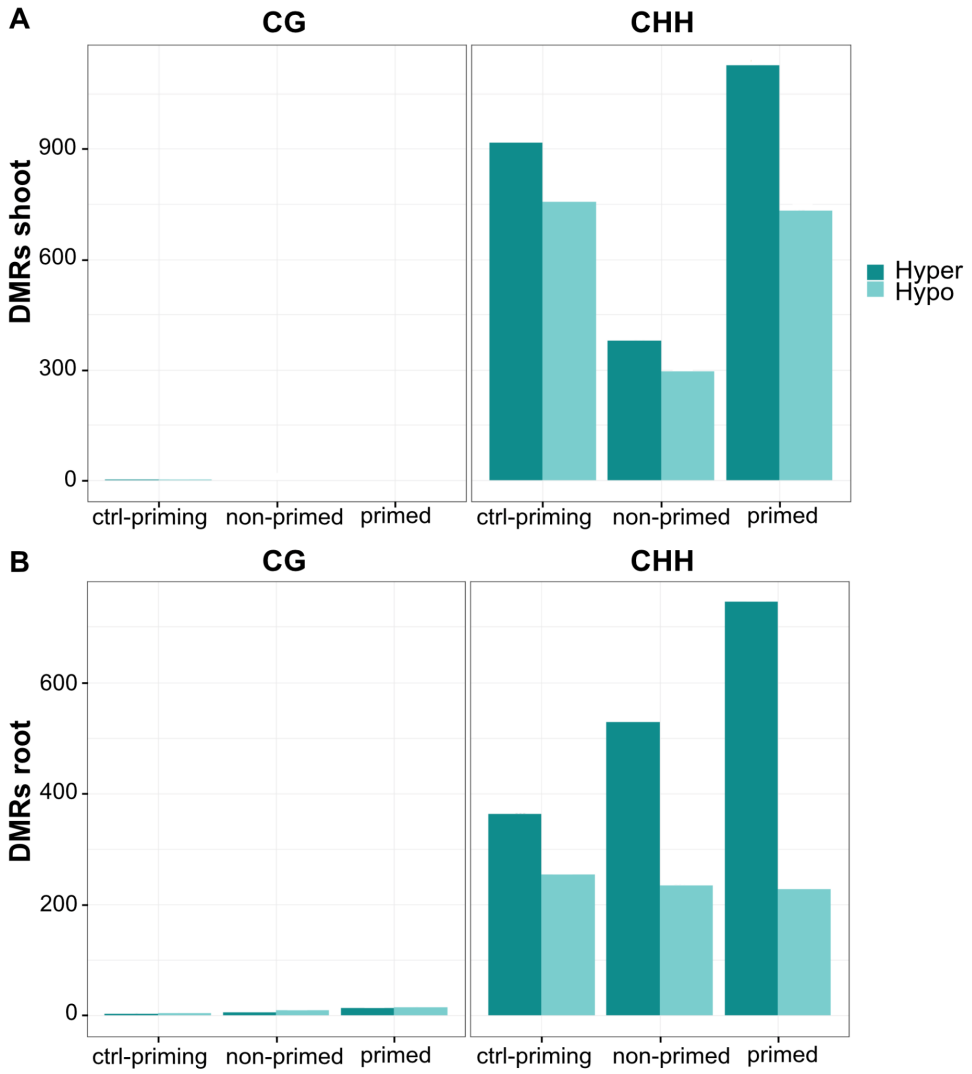


**Figure 17. APO stress-induced differentially methylated regions (DMRs) in *T. arvense*. A)** Amount of hyper and hypomethylated DMRs in shoot in CG and CHH contexts. **B)** Amount of hyper and hypomethylated DMRs in root tissues.

An analysis of mean methylation difference on these new DMRs datasets showed a clear cluster separation between control and APO-treated samples in roots, but not in shoots (Figure 18 and Figure 19). Roots are the tissue where APO is naturally perceived, we further focus on root DMRs to understand the epigenetic response to APO stress in *T. arvense*.

**Table 2.** Total number of hyper and hypomethylated DMRs in CG and CHH contexts in root and shoot samples.

| | CG | | CHH | |
|---|---|---|---|---|
| | Hyper | Hypo | Hyper | Hypo |
| **DMRs Shoot** | 4 | 2 | 2422 | 1783 |
| **DMRs Root** | 23 | 28 | 1637 | 716 |

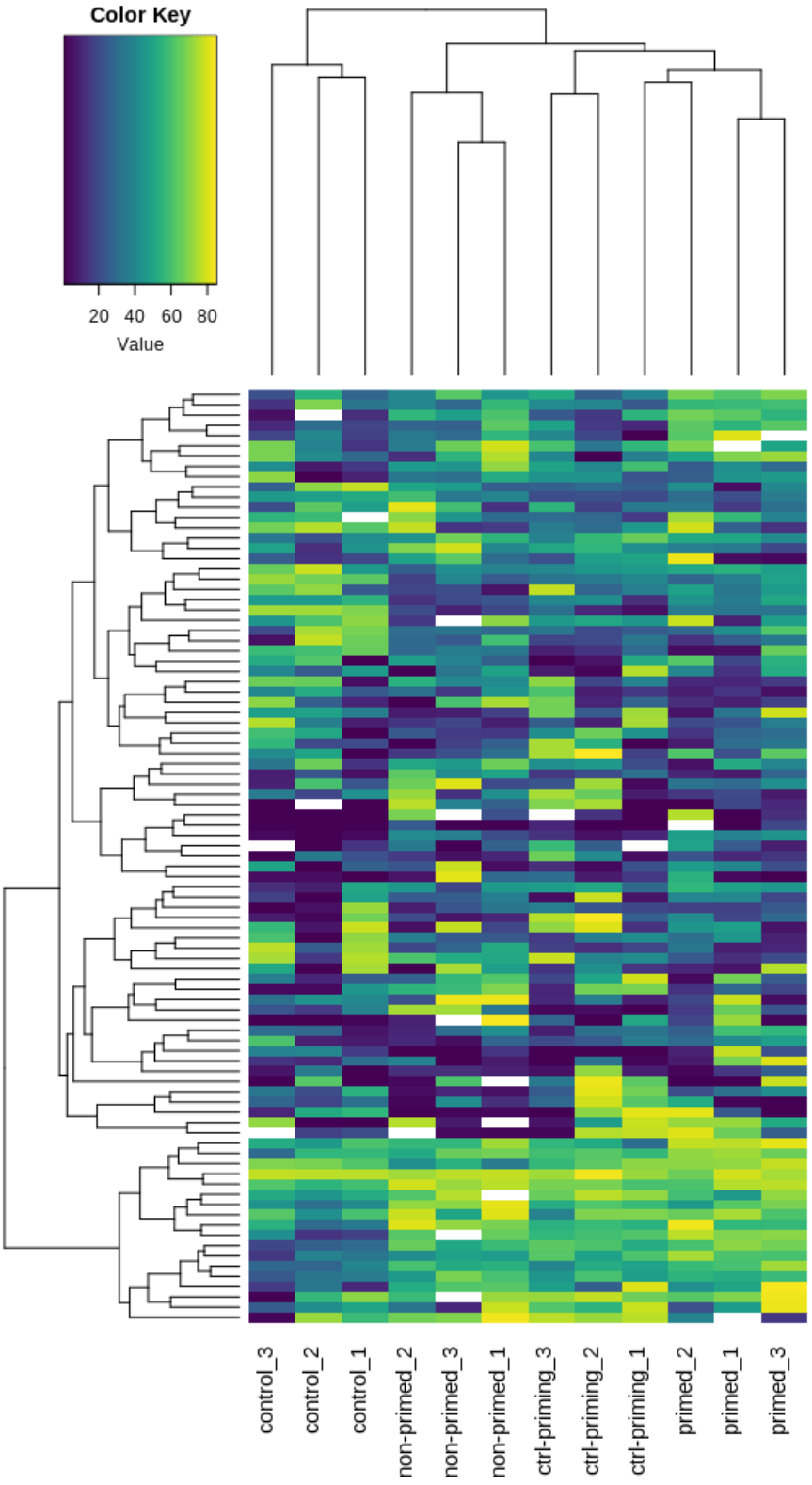


**Figure 18. APO stress-induced CHH DMRs in roots.** Heatmap of mean methylation level of filtered CHH DMRs (15% methylation difference, 0.001 FDR) in the three biological replicates of APO treated samples (non-primed, ctr-priming, primed) and control.

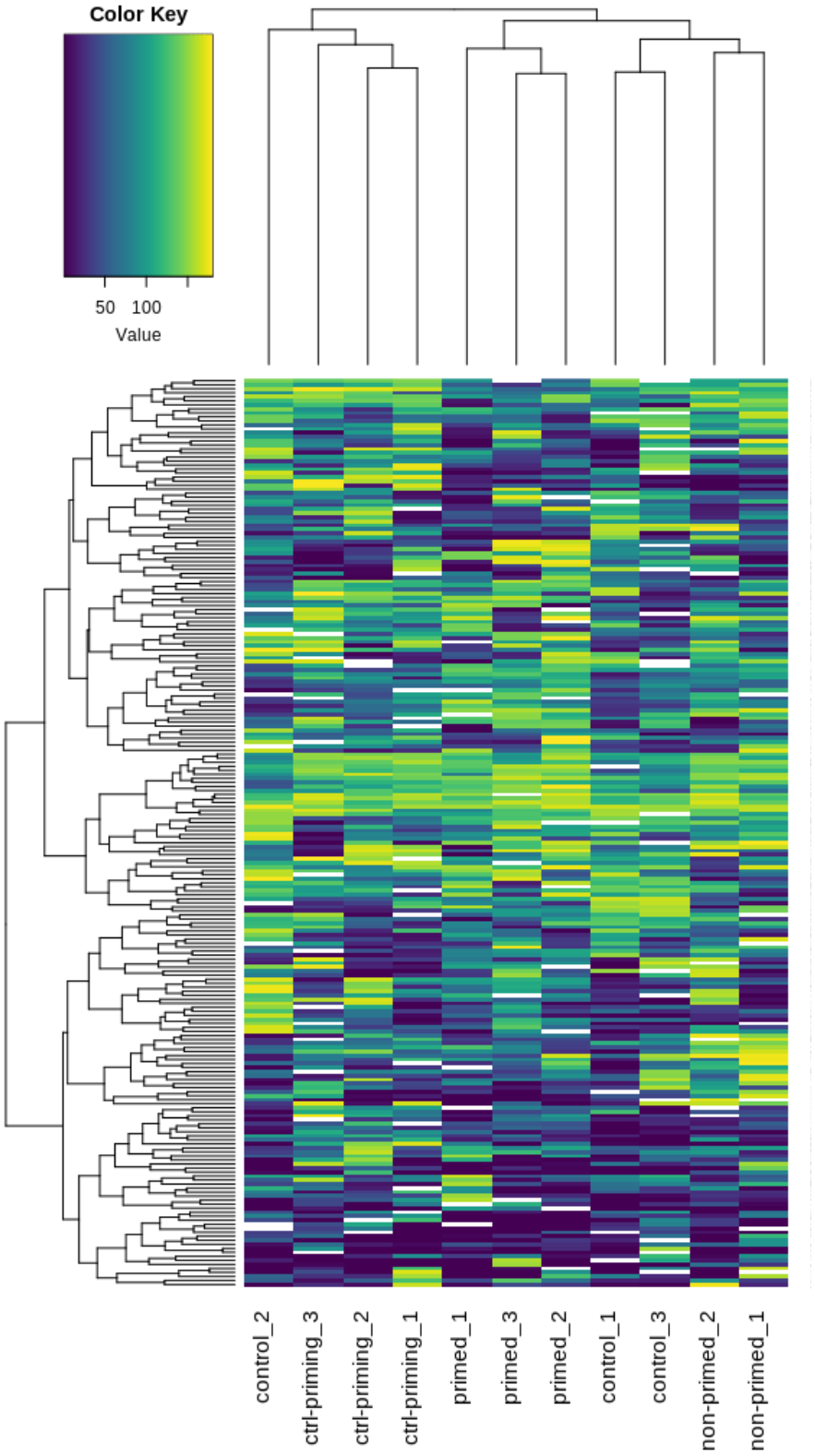


**Figure 19. APO stress-induced CHH DMRs in shoots.** Heatmap of mean methylation level of filtered CHH DMRs (15% methylation difference, 0.001 FDR) in the three biological replicates of APO treated samples (non-primed, ctrl-priming, primed) and control.

## 2.4 Candidate genes affected by APO stress

To better understand the potential functional role of the DMRs in APO stress response, we checked the root DMRs overlapping with TEs and gene promoters (defined as a 2 kb window). Our DMRs-genome intersection analysis yielded 58 candidate genes and 48 TEs in roots (Table 3 and Supplemental table 4). A functional annotation according to Arabidopsis orthologs revealed that many of these DMRs occur nearby genes related to cell growth and biotic/abiotic stress responses (Table 3). Examples are the Cyclin-dependent kinase A-1 (CDKA-1: Tarvense_01797, a core cell cycle regulator [275–277] and the B"BETA:Serin/threonine phosphatase 2A (Tarvense_14160), which is important in microtubule organization and cell elongation [278–281]. On the other hand, interesting stress related candidates included a subunit of the cytochrome *c* reductase complex (Tarvense_14345), important in oxidative stress [282,283], and the stress response regulator ERD7 (Tarvense_24043) [284−286].

To identify DMRs that generally affect the same set of genes, we searched for genes that appeared in all APO treatment conditions. No genes were shared between all APO stress conditions. However, three genes were shared between the long APO stress conditions; primed and non-primed (Table 3 and supplemental figure 5). Two of those genes encode for proteins of unknown function (Tarvense_08747 and Tarvense_14442), and one of them corresponds to the previously mentioned serine/threonine phosphatase 2A (Tarvense_14160), which is involved in microtubule arrangement and plays an important function in cell division and elongation [278–281]. The DMRs close to those genes varied between APO stress conditions. For Tarvense_08747 and Tarvense_14160 a slight increase in methylation was observed in all APO treated conditions with respect to control (Supplemental figure 6). In contrast, for Tarvense_14442 a slight decrease in methylation was observed in all APO treated conditions compared to control (Supplemental figure 6). All in all, our observations suggest that the epigenetic response to APO varies according to the duration and/or timing of the exposure to the chemical and point to interesting candidate genes which could mediate the APO stress response in *T. arvense*.

In conclusion, we observed that the allelochemical APO affects DNA methylation profiles in shoot and root tissues, with the CHH context being the most affected.

Additionally, we determine a small set of candidate genes that may be involved in the perception and response to APO stress in roots. Further investigation is needed to understand how these changes in DNA methylation affect gene expression and contribute to the APO growth inhibition related phenotype.

**Table 3.** Candidate genes and their putative functions according to Arabidopsis orthologs.

| Candidate gene | Gene ID | Ortholog | Putative funtion |
|---|---|---|---|
| PYRR Riboflavin biosynthesis protein PYRR, chloroplastic | Tarvense_01654 | AT3G47390 | Photooxidative damage |
| CDKA-1 Cyclin-dependent kinase A-1 | Tarvense_01797 | AT3G48750 | Cell cycle and allelopathy |
| Protein of unknown function | Tarvense_01871 | | |
| CID10:Polyadenylate-binding protein interacting protein 10 | Tarvense_01872 | AT3G49390 | RNA-binding protein |
| UPL7:E3 ubiquitin-proteinligase | Tarvense_02196 | AT3G53090 | Trichome development |
| UPL7:E3 ubiquitin-proteinligase | Tarvense_02197 | AT3G53090 | Trichome development |
| ARF:ADP-ribosylation factor 2 (O.sativa subsp japonica) | Tarvense_02957 | Os05g0489600 | GTP-binding protein involved in protein trafficking |
| DUF7:DUF724 domain containing protein 7 | Tarvense_02958 | AT3G62300 | DNA replication, transcription and chromatin remodeling |
| Protein of unknown function | Tarvense_04716 | | |
| ADK2: Adenylate kinase 3/ RCOM probable aspartylaminopeptidase | Tarvense_04810 | AT5G50370 | Adenylate kinase family protein |
| CIA1 protein | Tarvense_04954 | AT2G26060 | Embryo development and genome integrity |
| NDPK3: Nucleoside diphosphate kinase III; chloroplastic &mitochondrial | Tarvense_04958 | AT4G11010 | Oxidative stress |
| SPA2: Protein SPA1-Related 2 | Tarvense_04977 | AT4G11110 | Photomorphogenesis |
| AT4G00893 F-box protein | Tarvense_05081 | AT4G00893 | F-box/kelch-repeat protein |
| ENT5:Equilibrative nucleotide transporter 5 | Tarvense_05299 | AT4G05140 | Nucleoside transporter |
| AT2G29880 uncharachterized: Myb | Tarvense_05330 | AT2G29880 | Pollen germination and tube growth |
| LECRK44:L-type lectin-domain containing receptor kinase IV.4 | Tarvense_05442 | AT4G02420 | Auxin regulated gene |
| LECRK44:L-type lectin-domain containing receptor kinase IV.4 | Tarvense_05443 | AT4G02420 | Auxin regulated gene |

| | | | |
|---|---|---|---|
| WEB family protein | Tarvense_06021 | AT5G16730 | Microtubule-associated protein |
| SIED1: Protein salt-induced and EIN3/EI L1-dependent 1 | Tarvense_06867 | AT5G22270 | Salinity tolerance |
| AAE16: acyl-activating enzyme 16, chloroplastic | Tarvense_07911 | AT3G23790 | Lipid metabolisms |
| RPL29B:60S ribosomal protein L29-2 | Tarvense_08682 | AT3G06680 | Ribosomal L29e protein family involved in protein regulation |
| Unknown function | **Tarvense_08747** | | |
| AT5G01750 LURP-one-related 15 | Tarvense_09065 | AT5G01750 | Abiotic stress, root development |
| ARP1: RNA-binding protein | Tarvense_11448 | AT3G54770 | Seed germination under ABA or abiotic stress conditions |
| Unknown funcion | Tarvense_11555 | | |
| NPF5.2:NRT1/PTR Family 5.2 | Tarvense_13266 | AT5G46050 | Biotic and abiotic stress |
| XRI1 | Tarvense_13521 | AT5G48720 | Meiosis and gametogenesis |
| PHO1-H5 Phosphate transporter PHO1 homolog 5 | Tarvense_13605 | AT2G03240 | EXS (ERD1/XPR1/SYG1) family protein, stress |
| B"BETA: Serin/threonine protein phosphatase 2A regulatory subunit B"beta | **Tarvense_14160** | AT5G18580 | Microtubule array, cell orientation and elongation |
| QCR7-2 Cytochrome b-c1 complex subunit 7-2, mitochondrial | Tarvense_14345 | AT5G25450 | Development, biotic and abiotic stress, allelopathy |
| Protein of unknown function | **Tarvense_14442** | | |
| BASL:Breaking of asymmetry in the stomatal lineage | Tarvense_14526 | AT5G60880 | Assymetric cell division and stomatal development |
| MYB34: TF MYB34 | Tarvense_14527 | AT5G60890 | Tryptophan pathway |
| SRK6:Putative serine/threonine-protein kinase receptor (Brassica olareacea) | Tarvense_17158 | SRK6 | |
| MFDX2:Adrenodoxin-like protein 2, mitochondrial | Tarvense_17183 | AT4G21090 | Mithocondrial ferredoxin, redox metabolic pathways |
| DOGL3: Protein DOG1-like 3 | Tarvense_17409 | AT4G18690 | Seed dormancy |
| FTA: Protein farnesyltransferase/geranylgeranyltransferase type 1 subunit alpha | Tarvense_17829 | AT3G59380 | ABA stress response, drought, meristem and growth |
| AAE15:Long chain fatty acid (acyl-carier-protein) ligase AEE15, chloroplastic | Tarvense_18022 | AT4G14070 | Elongation of exogenous medium-chain fatty acids |

| | | | |
|---|---|---|---|
| MAPKKK20: Mitogen activated protein kinase kinase kinase 20 | Tarvense_18023 | AT3G50310 | Osmotic stress, cell division and cell elongation in the primary root |
| Protein of unknown function | Tarvense_18187 | | |
| Protein of unknown function | Tarvense_18306 | | |
| MKK3: Mitogen-activated protein kinase kinase 3 | Tarvense_18328 | AT5G40440 | Suggestive role in signaling during microtubule organization. |
| CYCB1-3: Cyclin B1-3 | Tarvense_18329 | AT3G11520 | Cell cycle |
| CAL1: Calmodulin (Medicago) | Tarvense_18729 | ATCAL1 | This is likely to be a pseudogene |
| Protein of unknown function | Tarvense_18766 | | |
| GLR2.8: Glutamate receptor 2.8 | Tarvense_19251 | AT2G29110 | Member of Putative ligand-gated ion channel subunit family |
| GLR2.9 Glutamate receptor 2.9 | Tarvense_19252 | AT2G29100 | Defense |
| F-box/LRR repeat protein | Tarvense_20374 | AT3G03360 | F-box/RNI-like superfamily protein involved in protein regulation |
| ALG11:GDP-Man:Man(3)GlcNAc(2)-PP_Dol alpha-1,2 mannosyltransferase | Tarvense_20375 | AT2G40190 | Cell-wall biosynthesis and abiotic stress response |
| ERD7: Early responsive to dehydration, chloroplastic | Tarvense_24043 | AT2G17840 | Abiotic stress responses |
| RNL: tRNA ligase 1 | Tarvense_24137 | AT1G07910 | Zygote division, auxin |
| GLR3.1 Glutamate receptor 3.1 | Tarvense_24138 | AT2G17260 | Involved in calcium-programmed stomatal closure. |
| THY-1: Bifunctional dihydrofolate reductase thymidylate synthase 1 | Tarvense_24256 | AT2G16370 | Synthesis of DNA precursors and some amino acids, seed development |
| Protein of unknown function | Tarvense_24594 | | |
| AT2G22730 probable sphingolipid transporter spinster homolog 3 | Tarvense_24719 | AT2G22730 | Major facilitator superfamily protein |
| NPY4:BTB/POZ domain containing protein NPY4 | Tarvense_24753 | AT2G23050 | Auxin-mediated organogenesis |
| AT1G64840: F-box/Kelch repeat protein A | Tarvense_24984 | AT1G64840 | Mitochondrial protein |

# DISCUSSION

## 1. A BX loss of synthesis mutant in hexaploid wheat generated by a non-transgenic TILLING approach

It is well known that polyploidy has a positive impact on several important agronomic traits. Not surprisingly, many of the world's most important crops are polyploid [287]. Yet, the generation of genomic tools for plant breeding of polyploid crops remains a substantial challenge. The major bottleneck is the often highly heterozygous genome of polyploid species, which makes mutant identification and generation harder and time consuming. Here, I have generated a BX loss-of-synthesis mutant in hexaploid bread wheat by combining mutations on the three different homoeologous *BX3* genes.

TILLING is an optimal approach to identify mutations at desired loci in polyploid species, because random point mutations caused by EMS treatment occur at a relatively high frequency regardless of the genome size [140]. Additionally, it might be preferred to other mutagenesis strategies because it can be applied to any species and does not rely on plant transformation, which is only available for a few plants and has variable success rates [145]. In fact, TILLING resources have been developed for a number of crops other than wheat [146,288–290], including rice, maize, barley, soybean, sorghum, potato, peanut, oat, and tomato [140]. In spite of that, to date, no TILLING variety has been released for commercialization.

Along with TILLING, targeted mutagenesis using CRISPR-Cas technologies has also proven to be very successful for gene editing of polyploid genomes. As opposed to TILLING, target mutagenesis is more precise, faster, and allows gene modification without any background mutations [145,291]. However, it presents other limitations such as off-target effects, loss of mutations in the next generation when only somatic tissues are modified, and legal constraints regarding its use in breeding programs [145,292], especially in countries where genome-edited plants are subjected to

GMO's legislation [293]. In contrast, the mutations generated by TILLING are stably inherited and non-transgenic, which makes TILLING a promising strategy for crop breeding in the future [288,294].

The main drawback of TILLING lies in the time it takes to obtain a candidate mutant. This of course depends on ploidy level, species generation time, and number of backcrosses needed to reduce undesired mutation load. For polyploid species, it is often necessary to combine mutations in the different homoeologs, because single gene mutations could be masked due to gene redundancy. Indeed, this is the case for BX synthesis homoeologous genes in hexaploid wheat [42]. Therefore, to obtain the *bx3* loss of synthesis mutant, it was necessary to combine, by crossing and selfing over three generations, all *BX3* individual mutations on the A, B and D genomes (Supplemental figure 1 and Figure 7B).

Although redundant, not all three BX homoeologs contribute equally to BX biosynthesis. Nomura et al. showed that BX homoeologs are differentially expressed and their translational products also differ in their catalytic properties. Overall, BX homoeologs of the B genome seemed to contribute the most to BX biosynthesis. Particularly for BX3 proteins, the highest catalytic activity comes from the BX3-A, followed by the BX3-B and D enzymes [42]. This explains why *BX3-ab* double mutants showed a higher reduction in DIMBOA and DIMBOA-glc production, compared to *BX3-bd* double mutants (Figure 7B). However, although small, the contribution of BX3-D enzyme is still necessary to reduce DIMBOA and DIMBOA-glc to undetectable levels (Figure 7B). Our results further confirm *in planta* the previously observed unequal contribution of BX homoeologs to BX biosynthesis.

Additionally, *bx3* mutants showed accumulation of intermediary compounds upstream of BX3 enzymatic reaction, such as indoline-2-one and tryptophan (Figure 7C). We did not detect free indole, which might be due to its channeling to tryptophan synthesis. These results were somehow expected, as interruption of metabolic pathways usually leads to accumulation and redirection of intermediary metabolites [295]. Similarly, accumulation of upstream intermediaries has been observed in maize BX deficient mutants and in transgenic Arabidopsis plants that

synthesize DIBOA-Glc [296]. However, the effect of the accumulation of these metabolites on plant physiology is not well understood. In transgenic Arabidopsis, indoline-2-one is phytotoxic and affects plant growth [296]. In contrast, *bx3* mutants in maize [296] and wheat (Figure 8 and supplemental Figure 2C) are not distinguishable from their WT counterparts. These could be due to a higher tolerance to indoline-2-one and a more efficient detoxification mechanism in plants that naturally synthesize BX.

As a matter of fact, indoline-2-one can be recognized as a xenobiotic and detoxified by several species across the plant kingdom. Detoxification occurs via hydroxylation at position C5 by P450s, followed by glycosylation to form indoline-2-one-5-O-*β*-D-glucopyranoside (5HIONG), which seems to be a stable storage compound [296]. It is likely that excess indoline-2-one is being detoxified through this mechanism in *bx3* mutants. This is supported by the lack of a phytotoxic phenotype in *bx3* plants (Figure 8). However, further identification of 5HIONG accumulation in our BX deficient lines is required to corroborate this hypothesis.

On the other hand, tryptophan accumulation could affect the metabolism of aromatic compounds, including auxins. This metabolic shift could impact plant growth and development. However, we did not observe any significant effect on plant growth on *bx3* mutants (Figure 8 and supplemental Figure 2C). Similarly, other studies in rice [297,298], potato [299], soybean [300], azuki bean [301] and Arabidopsis [302] have shown that overproduction of tryptophan in these species has only minor effects on the entire metabolome as well as on plant growth and development. These observations suggest that the flow from tryptophan into secondary metabolism is strictly regulated and intermediaries are effectively utilized. In future studies, it will be interesting to analyze the metabolome of *bx3* plants and determine if other physiological changes happen in these mutants.

So far, BX loss of synthesis mutants have only been reported in maize [18,24,25,44,296]. Here, I report the first BX mutant in hexaploid wheat. It is important to note that both independent *bx3* mutant lines behaved similarly in the phenotypes tested in this study. These give us confidence that our observations are due to *BX3* mutation and not other background mutations. Nonetheless,

backcrossing to WT to remove excess EMS mutations that might affect additional traits is needed. Currently, the *bx3* plants have been backcrossed to WT two times. It will be necessary to phenotype the backcrossed *bx3* lines to confirm my current observations.

## 2. Loss of BX does not affect biotic interactions in wheat

Plants adjust the synthesis of secondary metabolites to defend themselves under environmental pressure. Benzoxazinoids are a class of secondary metabolites, mainly found in grass species, that protect plants against a multitude of biotic stressors [100]. Several studies have addressed the toxicity of BX on different target species, including bacteria, fungi, herbivores and plants [30,303]. However, its toxic effect on wheat fungal pathogens and especially its potential allelopathic effect in ecological setups is still unclear and requires more investigation. Here, we investigated the role of BX on wheat defense to stem rust and blast diseases and its allelopathic potential against Arabidopsis in soil.

Several studies have addressed the role of BX in defense against fungal pathogens in cereals. Their association with disease resistance is not obvious, some pathogens are susceptible to BX, while others can tolerate or even be stimulated by BX[30,43]. Particularly, a link between BX and head blast disease caused by *M. oryzae* has not been reported so far. On the other hand, a few studies on wheat infected with *P. graminis* suggest that BX content confers protection to stem rust infection [304–306]. In our wheat infection experiments with *M. oryzae* (head blast) and *P. graminis* f.sp. *tritici* (stem rust), we did not observe an effect of BX on disease symptoms (Figure 9), suggesting that, for these fungal diseases, BX are not a prevalent defense mechanism. Although contradictory to previous BX susceptibility phenotypes in *P. graminis,* these observations might be due to a wide range of possible explanations.

For instance, it is possible that the wheat variety (Cadenza) we used does not produce the amount of BX in leaves necessary to inhibit *M. oryzae* and *P. graminis*. Indeed, previous studies have shown that BX content varies across wheat varieties

and that high BX content correlates with disease resistance [86,304,307–309]. Alternatively, the type of damage caused by the fungus during infection might affect the chemical state of BX in the plant, their concentration and hence their antifungal activity [305,310]. In line with this idea, detoxification could occur in *M. oryzae* and *P. graminis* similar to BX detoxification by other fungal species [311,312]. However, this scenario is less likely to occur in *P. graminis*, which has been shown to be susceptible to BX ([86,304,307,308]; [311]). Furthermore, BX content can be influenced by the environment [43]; It is therefore possible that in our controlled environmental conditions, production and release of BX are reduced. Further investigations are necessary to resolve the defensive role of BX against these fungal pathogens.

I also studied the allelopathic function of BX in wheat. BX have been previously described as allelochemicals based on their growth inhibitory effects under laboratory conditions and in the field [263,313]. Contrary to our expectation, we did not find clear evidence of allelopathy occurrence in our experimental setup (Figure 10 and 11). One reason might simply be related to the BX exudation capacity of our wheat variety. Previous studies have shown that DIMBOA exudation is variety-specific and that only a few varieties release considerable amounts of DIMBOA in their root exudates [29,79,308,314,315]. In addition, exudation not only depends on plant genotype but also on the identity and density of the competing weed species, as well as on the timing of plant exposure to competition [20–22,85]. It is therefore likely that Arabidopsis does not induce BX exudation because it is not a naturally occurring competitor, or because a higher density and/or earlier exposure is needed to induce allelopathy in wheat. Hence, it is necessary to check if cadenza exudes BX at a relevant concentration needed for plant growth inhibition and if so, to optimize our experimental design.

Additionally, It is important to note that, while most studies on BX inhibitory effects were done with crude extracts *in vitro*, or were observed as a consequence of BX accumulation in soil (also known as plant soil feedback effects, PSF) [23,27,316,317], we used a plant-plant competition strategy. This is relevant because, even if cadenza exudes good amounts of BX and accumulation in soil reaches inhibitory levels, the compounds might not be as biodisponible for

Arabidopsis in our system as they are in an *in-vitro* experiment. This could happen for several reasons. For instance, compound stability might be affected by abiotic factors or simply be degraded through microbial activity or adhering to soil particles that immobilize them [318–320]. In such a scenario, Arabidopsis would most likely face low concentrations of BX and detoxification of the residual amounts might account for the lack of allelopathic effects. Previous studies have demonstrated that Arabidopsis is able to detoxify BX via o-glycosylation, most likely requiring the sequential action of cytochrome P450 and UDP-glucosyltransferase activities [80,321]. Yet, this detoxification mechanism may be useful to some extent, as higher concentrations of DIMBOA, DIBOA and its derivative products are still phytotoxic to Arabidopsis [38,81].

Another factor that comes into play in our plant-plant interaction scenario is resource competition. In fact, I believe that the reduced growth effect I observed in Arabidopsis when growing it together with wheat (Figure 10 and 11) is mainly due to resource competition. Differentiating between resource competition and allelopathy is very challenging, as both are probably integrated. One way to distinguish between these two phenomena is by exploring the dependency between plant density and allelopathy [322,323]. Accordingly, Weidenhamer et al. showed that density-dependent growth response occurs in Bahiagrass at low concentrations of gallic acid and hydroquinone allelochemicals, but not at high concentrations, suggesting that resource competition is important until strong suppressing effects of the chemical occur [322]. It would be interesting to explore the density dependency to allelopathic induction in our biological setup to disentangle these two factors.

Demonstrating the occurrence of allelopathy in natural conditions is not trivial and has proven to be rather challenging [316,317]. This is in part due to the difficulty in designing experiments that disentangle the contribution of other environmental factors to plant-plant interaction. Experimental approaches that use contrasting plant genotypes that differ in their allelochemical production are good strategies to tackle this problem, nonetheless this type of approaches are still rare [324]. We think that further optimization of our experimental design could help to understand allelopathic interactions in natural environments.

# 3. The BX-derived compound APO impairs the epigenome and affects stress-related genes in *T. arvense*

Epigenetic changes play an important role in regulating stress responses in plants. Particularly, DNA methylation has been implicated in the response to several biotic and abiotic stresses in different plant species [156,185,189]. However, the epigenetic response to allelopathic compounds has not been explored yet. Here, we investigated the effect of the BX-derived allelochemical APO on DNA methylation at the genome-wide level in *T. arvense*.

Genome-wide, DNA methylation in *T. arvense* is structured similarly to other Brassicaceae in the three different sequence contexts, with higher methylation in CG, followed by CHG and CHH (Figure 14) [175,248]. This context-dependent methylation difference might be explained by the different DNA methylation maintenance mechanisms that in part account for their stability [155,157]. Additionally, as observed in other plant species [175], DNA methylation in *T. arvense* was unevenly distributed across different genomic features, with TEs and intergenic regions harboring the higher levels of DNA methylation, particularly in CG context (Figure 15) [248].

On the other hand, gene body methylation, which is a common feature of constitutively expressed housekeeping genes in other species [175]; [163,325], seemed to be depleted in *T. arvense*. Similar lack of gbM has been observed in other Brassicaceae, in particular in the close relative *Eutrema salsugineum [175,269],* which suggest that gbM loss occurred before the speciation between *T. arvense* and *E. salsugineum* [248]. Previous studies have associated the loss of gbM with mutation in the *CHROMOMETHYLTRANSFERASE 3 (CMT3)* gene *[269].* However, whether *CMT3* mutation accounts for the loss of gbM in *T. arvense* is unknown. A recent study analyzed the epigenomes of more than 200 *T. arvense* accessions and did not find any variant in proximity to *CMT3* associated with variation in the number of gbM genes. Instead, a genome wide association (GWA) pick was found closeby the uncharacterized gene *LOG2-LIKE UBIQUITIN LIGASE3* (*LUL3*), which could account for gbM variation [250,326,327]. Overall, these findings support the well-established role of DNA methylation in regulating gene transcription and TE

silencing and show that gbM in *T. arvense* differs from most previously studied plant species.

After having established a clear genome-wide DNA methylation pattern, I proceeded to analyze global DNA methylation changes upon APO treatment in *T. arvense* root and shoot tissues. Interestingly, most variation in global DNA methylation was explained by tissue type (Figure 16A), and only a small fraction of the variation was observed between control and APO-treated samples (Figure 16B). Epigenetic differences between roots and shoots have been found in other plant species [270–272,328,329]. These differences might be involved in regulating distinct developmental and environmental transcriptional responses in a tissue-specific manner [270,272]. Because most variation was observed between tissues, this indicates that the overall tissue-specific DNA methylation signature is quite stable [270,274]. Similarly, Seymour et al. observed that DNA methylation is more affected by tissue type than by environmental differences in 3 Brassicaceae species [270]. These observations suggest that, although DNA methylation is a mark associated with stress responses, the changes in response to environmental perturbations, and specifically to APO, must be local, probably occurring only on a few targeted genes related to the stress response.

While genome-wide I only observed slight variations between control and APO treated samples, I detected extensive differences at specific loci when investigating DMRs, especially in the CHH context (Figure 17 and table 2). This is in agreement with previous studies that described CHH methylation as the most dynamic mark in response to the environment [187,330]. For *T. arvense*, climate was found to be a strong predictor of CHH methylation variation in natural populations [250]. In addition, global changes in CHH DNA methylation have been observed in response to various abiotic and biotic stresses in different plant species [190–194,203]. However, a clear pattern in the response of DNA methylation to stress does not seem to exist; some stress signals causes DNA hypermethylation [194,196,203], while others are characterized by a hypomethylated state [190–194,331]. In particular, for the case of APO-induced stress in *T. arvense*, we observed more hypermethylated DMRs in both tissues across the different stress treatments (Figure 17). This suggests that DNA hypermethylation might be a specific APO stress

response in *T. arvense*. Whether this response is maintained in longer stress periods or if it is stable enough to give rise to epigenetic plant memory remains to be tested. Here, we did not find evidence of somatic epigenetic memory. However, this might be a limitation of our experimental design, which allowed for only a short stress exposure.

From our DMRs analysis, we found several DMRs close to genes with predicted functions in stress response, cell growth and plant development (Table 3). Some of the interesting candidate genes were Tarvense_01797, Tarvense_14345, Tarvense_24043, and Tarvense_14160. Previous studies in Arabidopsis have shown that the expression of the Arabidopsis ortholog of Tarvense_01797, AT3G48750, which encodes for a Cyclin-dependent kinase A-1 (CDKA-1), is affected upon exposure to allelochemicals from apple [332]. Similarly, the Arabidopsis ortholog of Tarvense_14345, AT5G25450, which encodes for a Ubiquinol–cytochrome *c* reductase subunit, has been shown to be induced in response to buckwheat allelochemicals [333]. Here, we found that DNA methylation changes occur in the neighboring region of these genes upon APO treatment in *T. arvense*, suggesting that epigenetic modifications might be involved in the transcriptional stress response to allelochemicals. In accordance with this, the expression of AT2G17840, the Arabidopsis ortholog of Tarvense_24043, which is also a stress related gene in Arabidopsis and *T. arvense* [286], is downregulated upon application of histone deacetylase and DNA methyltransferase inhibitors [334]. In addition, Tarvense_14160 (AT5G18580), which was shared between the long APO stress conditions (primed and non-primed), seems to be important for plant growth and development along with other candidates (AT4G11110, AT2G29880, AT3G50310, AT3G11520 and AT2G26060) found in our dataset [335,336]). All in all, we identified DNA methylation changes in candidate genes important for stress response as well as for plant growth and development, which could be related to the APO growth inhibition phenotype.

# CONCLUSION

In summary, this study reports the first BX loss of synthesis mutant generated by TILLING technology in wheat. We found that the interruption of BX synthesis in *bx3* mutants leads to accumulation of upstream intermediary compounds without any striking effect in plant phenotype, indicating that intermediaries are effectively utilized and/or detoxified in wheat. Additionally, by making use of this new genetic resource, we determined that BX does not affect allelopathic interactions and plant defense of wheat in our biological setup. Further experimental research, in particular to optimize allelopathic experimental designs and to study the defense responses to other pathogens in wheat, is necessary to corroborate these observations. The wheat genetic material generated in this study will facilitate future research on BX biological functions in this highly relevant crop.

On the other hand, this study also provides new insights into the molecular role of the BX derived allelochemical APO at the epigenomic level. Here, we observed global DNA methylation changes, particularly in the CHH context, in *T. arvense* under APO stress. Our data also revealed local changes in DNA methylation proximal to genes with potential implication in APO stress response. Further studies will determine the functional implication of DNA methylation on these candidate genes. Over the last few years, efforts have been undertaken to develop *T*. *arvense* into a new model organism and a biofuel and winter cash cover crop [248,337,338]; thus, any insights into the molecular bases of environmental stress response in *T. arvense* would be of great value for this translational research.

# SUPPLEMENTARY MATERIALS

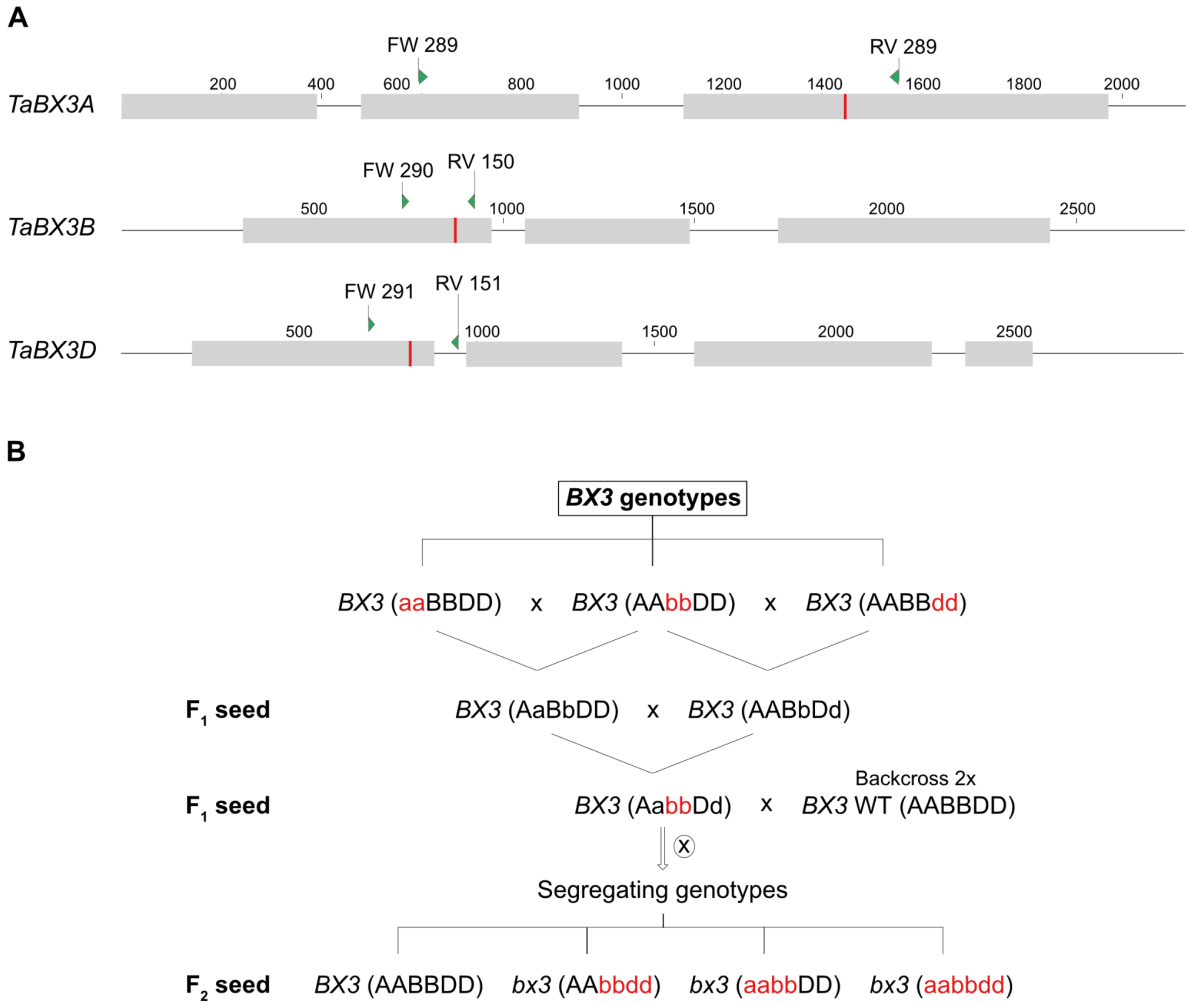


**Supplemental figure 1. Generation of *bx3* mutant using wheat TILLING lines. A)** Schematic representation of the *BX3* homeologous genes in wheat. Gray boxes represent exons and the red lines indicate the position of the mutation on the TILLIN lines used to generate *bx3* mutants. Primer pairs used for genotyping are indicated as green arrows. **B)** Crossing scheme between the three single homozygous mutant lines and genotypes selected on each generation to obtain triple homozygous *bx3* mutants. From the F1 segregant population, plants with the AabbDd genotype were self-pollinated to produce *bx3* mutant lines and other segregating genotypes including wild type (WT), as well as backcrossed to (WT) to clean any background mutations. Self-pollination is represented by an X inside a circle.

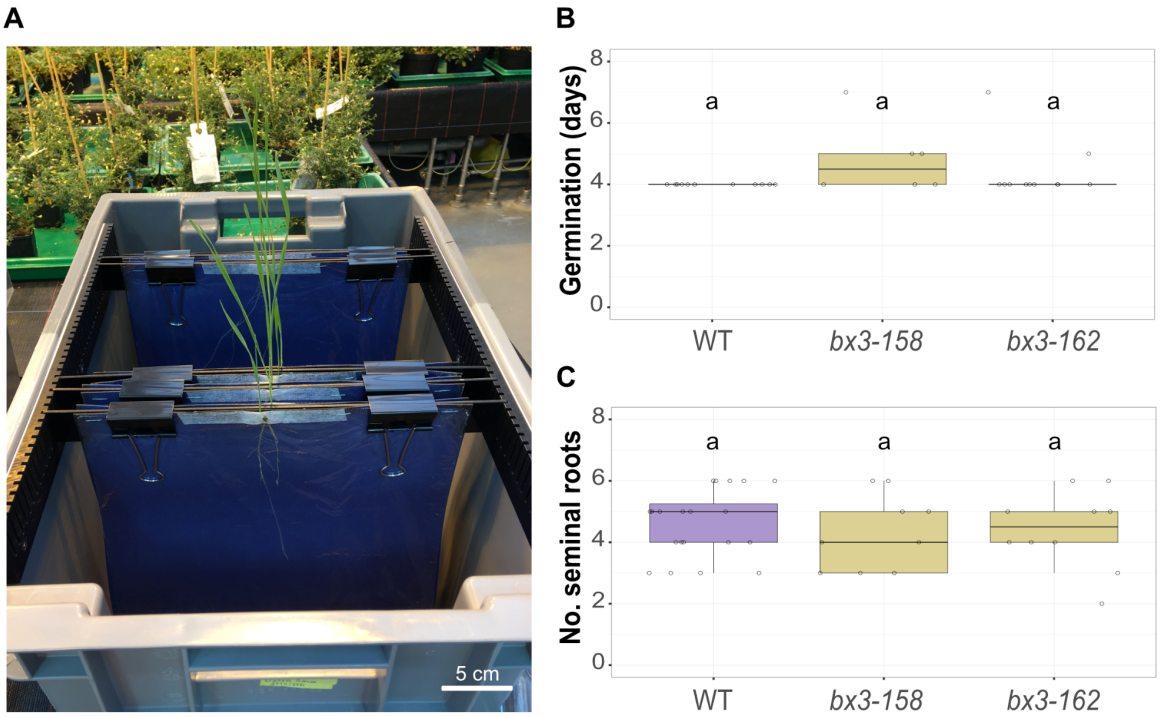


**Supplemental figure 2. Plant phenotyping of wheat seedlings. A)** Picture of the plant phenotyping system. Two filter papers (blue) are stacked together in a rack box filled with 5 L of half-strength Hoagland nutrient solution. Seeds are taped to the top of the filter paper. The root growth area is covered with a black foil (in the picture a transparent foil was used for visualization of the roots). **B)** Germination time of wild type (WT) and *bx3* wheat mutants (*bx3-158* and *bx3-162*). **C)** Number of seminal roots in 2.5-week-old wheat WT and *bx3* mutants (*bx3-158* and *bx3-162*). Circles indicate biological replicates [**A)** n = 7-12 and **B)** n = 9-20]. Different letters indicate different statistical groups (ANOVA, posthoc Tukey, $p \leq 0.05$).

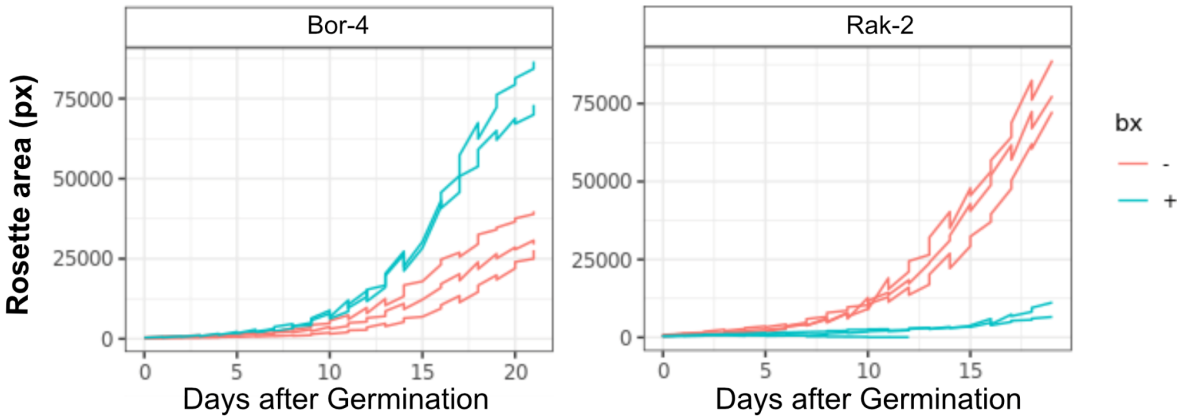


**Supplemental figure 3. Arabidopsis growth in benzoxazinoid-conditioned soil.** Temporal dynamics of rosette growth of the Arabidopsis accessions Bor-4 (left) and Rak-2 (right) growth on conditioned maize wild type (blue) and *bx1* mutant (red) soil. Data from an independent experiment by Dr. Niklas Schandry et al. unpublished.

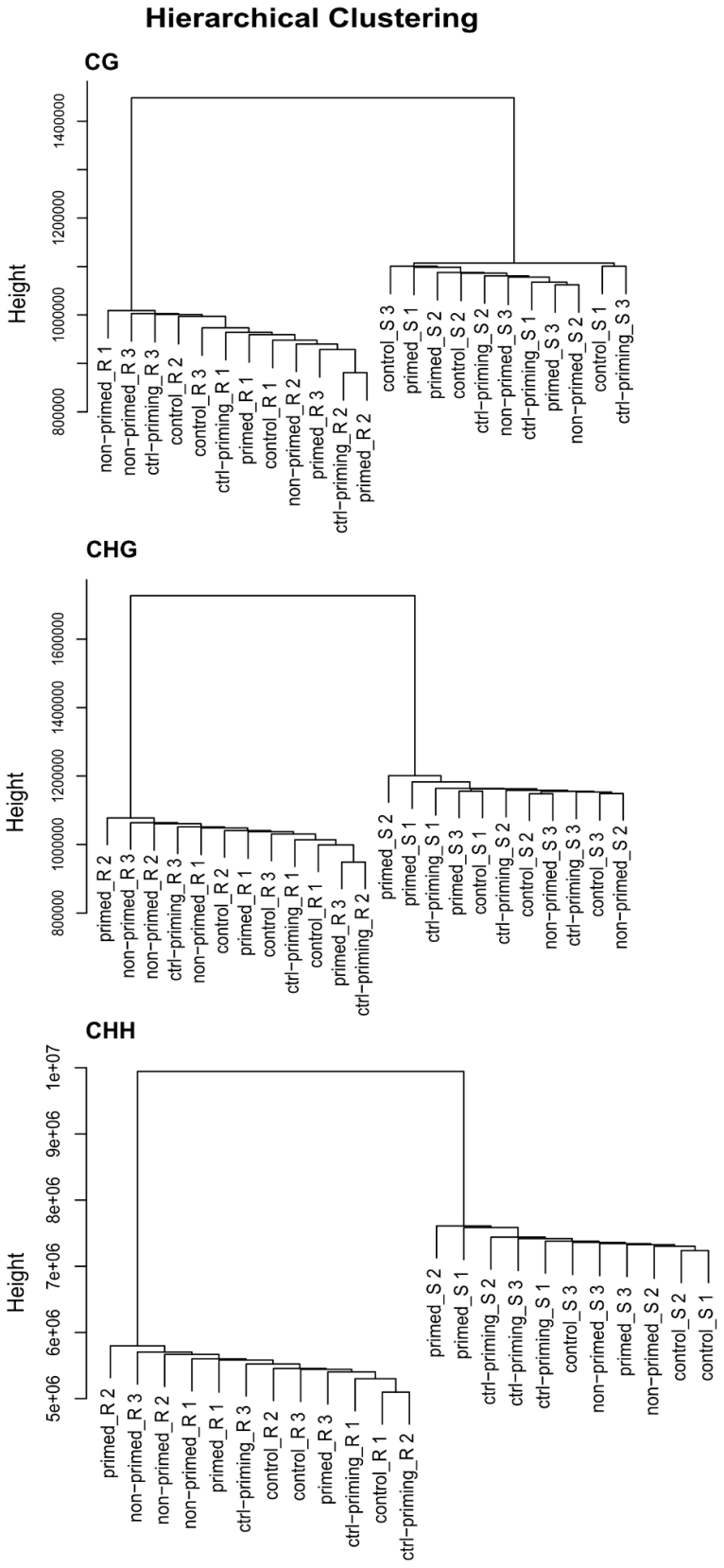


**Supplemental figure 4. Dynamics on DNA methylation in stress samples.** Hierarchical clustering on global levels of DNA methylation by sequence context in APO-treated and

control samples. The two main clusters correspond to root (R) and shoot (S) samples. The three biological replicates on each condition are enumerated from 1 to 3.

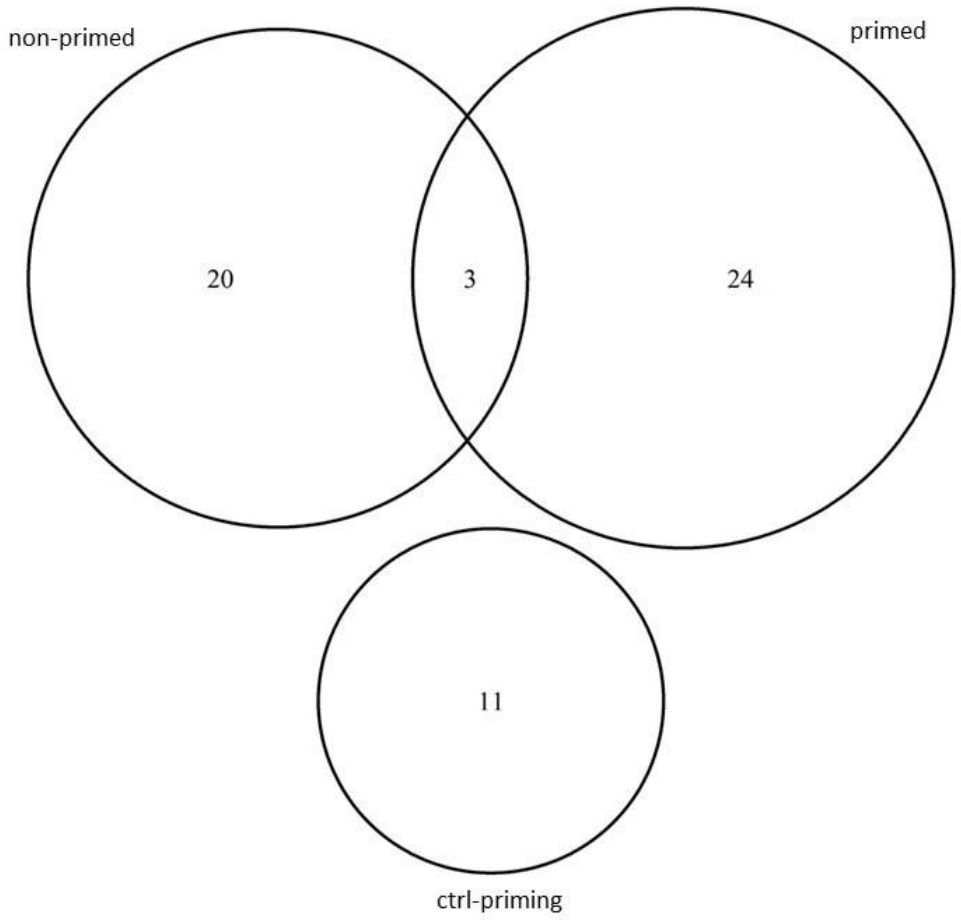


**Supplemental figure 5. Shared APO stress-response candidate genes.** Venn diagram of candidate genes separated by APO treatment condition. Note that only 3 genes are shared between the long APO treatment conditions “primed” and “non-primed”.

**Tarvense_08747**

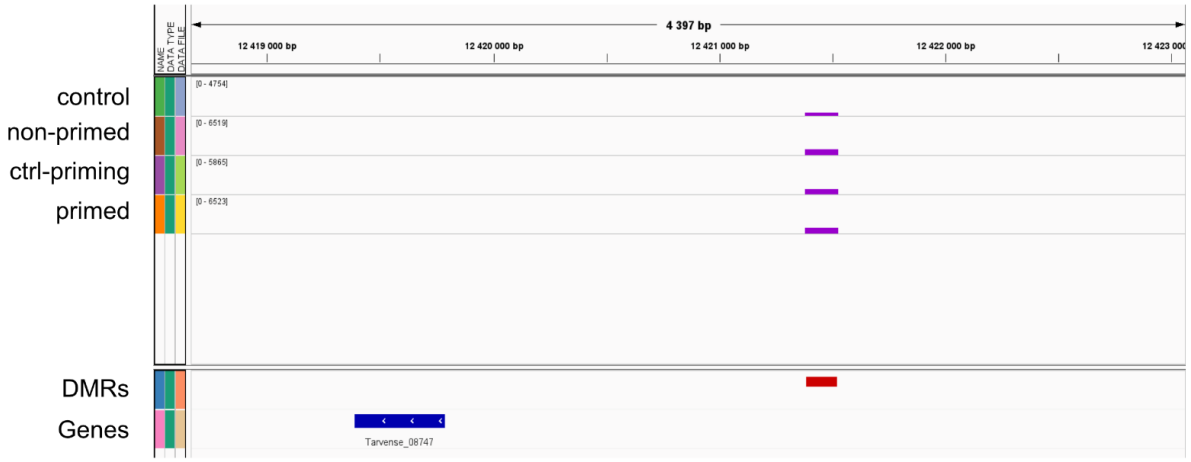


**Tarvense_14442**

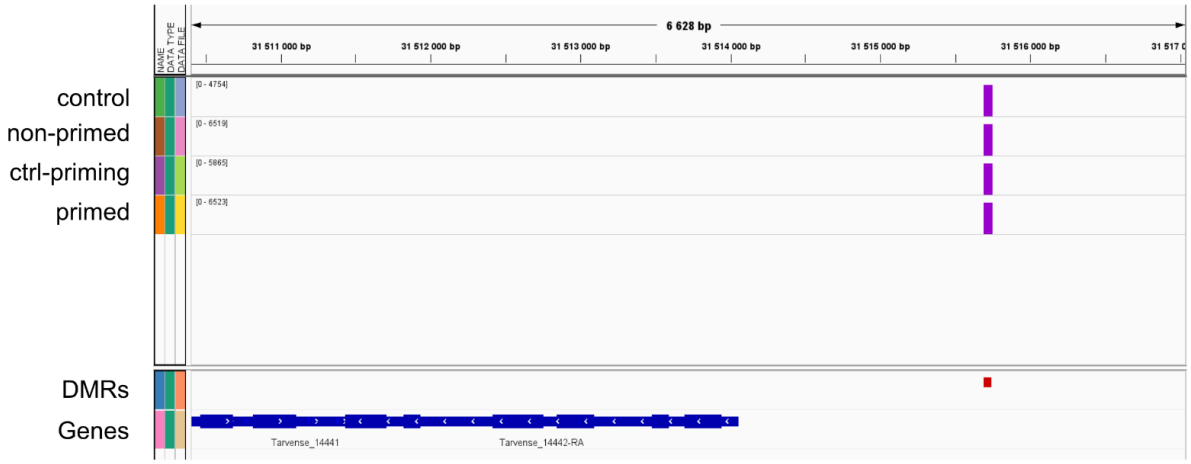


**Tarvense_14160**

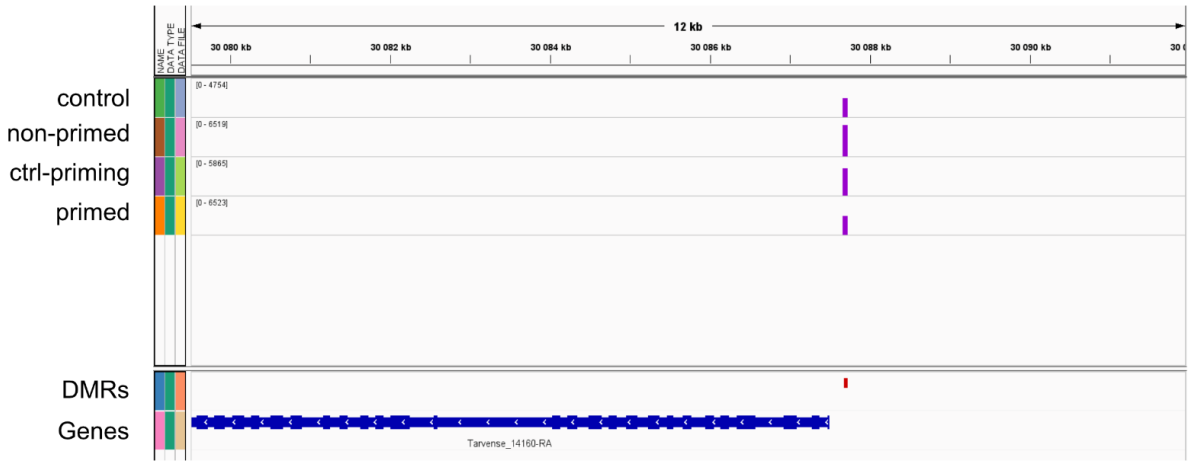


**Supplemental figure 6. Root DMRs close to candidate genes.** Genome browser view (igv) of DMRs (display in red) located in promoter regions of three candidate genes (Tarvense_08747, Tarvense_14442 and Tarvense_14160) shown in blue in each panel on the bottom. Average methylation for each condition (control, non-primed, ctrl-priming and primed) is displayed as purple bars.

**Supplemental Table 1.** List of primer pairs used for genotyping wheat TILLING lines during crossing.

| Gene | Primer No. | Primer name | Primer sequence (5´→ 3´) | Tm (°C) | Fragment size (bp) | SNP WT | SNP mutant |
|---|---|---|---|---|---|---|---|
| ***BX3* A** | 529 | FW 289 | AGAATCCCACCGCAAGGAAG | 64.6 | 962 | tgG | tgA |
| | 530 | RV 289 | GAACCCAAATGGCAGGAACC | | | | |
| ***BX3* B** | 531 | FW 290 | CCGTACCCACCTTGTTCGTG | 64.8 | 265 | tGg | tAg |
| | 263 | RV 150 | TGAGCATATGCGTGGTTAAC | | | | |
| ***BX3* D** | 532 | FW 291 | TGCGTACCCACGACCAAATC | 63.3 | 255 | tgG | tgA |
| | 265 | RV 151 | TCAGATGATGAGTGACGGACTA | | | | |

**Supplemental Table 2.** List of filtered DMRs in roots of APO-treated samples (np:non-primed,cp: ctrl-priming, p: primed) and control (c). Chromosomal DMR position is indicated (chr:start-end) and methylation level is shown for each biological replicate (3).

| DMR | chrom | start | end | c_1 | c_2 | c_3 | np_1 | np_2 | np_3 | cp_1 | cp_2 | cp_3 | p_1 | p_2 | p_3 |
|---|---|---|---|---|---|---|---|---|---|---|---|---|---|---|---|
| 1 | Chr1 | 8632 | 8663 | 0 | 0 | 0 | 0 | 20 | 0 | 0 | 0 | 14 | 0 | NA | 18 |
| 2 | Chr1 | 4854138 | 4854191 | 3,21429 | 2,28571 | 3,14286 | 3,71429 | 0 | 25,42857 | 7,57143 | 0,57143 | 12,14286 | 16,85714 | 28,07143 | 4,5 |
| 3 | Chr1 | 5087593 | 5087615 | 16,71429 | 32,14286 | 29,85714 | 11,42857 | 0 | 0 | 0 | 0 | 0 | 8,28571 | 14,16667 | 18,71429 |
| 4 | Chr1 | 6382770 | 6382807 | 23,1 | 15,1 | 24,2 | 11 | 1,1 | 3,7 | 5 | 8,1 | 2,9 | 1,5 | 4 | 0 |
| 5 | Chr1 | 31432950 | 31433006 | 10,17647 | 19,36364 | 10,75 | 30,72222 | 45,66667 | 29,66667 | 21,72222 | 15,66667 | 15,44444 | 12,94118 | 15 | 21,625 |
| 6 | Chr1 | 31529382 | 31529448 | 21,9375 | 21,25 | 19,625 | 38,25 | 46,875 | 37,1875 | 41,875 | 46,9375 | 56,26667 | 55 | 48,5 | 50,75 |
| 7 | Chr1 | 33667677 | 33667797 | 11 | 25,27273 | 25,54545 | 28,63636 | 13,27273 | 25,09091 | 22,5 | 19,63636 | 12,27273 | 43,18182 | 22,81818 | 41,09091 |
| 8 | Chr1 | 35159639 | 35159812 | 5,34286 | 5,375 | 5,42857 | 24,1 | 23,03333 | 27,58621 | 21,11111 | 12,05714 | 12,6 | 10,42857 | 10,48387 | 5,71429 |

| | | | | | | | | | | | | | | | |
|---|---|---|---|---|---|---|---|---|---|---|---|---|---|---|---|
| 9 | Chr1 | 35822156 | 35822183 | 0 | 4,4 | 5,7 | 11,7 | 2,3 | 13,9 | 3 | 5,1 | 3,2 | 21,5 | 18,5 | 22,5 |
| 10 | Chr1 | 37653033 | 37653085 | 63 | 44 | 0 | 57 | 41 | NA | 58 | 76 | 70 | 50 | 50 | 88 |
| 11 | Chr1 | 41215802 | 41215869 | 44 | 33,5 | 56,5 | 75,5 | 80 | 36,5 | 62,5 | 57,5 | 25 | 61,5 | 53 | 45 |
| 12 | Chr1 | 47402810 | 47402897 | 30,5 | 33,16667 | 21,64286 | 7,92857 | 24,07143 | 11,07143 | 8,57143 | 4,64286 | 5,33333 | 34,25 | 21,5 | 8 |
| 13 | Chr1 | 50734663 | 50734696 | 20,15385 | 0 | 39,30769 | 1,07692 | 2,15385 | 8,61538 | 17 | 1 | 14,66667 | 27,53846 | 32,38462 | 18,30769 |
| 14 | Chr2 | 13301652 | 13301703 | 23,38462 | 7 | 14,92308 | 36,75 | 29 | 23,69231 | 18,38462 | 22,38462 | 28,30769 | 42,41667 | 43,61538 | 43,53846 |
| 15 | Chr2 | 27910281 | 27910325 | 12,7 | 0 | 7 | 32,9 | 24,5 | 25,3 | 17,4 | 26,6 | 31 | 3,7 | 22,8 | 34,4 |
| 16 | Chr2 | 28626401 | 28626444 | 6,8 | 8,6 | 2,7 | 20,5 | 23,33333 | 25,4 | 19,2 | 14,9 | 22,7 | 29,7 | 23,6 | 46,6 |
| 17 | Chr2 | 32765806 | 32765941 | 32,55556 | 16,05 | 26,6 | 1,72222 | 1,4 | 10,85 | 6,2 | 8,5 | 19 | 23,25 | 20,6 | 31,75 |
| 18 | Chr2 | 33075609 | 33075658 | 31,92308 | 34,84615 | 41,76923 | NA | 44,07692 | 75,92308 | 66,23077 | 74,15385 | 59,4 | 32,53846 | 46,61538 | 52,38462 |

| | | | | | | | | | | | | | | | |
|---|---|---|---|---|---|---|---|---|---|---|---|---|---|---|---|
| 19 | Chr2 | 33139150 | 33139230 | 63 | 50 | 33 | 50 | 16 | NA | 30 | 33 | 33 | 14 | 88 | 35 |
| 20 | Chr2 | 33417120 | 33417165 | 27 | 16,66667 | 26,71429 | 34,28571 | 32 | 55,16667 | 51,71429 | 43,14286 | 25 | 36,14286 | 39,14286 | 31 |
| 21 | Chr2 | 34855287 | 34855416 | 6,86667 | 8 | 7,9 | 12,03333 | 19,8 | 10,7 | 11,86667 | 11,43333 | 20,86667 | 24,66667 | 25,86207 | 23,73333 |
| 22 | Chr2 | 37028499 | 37028557 | 8,15 | 2,38462 | 9,85 | 32,85 | 17,75 | 23,05 | 15,4 | 11,65 | 15,95 | 13,55 | 24,7 | 13,5 |
| 23 | Chr2 | 37840431 | 37840489 | 17 | 32,5 | 18,5 | 35 | 25 | 25 | 0 | 14,5 | 28 | 9 | 50 | NA |
| 24 | Chr2 | 40687865 | 40687940 | 1,77778 | 0 | 1,55556 | 14 | 3 | 27,66667 | 12,66667 | 1,77778 | 14,77778 | 27,22222 | 32,5 | 32,22222 |
| 25 | Chr2 | 44438131 | 44438243 | 20,66667 | 40,44444 | 20 | 28,88889 | 29,5 | 51,2 | 25,2 | 17 | 38,22222 | 46,55556 | 59,66667 | 51,88889 |
| 26 | Chr3 | 5637365 | 5637430 | 2,75 | 4,9 | 3,3 | 28,8 | 24 | 13,4 | 14 | 11 | 5 | 16,88889 | 12,66667 | 12 |
| 27 | Chr3 | 24082052 | 24082086 | 28 | 14 | 38 | 27 | 52 | 9 | 28 | 40 | 38 | 25 | 26 | 18 |
| 28 | Chr3 | 27361352 | 27361422 | 3,26667 | 6,26667 | 2,8 | 11,13333 | 9,66667 | 5,44444 | 23,33333 | 13,86667 | 4,4 | 17,6 | 24,93333 | 22,53333 |

| | | | | | | | | | | | | | | | |
|---|---|---|---|---|---|---|---|---|---|---|---|---|---|---|---|
| 29 | Chr3 | 31467038 | 31467090 | NA | 47,08333 | 48 | 20,66667 | 52,27273 | 32,75 | 14,75 | 18,83333 | 20,41667 | 42,25 | 7,5 | 26,5 |
| 30 | Chr4 | 1065082 | 1065113 | 5,3 | 6,9 | 7,8 | 18 | 16,7 | 28,3 | 25,3 | 21,3 | 21,3 | 27,2 | 23,5 | 36 |
| 31 | Chr4 | 12421385 | 12421524 | 0 | 3,33333 | 10,28571 | 10,85714 | 14 | 11,42857 | 12,42857 | 6,28571 | 11,14286 | 17,42857 | 10 | 21,14286 |
| 32 | Chr4 | 14503989 | 14504020 | 25,53846 | 39,22222 | 34,30769 | 11,92308 | 12,69231 | 10,61538 | 7,38462 | 16,92308 | 6,66667 | 23,61538 | 11,76923 | 7,46154 |
| 33 | Chr4 | 32748817 | 32748956 | 11,125 | 12,40625 | 5,9375 | 20,15625 | 13,3871 | 10,125 | 23,34375 | 16,90625 | 16,8125 | 29,03125 | 23,71429 | 35 |
| 34 | Chr5 | 4586921 | 4586964 | 21 | 33 | 62 | 60 | 14 | 42 | 25 | 0 | 28 | 50 | 37 | 53 |
| 35 | Chr5 | 9023591 | 9023620 | 48,4 | 60,2 | 62,5 | 24,8 | 30,8 | 40,85714 | 64,8 | 48,8 | 40,9 | 57,2 | 67,4 | 63,4 |
| 36 | Chr5 | 9122774 | 9122819 | 18 | 16 | 5 | 20 | 0 | 14 | 0 | 4 | 8 | 23 | 12 | 25 |
| 37 | Chr5 | 16735122 | 16735232 | 0 | 57 | 42 | 20 | 37 | 28 | 40 | 10 | 0 | 18 | 50 | 40 |
| 38 | Chr6 | 556168 | 556215 | 1,25 | 0 | 0 | 9,25 | 13,25 | NA | 4,375 | 0 | 2,75 | 6 | 2,85714 | 1,75 |

| | | | | | | | | | | | | | | | |
|---|---|---|---|---|---|---|---|---|---|---|---|---|---|---|---|
| 39 | Chr6 | 3599850 | 3599909 | 8,33333 | 0 | 4,16667 | 3,66667 | 0 | 7,33333 | 13,83333 | 26,33333 | 15 | 11,16667 | 15 | 6 |
| 40 | Chr6 | 8920700 | 8920765 | 20 | 7,83333 | 6 | 10 | 17,16667 | 16,66667 | 25 | 18,16667 | 9,83333 | 24,66667 | 33 | 34,5 |
| 41 | Chr6 | 9047413 | 9047450 | 0 | 0 | 0 | 14,5 | 5,5 | NA | 0 | 12 | NA | 0 | 8 | 15 |
| 42 | Chr7 | 23001451 | 23001483 | 5,7 | 9,2 | 10 | 38,5 | 23,2 | 21,8 | 22,8 | 14,9 | 16,4 | 20,4 | 18 | 25,5 |
| 43 | Chr7 | 25218116 | 25218215 | 10,15789 | 6,78947 | 6,89474 | 27,36842 | 39,8 | 29,33333 | 25,05263 | 14,4375 | 7,33333 | 14,57895 | 16,10526 | 16,21053 |
| 44 | Chr7 | 26734344 | 26734380 | 2,66667 | 3 | 0 | 10,91667 | 16,58333 | 10,16667 | 10,66667 | 25,33333 | 6,16667 | 14,85714 | 22,25 | 15,66667 |
| 45 | Chr7 | 27245590 | 27245667 | 0 | 0 | 7,28571 | NA | 7,42857 | 10,25 | 8,57143 | 3,57143 | 11,57143 | 6 | 7,28571 | 4 |
| 46 | Chr7 | 27288648 | 27288766 | 37,53333 | 4,6 | 13,53333 | 1,06667 | 0 | 0,46667 | 9,66667 | 6 | 0 | 2,13333 | 9,6 | 0 |
| 47 | Chr7 | 30087674 | 30087721 | 26,5625 | 27 | 32,75 | 77,30769 | 54,6875 | 62,125 | 45,375 | 47,3125 | 38,375 | 46,6875 | 31,33333 | 50,9375 |
| 48 | Chr7 | 30944276 | 30944338 | 17 | 14,25 | 31 | 45 | 45 | NA | 49,25 | 45,25 | 40 | 50 | 80 | 52 |

| | | | | | | | | | | | | | | | |
|---|---|---|---|---|---|---|---|---|---|---|---|---|---|---|---|
| 49 | Chr7 | 31515695 | 31515744 | 80 | 87,25 | 96,25 | 68,2 | 63 | 78,6 | 68,6 | 83,6 | 75 | 80 | 53,2 | 56,2 |
| 50 | Chr7 | 31921062 | 31921171 | 43,75 | 40,83333 | 53,11111 | 61,38889 | 83,27273 | 68,41667 | 47,44444 | 57,05556 | 67,72222 | 69,6 | 48,61111 | 60,16667 |
| 51 | Scaffold_2 | 8360251 | 8360311 | 16,58333 | 11,92857 | 3,63636 | 50,71429 | 36,92857 | 30,91667 | 46,71429 | 23,71429 | 37 | 29,71429 | 22,78571 | 21,78571 |
| 52 | Scaffold_2 | 9725180 | 9725255 | 9,7 | 10,5 | 5,05263 | 12 | 10,2 | 8,25 | 13,5 | 8,3 | 7,8 | 34,95 | 30,75 | 12,2 |
| 53 | Scaffold_2 | 11548358 | 11548464 | 2,7 | 5,86667 | 12,76667 | 13 | 5,3 | 9,26667 | 10,3 | 6,86667 | 18,3 | 22,86667 | 24,14815 | 31,86667 |
| 54 | Scaffold_2 | 12836466 | 12836516 | 13,08333 | 28,33333 | 15,91667 | 40,66667 | 39,33333 | 51 | 9,33333 | 17,41667 | 35 | 36,08333 | 29,83333 | 9,5 |
| 55 | Scaffold_2 | 14254645 | 14254733 | 7,13636 | 0 | 5,86364 | 17,90909 | 27,36364 | 20,41176 | 27,63636 | 22,22727 | 15,90909 | 30 | 24,11111 | 13,22727 |
| 56 | Scaffold_2 | 17765173 | 17765240 | 17,21739 | 14,21739 | 23,69565 | 21,22222 | 37,21739 | 53,10526 | 39,95652 | 30,56522 | 18,13043 | 10 | 9,69565 | 10,6087 |
| 57 | Scaffold_3 | 741710 | 741752 | 24,16667 | 30 | 15,33333 | 29,91667 | 30 | 35,83333 | 48,5 | 30,83333 | 50 | 44,58333 | 70,5 | 43,83333 |
| 58 | Scaffold_3 | 914678 | 914738 | 26,28571 | 24,19048 | 24,33333 | 33,7619 | 43,19048 | 37,19048 | 35,42857 | 36,2381 | 27,71429 | 44,28571 | 45,33333 | 56,14286 |

| | | | | | | | | | | | | | | | |
|---|---|---|---|---|---|---|---|---|---|---|---|---|---|---|---|
| 59 | Scaffold_3 | 1879031 | 1879100 | 4,95455 | 7,86364 | 0,95455 | 8,59091 | 5,40909 | 6,22727 | 7,59091 | 6,72727 | 9,09524 | NA | 27,63636 | 15,85714 |
| 60 | Scaffold_3 | 2024272 | 2024322 | 0 | 1,77778 | 1,6 | 20,5 | 10,22222 | 9,6 | 14 | 10,5 | 20,6 | 1,77778 | 4,2 | 0 |
| 61 | Scaffold_3 | 3346606 | 3346702 | 0 | 4,2 | 3,52941 | 22,5 | 16 | 17,70588 | 15,18182 | 9,94118 | 8 | 19 | 5,82353 | 5,17647 |
| 62 | Scaffold_3 | 4840118 | 4840221 | 31,625 | 12,125 | 14,75 | 29,75 | 34 | 14,66667 | 20,25 | 33 | 33,75 | 35,625 | 43,28571 | 33 |
| 63 | Scaffold_3 | 5145495 | 5145632 | 0 | 6,14286 | 0 | NA | 1,14286 | 5,71429 | 5,14286 | 8,85714 | 22,85714 | 0 | 0 | 7,42857 |
| 64 | Scaffold_3 | 7592880 | 7593001 | 5,04348 | 8,68182 | 6,95455 | 11,82609 | 8,52381 | 11,86957 | 31,86957 | 19,47826 | 23,47826 | 21 | 9,04348 | 15,56522 |
| 65 | Scaffold_3 | 7951148 | 7951205 | 24,21429 | 25,71429 | 45,71429 | 49,33333 | 85,27273 | 66,86667 | 43,25 | 44,4 | 38,5 | 42,06667 | 94,5 | 42,06667 |
| 66 | Scaffold_3 | 8813968 | 8814009 | 14 | 30 | 62 | 75 | 27 | 55 | 45 | 21 | 44 | NA | 66 | 37 |
| 67 | Scaffold_3 | 9663043 | 9663100 | 3,07692 | 1,625 | 1,55556 | 5,75 | 4,9375 | 5,4375 | 6,4375 | 5,4375 | 14 | 22,375 | 18 | 16,5625 |
| 68 | Scaffold_3 | 10754459 | 10754504 | 0 | NA | 0 | 20 | 8 | 28 | 0 | 7 | 7 | 18 | 0 | 14 |

| | | | | | | | | | | | | | | | |
|---|---|---|---|---|---|---|---|---|---|---|---|---|---|---|---|
| 69 | Scaffold_3 | 12524146 | 12524216 | 5,8 | 0,6 | 10,6 | 10,95 | 18,15 | 10,2 | 19,6 | 9,65 | 8,85 | 17,7 | 28,1 | 21,70588 |
| 70 | Scaffold_3 | 12525567 | 12525700 | 26,41667 | 34,36364 | 25,70833 | 8,5 | 19,84211 | 9,7619 | 12,6087 | 21,41667 | 14,08333 | 8,63636 | 20,14286 | 11,58333 |
| 71 | Scaffold_4 | 3321227 | 3321451 | 24,27273 | 27,3 | 21,38462 | 38,81818 | 36,61538 | 56 | 34,15385 | 45,53846 | 31,07692 | 40,61538 | 41,88889 | 42,53846 |
| 72 | Scaffold_4 | 7995311 | 7995365 | 31,85714 | 38,28571 | 33,57143 | 26,57143 | 43,08333 | 27,21429 | 16 | 15,85714 | 16,85714 | 18,9 | 23,78571 | 25,78571 |
| 73 | Scaffold_4 | 11076506 | 11076536 | 8,63636 | 14,27273 | 9 | 32,8 | 43,27273 | 40 | 26,45455 | 22,27273 | 9,90909 | 16,45455 | 22,27273 | 18,27273 |
| 74 | Scaffold_4 | 13843958 | 13843999 | 45 | 35,28571 | 42 | 59,57143 | 40,57143 | 42,14286 | 21,4 | 33,14286 | 40 | 74,28571 | 81,42857 | 71,42857 |
| 75 | Scaffold_5 | 9107991 | 9108063 | 12,8 | 21 | 7 | 6,8 | 0 | 5,6 | 2,8 | 11,2 | 6,66667 | 14 | 16,6 | 16,33333 |
| 76 | Scaffold_5 | 11098147 | 11098287 | 27,27273 | 15,69231 | 28,15385 | 28,15385 | 6,58333 | 11,46154 | 12,15385 | 5,07692 | 8 | 18,15385 | 18,58333 | 12,4 |
| 77 | Scaffold_6 | 1787919 | 1787988 | 9,29412 | 7,82353 | 24 | 19,64286 | 37,64706 | 34 | 19,52941 | 19,05882 | 19,64706 | 10 | 28,93333 | 28,14286 |
| 78 | Scaffold_6 | 4616703 | 4616781 | 17,08333 | 26,66667 | 13,6 | 41,08333 | 22,91667 | 22,66667 | 12,9 | 12,91667 | 36 | 41,44444 | 51,33333 | 46,91667 |

| | | | | | | | | | | | | | | | |
|---|---|---|---|---|---|---|---|---|---|---|---|---|---|---|---|
| 79 | Scaffold_6 | 6746469 | 6746555 | 3,11111 | 9,66667 | 6,55556 | 25,66667 | 20,22222 | 30,22222 | 33 | 28 | 28 | 40,77778 | 37,88889 | 35 |
| 80 | Scaffold_6 | 10685303 | 10685367 | 14 | 0 | NA | 20 | 25 | 0 | NA | 17 | 42 | 20 | 33 | 13 |
| 81 | Scaffold_7 | 576137 | 576232 | 11,4 | 3,52381 | 9,16 | 10,70833 | 15,95833 | 14,78947 | 7,44 | 11,08 | 19,12 | 19,83333 | 20,22222 | 26,48 |
| 82 | Scaffold_7 | 1552024 | 1552169 | 13,2 | NA | 10 | 39,8 | 40,4 | 35 | 44,8 | 12,2 | 18,6 | 49,6 | 53,6 | 40,8 |
| 83 | Scaffold_7 | 1691172 | 1691254 | 33,2 | 35,4 | 34 | 14,8 | 15,2 | 16,6 | 13,33333 | 25,8 | 28 | 25,25 | 30 | 37,8 |
| 84 | Scaffold_7 | 1799126 | 1799255 | 39,51724 | 41,5 | 24,37931 | 48,43478 | 38,86207 | 54,15789 | 45,21739 | 47,44828 | 42,06897 | 61,03571 | 68,13793 | 50,65517 |
| 85 | Scaffold_7 | 2974604 | 2974650 | 7,23077 | 1,84615 | 0 | 23,30769 | 13,23077 | 2,61538 | 15,84615 | 15,92308 | 24,84615 | 17,69231 | 2,76923 | 2,33333 |
| 86 | Scaffold_7 | 4705687 | 4705725 | 20,13333 | 12,8 | 28,26667 | 4,92857 | 21,4 | 5,4 | 9,2 | 31,5 | 16,6 | 5,66667 | 10,16667 | 2,5 |
| 87 | Scaffold_7 | 5524868 | 5524899 | 19,5 | 14,83333 | NA | 1 | NA | 1,75 | 8,25 | 7,5 | 1 | 5,41667 | 9,41667 | 2,83333 |
| 88 | Scaffold_7 | 10142836 | 10142852 | 30 | 0 | 18 | 25 | 20 | 22 | 12 | 8 | 11 | 28 | 28 | 18 |

| | | | | | | | | | | | | | | | |
|---|---|---|---|---|---|---|---|---|---|---|---|---|---|---|---|
| 89 | Scaffold_7 | 13240135 | 13240180 | 26,2 | 14,6 | 20,8 | 23,5 | 7,2 | 7 | 0 | 1,4 | 1,4 | 5,4 | 2 | 2,2 |
| 90 | Scaffold_9 | 4143562 | 4143589 | 22,58333 | 13 | 15,16667 | 10,16667 | 28,16667 | 0 | 0,75 | 2,08333 | 0 | 5,83333 | 12 | 7,5 |
| 91 | Scaffold_9 | 6945791 | 6945830 | 13,6 | 6,8 | 25,88889 | 46,66667 | 37,9 | 32,8 | 16,5 | 3,3 | 3,4 | 4,4 | 11 | 27,9 |

**Supplemental Table 3.** List of filtered DMRs in shoots of APO-treated samples (np:non-primed, cp:ctrl-priming, p: primed) and control (c). Chromosomal DMR position is indicated (chr:start-end) and methylation level is shown for each biological replicate (3).

| DMR | chrom | start | end | c_1 | c_2 | c_3 | np_1 | np_2 | cp_1 | cp_2 | cp_3 | p_1 | p_2 | p_3 |
|---|---|---|---|---|---|---|---|---|---|---|---|---|---|---|
| 1 | Chr1 | 1269096 | 1269125 | 37 | 7,4 | 18,6 | 25,2 | 12 | 39,8 | 28 | 40,2 | 7,5 | 2,7 | 7,7 |
| 2 | Chr1 | 1324862 | 1324945 | 0 | 7,75 | 0 | 15 | 13 | 10 | 24,5 | 14,75 | 22,5 | 10 | 19 |
| 3 | Chr1 | 1672259 | 1672308 | 0,46667 | 0,46667 | 0 | 14,26667 | 23 | 0 | 0 | 1 | 0 | 0 | 6,06667 |

| | | | | | | | | | | | | | | |
|---|---|---|---|---|---|---|---|---|---|---|---|---|---|---|
| 4 | Chr1 | 2257582 | 2257618 | 30,16667 | 38,66667 | 40,83333 | 10 | 20 | 13 | 29,5 | 28,66667 | 8 | 8,16667 | 13,33333 |
| 5 | Chr1 | 3881337 | 3881367 | 49,14286 | 34,42857 | 54,85714 | 45,71429 | 88,28571 | 68,28571 | 46,42857 | 60,85714 | 73,57143 | 75,14286 | NA |
| 6 | Chr1 | 4829450 | 4829542 | 66 | 75 | NA | 55 | 33 | 12 | NA | 66 | 0 | 66 | 36 |
| 7 | Chr1 | 5243636 | 5243682 | 31,6 | 27,2 | 27,6 | 13,6 | 21,25 | 10,7 | 8,4 | 19,2 | 15 | 2,2 | 12,4 |
| 8 | Chr1 | 6314197 | 6314244 | 14 | 30,66667 | 15,55556 | 20,33333 | 4,44444 | 6,44444 | 0 | 5,44444 | 16 | 23,11111 | 7,66667 |
| 9 | Chr1 | 6521561 | 6521589 | 16 | 50 | 20 | 12 | 16 | 0 | 33 | NA | 20 | 14 | 37 |
| 10 | Chr1 | 6769948 | 6769999 | 26,66667 | 29 | 38 | 12,33333 | 11,33333 | 20,66667 | 16,66667 | 0 | 6,66667 | 60 | 31 |
| 11 | Chr1 | 7520505 | 7520547 | 15,5 | 11,83333 | 8,08333 | 16,08333 | 30,25 | 17,33333 | 26,14286 | 30,83333 | 13,9 | 17,45455 | 11,91667 |
| 12 | Chr1 | 31180010 | 31180104 | 14,10345 | 8,93103 | 2,28571 | 11,35714 | 7,03448 | 3,75862 | 8,03448 | 12,93103 | 22,28 | 16,6087 | 34,71429 |
| 13 | Chr1 | 33347697 | 33347766 | 28,33333 | 21,75 | 52,14286 | 13,5 | 9,25 | 6 | 8,375 | 1,5 | 0 | 5,625 | 25 |

| | | | | | | | | | | | | | | |
|---|---|---|---|---|---|---|---|---|---|---|---|---|---|---|
| 14 | Chr1 | 33660978 | 33661081 | 33,5 | 42,8125 | 44,46667 | 48,35294 | 82,64706 | 52,52941 | 38,72727 | 58,64706 | 58,47059 | 62,94118 | 76,47059 |
| 15 | Chr1 | 34654224 | 34654316 | 0 | 2,875 | 1,125 | 13 | 14,5 | 18,125 | 19,75 | 19,75 | 8 | 13,625 | 12,375 |
| 16 | Chr1 | 35078894 | 35078922 | 33,11111 | 16 | 21,11111 | 23,77778 | 11,77778 | 1,55556 | 8,44444 | 5,77778 | 20,66667 | 3,11111 | 15,33333 |
| 17 | Chr1 | 36377584 | 36377622 | 28 | 6,76471 | 18,14286 | 41,52941 | 40,5 | 50 | 47,58824 | 57,17647 | 33,05882 | 50,4 | 26,05882 |
| 18 | Chr1 | 37099249 | 37099514 | 8,57143 | 16,57895 | 6,95833 | 16,70833 | 9,83333 | 26,25 | 25,5 | 30,57895 | 14,1875 | 13,54167 | 19,54167 |
| 19 | Chr1 | 38041165 | 38041234 | 22,2 | 28,2 | 29 | 6,4 | 57,7 | 52,6 | 81,3 | 45,7 | 25 | 42,4 | 56,5 |
| 20 | Chr1 | 39988438 | 39988513 | 92,09091 | 84,54545 | 61,5 | 63,9 | 64,09091 | 61,66667 | 44,66667 | 46,72727 | 83,27273 | 70,1 | 52,81818 |
| 21 | Chr1 | 41282590 | 41282628 | NA | 14 | 14 | 0 | 11 | 0 | NA | 16 | 0 | 20 | 0 |
| 22 | Chr1 | 41830253 | 41830545 | 17,2 | 7,5625 | 10,6875 | 8,375 | 12,16667 | 13,75 | 11,9375 | 14,78571 | 8,8 | 46,61538 | 18,9375 |
| 23 | Chr1 | 42293760 | 42293881 | 24,5 | 20,5 | 34 | 49,5 | 0 | NA | 18 | 60 | 50 | 36,5 | 53,5 |

| | | | | | | | | | | | | | | |
|---|---|---|---|---|---|---|---|---|---|---|---|---|---|---|
| 24 | Chr1 | 43660569 | 43660714 | 7 | 10 | 7,71429 | 5 | 10,28571 | 5,5 | 13 | 13,71429 | 9,42857 | 24,14286 | 19 |
| 25 | Chr1 | 44034500 | 44034665 | 15 | NA | 13,5 | 50 | 12,5 | 20,5 | 29,75 | 24 | 17,66667 | 35,5 | 16,5 |
| 26 | Chr1 | 45991211 | 45991330 | 32,83333 | 31,36364 | 7,90909 | 20,18182 | 23,63636 | 9,63636 | 7 | 3,63636 | 10,25 | 11,33333 | 12,72727 |
| 27 | Chr1 | 46100427 | 46100494 | 2,90476 | 10,47619 | 7,33333 | 9,66667 | 9,47619 | 23,61905 | 27,88889 | 21,7619 | 21,61905 | 7,90476 | 16,76923 |
| 28 | Chr1 | 47388006 | 47388043 | 10,93333 | 0,6 | 3,4 | 5,8 | 9,4 | 23,07692 | 4,66667 | 10,33333 | 14 | 22,93333 | 24,73333 |
| 29 | Chr1 | 47712252 | 47712283 | 0 | 5,33333 | 6,66667 | 20 | 6,66667 | 11,11111 | 13,33333 | 8,55556 | 34,11111 | NA | 37,11111 |
| 30 | Chr1 | 48200569 | 48200625 | 22,375 | 25,625 | 15,75 | 10,1875 | 31,625 | 2 | 24,125 | 28,2 | 9,16667 | 1 | 5,5 |
| 31 | Chr1 | 48820346 | 48820420 | 38,70588 | 42,29412 | 35,17647 | 35,85714 | 26,18182 | 19,70588 | 36,66667 | 17,35294 | 20,92857 | 3,76471 | 8,0625 |
| 32 | Chr1 | 49277160 | 49277221 | 22,23077 | 57 | 40 | 38,30769 | 36,92308 | 7,85714 | 9,42857 | 8,76923 | 3,07692 | 2,22222 | 20,46154 |
| 33 | Chr1 | 49370688 | 49370786 | 20 | 8,90909 | 12,54545 | 38,36364 | 24,81818 | 25,81818 | 27 | 10,63636 | 29 | 17,72727 | 59,09091 |

| | | | | | | | | | | | | | | |
|---|---|---|---|---|---|---|---|---|---|---|---|---|---|---|
| 34 | Chr1 | 49429544 | 49429588 | 5,90909 | 3 | 1,45455 | 33,45455 | 37,36364 | 11,45455 | 12,72727 | NA | 20 | 6 | 13,33333 |
| 35 | Chr1 | 49675162 | 49675366 | 15,43333 | 13,96667 | 16,62963 | 27,59259 | 31 | 32,61538 | 25,2 | 19,7931 | 9,83333 | 22,06667 | 30,37037 |
| 36 | Chr1 | 50370395 | 50370443 | 39,66667 | 26,66667 | 39 | 20 | 17,66667 | 11 | 20 | 24,5 | 10 | NA | 9,33333 |
| 37 | Chr1 | 51404310 | 51404390 | 28,57143 | 16,625 | 30,28571 | 46,66667 | 35,80952 | 35,75 | 36,52381 | 22,33333 | 50,09524 | 34,11111 | 46,52381 |
| 38 | Chr1 | 52140932 | 52140963 | 23,9 | 17,2 | 12,5 | 43,4 | 33,8 | 19,4 | 10,5 | 18,9 | 20,5 | 14,5 | 9,6 |
| 39 | Chr1 | 53067702 | 53067745 | 18,4 | 17,2 | 38,1 | 1,6 | 4,2 | 6 | 16,2 | 0 | 12 | 8,7 | 9,1 |
| 40 | Chr1 | 53355530 | 53355576 | 1,6 | 1,2 | 22 | 3,5 | 21 | 10 | 12,2 | 2,6 | 20 | 14,3 | 14,5 |
| 41 | Chr1 | 53396929 | 53396965 | 30,45455 | 23 | 36,72727 | 34,2 | 54 | 55 | 70,45455 | 54,72727 | 43 | 66,625 | 30,27273 |
| 42 | Chr1 | 53516885 | 53516934 | 10 | 20,33333 | 6,66667 | 47 | 26 | 29,66667 | 27 | NA | 23,33333 | 24 | 15 |
| 43 | Chr1 | 53726237 | 53726283 | 14 | NA | 16 | NA | 0 | 0 | 25 | 14 | 0 | 0 | 0 |

| | | | | | | | | | | | | | | |
|---|---|---|---|---|---|---|---|---|---|---|---|---|---|---|
| 44 | Chr1 | 55597746 | 55597778 | 13,6 | 14,6 | 28 | 16,8 | 4 | 3,2 | 2,8 | NA | 3,2 | NA | 5 |
| 45 | Chr1 | 57496459 | 57496558 | 1,71429 | 2 | 4,66667 | 22,57143 | 10,42857 | NA | 16 | 4 | 0 | 5,71429 | 5,28571 |
| 46 | Chr1 | 62257807 | 62257837 | 0 | 0 | 22 | 36 | 36 | 16 | 11 | 25 | NA | 38 | 18 |
| 47 | Chr2 | 22984894 | 22985010 | 36,14286 | 33,5 | 50,14286 | 19 | 32,57143 | 24,57143 | 29,33333 | 40 | 6,66667 | 7 | 12,28571 |
| 48 | Chr2 | 23797108 | 23797156 | 0 | 2,78571 | 2,85714 | 7,28571 | 5,71429 | 2,57143 | 6,85714 | 4,85714 | 29,69231 | 14,42857 | 28,28571 |
| 49 | Chr2 | 24924518 | 24924592 | 25,33333 | 32,08333 | 33,28571 | 24,41667 | 16,33333 | 7 | 9,83333 | 3,58333 | 29,3 | 28,33333 | NA |
| 50 | Chr2 | 27561219 | 27561257 | 57,625 | 22,23077 | 33,07692 | 30,69231 | 12,25 | 1,33333 | 5 | 11,23077 | 20 | 21 | 14,76923 |
| 51 | Chr2 | 30052811 | 30052882 | 0 | 11,22222 | 9,55556 | 10,11111 | NA | 0 | 12,83333 | 30,11111 | 30 | 26,72222 | 29,77778 |
| 52 | Chr2 | 30583108 | 30583139 | 6 | 7 | 19,66667 | 15 | 20,5 | 40 | 13,33333 | 23,33333 | 25 | 0 | 22 |
| 53 | Chr2 | 32296652 | 32296813 | 39,83333 | 23,16667 | 20 | 26,83333 | 49,66667 | 11,5 | 2,66667 | NA | 27,66667 | 31,33333 | 30,83333 |

| | | | | | | | | | | | | | | |
|---|---|---|---|---|---|---|---|---|---|---|---|---|---|---|
| 54 | Chr2 | 37008206 | 37008252 | 21,75 | 17,14286 | 15,125 | 15 | 0 | 2,75 | 0 | 0 | 23,16667 | 6,25 | 13 |
| 55 | Chr2 | 37830589 | 37830645 | 0 | 4,54545 | 3,72727 | 9,63636 | 1,45455 | 37,09091 | 19,72727 | 21,45455 | 0 | 20,81818 | 29,3 |
| 56 | Chr2 | 37890079 | 37890186 | 4,73333 | 9,26667 | 5 | 14,53333 | 10,2 | 19,75 | 21,33333 | 25,73333 | 30,86667 | 22,33333 | 8,73333 |
| 57 | Chr2 | 38770961 | 38771057 | 49,30769 | 39,25 | 34,76923 | 5,84615 | 30,84615 | 51,63636 | 34,375 | 26 | 20,76923 | 23,75 | 14,08333 |
| 58 | Chr2 | 39674261 | 39674321 | 7 | 12 | NA | 12 | 30 | 7 | 10 | 0 | 0 | 25 | 13 |
| 59 | Chr2 | 39687695 | 39687720 | 46,42857 | 31,28571 | 35,42857 | 25,14286 | 41,14286 | 17 | 32 | 26,42857 | 9,71429 | NA | 14,28571 |
| 60 | Chr2 | 40461556 | 40461607 | 0 | 1,1 | 1 | 25,6 | 19,5 | 0 | 4,7 | 0 | 0 | 1,1 | 0 |
| 61 | Chr2 | 45272884 | 45272907 | 10,5 | 12,75 | 20 | 8,25 | NA | 42 | 21,75 | NA | 17,25 | 18,5 | 15 |
| 62 | Chr3 | 3268046 | 3268133 | 13,44828 | 15,03448 | 20 | 33,89655 | 24,2069 | 11,37931 | 3,65517 | 40,66667 | 31,65517 | 33,31034 | 36,04167 |
| 63 | Chr3 | 10668157 | 10668322 | 23 | 28,57143 | NA | 18,28571 | 15,85714 | 2,28571 | 0 | 11,42857 | 15,28571 | 8 | 9,57143 |

| | | | | | | | | | | | | | | |
|---|---|---|---|---|---|---|---|---|---|---|---|---|---|---|
| 64 | Chr3 | 12364455 | 12364584 | 31,625 | 43,8125 | 29,85714 | 11 | 19,25 | 10,6875 | 11,75 | 11,125 | 34 | 13,625 | 20,625 |
| 65 | Chr3 | 13014186 | 13014313 | 5,33333 | 19,33333 | 12,33333 | 14 | 6,66667 | 16,33333 | 33,33333 | 22,33333 | 0 | 0 | 0 |
| 66 | Chr3 | 20903831 | 20903946 | 21 | 15,14286 | 26,05 | 4,38095 | 2,90476 | 1,55556 | 11,66667 | 19,57143 | 9 | 10,05882 | 18,3 |
| 67 | Chr3 | 21002905 | 21002944 | 1,27273 | 0 | 0 | 1,81818 | 0 | 9,27273 | 6,8 | 3,45455 | 26,54545 | 23,18182 | 0 |
| 68 | Chr3 | 22397184 | 22397293 | 21,25 | 8,5 | 18,25 | 12,75 | 25,66667 | 32,75 | 18,5 | NA | 35,5 | 53,75 | 51,75 |
| 69 | Chr3 | 22421948 | 22421994 | 42,5 | 33,36364 | 25,18182 | 23 | 20,72727 | 52,09091 | 30,09091 | 19,33333 | 17 | 9,33333 | 15,90909 |
| 70 | Chr3 | 23198273 | 23198311 | 2 | 1,2 | 8,5 | 9,2 | 24,33333 | 11,55556 | 8,33333 | 12,1 | 24,4 | 20,4 | 26,6 |
| 71 | Chr3 | 24130312 | 24130415 | 19,33333 | NA | 23,16667 | NA | 35,5 | 30,5 | 18,83333 | 32,5 | 39,83333 | 39,66667 | 46,83333 |
| 72 | Chr3 | 24657376 | 24657435 | 10,25 | 15,375 | 20 | 4,66667 | 0 | 0 | 0 | 2,75 | 1,5 | 0 | 14 |
| 73 | Chr3 | 27360896 | 27360932 | 0 | 0 | 12,42857 | 1,71429 | 2,28571 | 24,75 | 0 | 15 | NA | 13,71429 | 37,14286 |

| | | | | | | | | | | | | | | |
|---|---|---|---|---|---|---|---|---|---|---|---|---|---|---|
| 74 | Chr3 | 29215841 | 29215874 | 11 | 10,875 | 6,5 | 9,25 | 22,125 | 38,5 | 18,375 | 22 | 33,125 | 36,375 | 27 |
| 75 | Chr3 | 30667776 | 30667993 | 25,45833 | 16,34783 | 16,68421 | 31,30435 | 14,47826 | 36,04762 | 33,04167 | 44,91667 | 38,33333 | 49,54167 | 44,25 |
| 76 | Chr3 | 31551783 | 31551853 | 19,57895 | 21,40909 | 10,8 | 6,27273 | 8,86364 | 3,4 | 3 | 6,95455 | 9,86364 | 9,18182 | 15,54545 |
| 77 | Chr3 | 33034767 | 33034847 | 12 | 4 | NA | 0 | 7,5 | 26 | 33 | 18 | 40,5 | 26,5 | NA |
| 78 | Chr3 | 33627492 | 33627613 | 27,61905 | 28 | 22,2381 | 21,85 | 30,14286 | 19,71429 | 16,66667 | 14,83333 | 19,61538 | 7,10526 | 9,875 |
| 79 | Chr3 | 33744652 | 33744706 | 17,28571 | 23 | 13 | 23,625 | 11,5 | 3,25 | 20 | 14,42857 | 0 | 0 | 0 |
| 80 | Chr3 | 33949193 | 33949259 | 21,61538 | 28,44444 | 36,875 | 51 | 57,6 | 65 | 51,30769 | 44,84615 | 54,63636 | 39,38462 | 32,72727 |
| 81 | Chr3 | 34876497 | 34876571 | 23,38462 | 12,46154 | 21,30769 | 42,85714 | 16,69231 | 37,92308 | 66,84615 | 46,3 | 24,15385 | 41,2 | 60,625 |
| 82 | Chr3 | 39220576 | 39220651 | NA | 30,66667 | 18,75 | 4 | 19 | 2,5 | 4 | 19 | 0 | 20 | 5 |
| 83 | Chr3 | 41408018 | 41408144 | 17,15789 | 28,89474 | 11,5 | 13,63636 | 13,66667 | 3,94737 | 6,05556 | 5,15789 | 7,72222 | 4 | 7,55556 |

| | | | | | | | | | | | | | | |
|---|---|---|---|---|---|---|---|---|---|---|---|---|---|---|
| 84 | Chr3 | 41410923 | 41410968 | 27,55556 | 10,08333 | 30,16667 | 3,22222 | 3,77778 | 6,30769 | 11,44444 | 13,38889 | 0 | 7,9375 | 16,05556 |
| 85 | Chr4 | 111578 | 111655 | 24,57143 | 17,35714 | 30,21429 | 20 | 10,78571 | 28,5 | 2 | 6 | 6,92857 | 2,5 | 10,42857 |
| 86 | Chr4 | 811445 | 811467 | 33 | 25 | 18 | 20 | 57 | 33 | 22 | 33 | 40 | NA | 16 |
| 87 | Chr4 | 3967767 | 3967902 | 7,5625 | 16,53333 | 13,6875 | 30,0625 | 24,3125 | 21 | 36,125 | 4,54545 | 19,375 | 37,71429 | 43,15385 |
| 88 | Chr4 | 32433390 | 32433497 | 28,28571 | 40,57143 | 41,85714 | 31,375 | 25,625 | 15,35714 | 24,21429 | 14,78571 | 21,53846 | 30,92857 | 25,64286 |
| 89 | Chr4 | 35728637 | 35728770 | 4,44444 | 3,33333 | 3,06667 | 12,41667 | 11 | 33,33333 | 3,46667 | 14 | 13,8 | 18,14286 | 33,13333 |
| 90 | Chr4 | 36938619 | 36938681 | 10,25 | 8,9375 | 1,75 | 10,0625 | 20,61538 | 13,33333 | 6,5 | 15,8 | 23,625 | 24,5 | 36,875 |
| 91 | Chr5 | 1277312 | 1277389 | NA | 56 | 46,5 | 30 | 52,5 | 25 | 20 | 0 | 41 | NA | 56,5 |
| 92 | Chr5 | 3094016 | 3094099 | 44 | 41,66667 | 45,75 | 63 | 31,375 | 22,22222 | 14,66667 | 30,22222 | 22 | 10,44444 | 20,66667 |
| 93 | Chr5 | 4109097 | 4109136 | 0 | 2 | 0 | 11,4 | 3,2 | 35 | 20,6 | 20,4 | 12 | 13,33333 | 17 |

| | | | | | | | | | | | | | | |
|---|---|---|---|---|---|---|---|---|---|---|---|---|---|---|
| 94 | Chr5 | 4245953 | 4246074 | 26,58824 | 30,3125 | 20,11765 | 17,88235 | 12,33333 | 5,58824 | 16,23529 | 10,57143 | 10,17647 | 8,64706 | 8,11765 |
| 95 | Chr5 | 7373320 | 7373414 | NA | 32,85714 | 28,35714 | 45,64286 | 42 | 49,14286 | 44,92857 | 47,92857 | 51,78571 | 67,85714 | 62,14286 |
| 96 | Chr5 | 9123812 | 9123851 | 22 | 0 | 11,88889 | 6,33333 | 2,44444 | 1 | 5 | 6,88889 | 0 | 1,75 | 0,66667 |
| 97 | Chr5 | 9345833 | 9345907 | 0 | 21,9 | 37,14286 | 11,85714 | 8,7 | 13,5 | 0 | 15,8 | 15,7 | 20,2 | 6 |
| 98 | Chr5 | 11841370 | 11841431 | 18,18182 | 14 | 29,54545 | 12,09091 | 3,27273 | 16,88889 | 8,54545 | 2,88889 | 4,90909 | 2,54545 | 4 |
| 99 | Chr5 | 31364003 | 31364041 | 23,61538 | 11,30769 | 19,57143 | 0,92308 | 5,07692 | 4,07692 | 2,07692 | 0 | 6,07692 | 4,76923 | 8,14286 |
| 100 | Chr5 | 32674155 | 32674212 | 0 | 17,25 | 2,25 | 14,25 | 21,5 | 2,5 | 5 | 2,25 | 8,25 | 3,75 | 0 |
| 101 | Chr6 | 2600194 | 2600217 | 12 | 50 | 15 | 17,8 | 7,6 | 7,2 | 23,7 | 6,9 | NA | 29,5 | 32,5 |
| 102 | Chr6 | 3093307 | 3093357 | 1,75 | 12,07143 | 6,71429 | 14,5 | 7,5 | 17,14286 | 17,14286 | 7,28571 | 24,88889 | 23,2 | 13,42857 |
| 103 | Chr6 | 3506344 | 3506384 | 0 | 7 | 0 | 0 | 7 | 0 | 9 | 14 | 11 | 0 | 28 |

| | | | | | | | | | | | | | | |
|---|---|---|---|---|---|---|---|---|---|---|---|---|---|---|
| 104 | Chr6 | 4287698 | 4287749 | 11 | 0 | 12 | 14 | 12 | 20 | 16 | NA | 0 | 25 | 25 |
| 105 | Chr6 | 4303781 | 4303865 | 60 | NA | 80 | 10 | 20 | 40 | 18 | 12 | 29 | 14 | 29 |
| 106 | Chr6 | 4720671 | 4720699 | 15,83333 | 18,75 | NA | 28,16667 | 26 | 29,91667 | 41 | 58,16667 | 43,66667 | 48,33333 | 13,91667 |
| 107 | Chr6 | 5224040 | 5224136 | 59,33333 | 43,5 | NA | 30,5 | 31 | 53,5 | 57 | 40,66667 | 30 | 20,33333 | NA |
| 108 | Chr6 | 5453776 | 5453946 | 20,7931 | 20,82353 | 28,54286 | 20,86111 | 23,77778 | 8,05556 | 9,61111 | 10,13889 | 20,36111 | 8,38889 | 8,33333 |
| 109 | Chr6 | 5500171 | 5500339 | 7,6 | 15,9 | 9,3 | 16,4 | 8,4 | 17,9 | 4,2 | 11,2 | 30,1 | 23,33333 | 19 |
| 110 | Chr6 | 6357838 | 6357872 | 0 | 0 | 7 | 0 | 0 | 0 | 0 | 25 | 11 | 14 | 0 |
| 111 | Chr6 | 8245479 | 8245672 | NA | 11,6 | 33,8 | 22 | 11,2 | 0 | 0 | 0 | 0 | 0 | 6,6 |
| 112 | Chr6 | 16834532 | 16834563 | 20 | 12 | 0 | 14 | NA | 30 | 28 | 40 | NA | 20 | 28 |
| 113 | Chr6 | 20276236 | 20276254 | 0 | 2,77778 | 2,22222 | 9,77778 | 34,28571 | NA | 17,11111 | 18,66667 | 15 | 5 | 2,22222 |

| | | | | | | | | | | | | | | |
|---|---|---|---|---|---|---|---|---|---|---|---|---|---|---|
| 114 | Chr6 | 23949629 | 23949654 | 0 | 3,3 | 6,8 | 12,6 | 3,3 | 9,8 | 3,4 | 11,4 | 17,9 | 24,5 | 13,33333 |
| 115 | Chr6 | 25746121 | 25746278 | 2 | 2,625 | 6,05882 | 9,11765 | 2,47059 | 18,75 | 2,25 | 10,4375 | 13,17647 | 26,88235 | 18,52941 |
| 116 | Chr6 | 30837200 | 30837465 | 17,55814 | 12,275 | 23,60465 | 19,90698 | 26,11628 | 25,48718 | 28,32 | 21,2973 | 37,05405 | 38,5 | 28,53488 |
| 117 | Chr6 | 31029400 | 31029464 | 4,53846 | 4,69231 | 6 | 8 | 15,53846 | 6,85714 | 26,38462 | 22,22222 | 8,33333 | 8,4 | 4,84615 |
| 118 | Chr6 | 31029520 | 31029597 | 13,17647 | 11,70588 | 2,94118 | 7,6 | 5,41176 | 24,85714 | 22,8 | 24,76471 | 7,11765 | 6,625 | 6,41176 |
| 119 | Chr7 | 4638863 | 4639028 | 12,9 | 3,10526 | 9,28571 | 15,26316 | 22,6 | 29,84615 | 21,95 | 17,11765 | 10,25 | 11,94118 | 6,1 |
| 120 | Chr7 | 4873462 | 4873515 | 1,8 | 0 | 5 | 6,2 | 3,2 | 18 | 20 | 33,2 | 3,2 | 13,8 | 0 |
| 121 | Chr7 | 5194418 | 5194438 | NA | 17,9 | 16 | 6 | 4 | 0 | 0 | 4,8 | 16,85714 | 2,1 | 0 |
| 122 | Chr7 | 8713895 | 8714098 | 14,83784 | 8,43243 | 12,18919 | 15,16667 | 32,16667 | 21,16216 | 17,82353 | 23,19444 | 21,37838 | 20,62857 | 45,45946 |
| 123 | Chr7 | 10878643 | 10878709 | 16,33333 | 30,6 | 22,66667 | 38,93333 | 44,66667 | 48,26667 | 39,53333 | 55,8 | 46,33333 | 51,44444 | 53,4 |

| | | | | | | | | | | | | | | |
|---|---|---|---|---|---|---|---|---|---|---|---|---|---|---|
| 124 | Chr7 | 16596013 | 16596093 | 24,25 | 19,11111 | 12 | 6,77778 | 0 | 6,88889 | 14,33333 | 12,44444 | 0 | 4,71429 | 0 |
| 125 | Chr7 | 20444032 | 20444092 | 7,1 | 1,6 | 0 | 28,2 | 24,1 | 31,5 | 8,7 | 13,5 | 10,22222 | 16 | 12,1 |
| 126 | Chr7 | 21711990 | 21712021 | 4 | 0 | 0 | 15,76923 | 19,30769 | 24 | 3,84615 | 3,33333 | 0 | 2,30769 | 16,57143 |
| 127 | Chr7 | 22576569 | 22576588 | 11,5 | 0 | 20 | 40 | 16,5 | NA | 20 | 14 | NA | 55 | 38,5 |
| 128 | Chr7 | 24039000 | 24039071 | 12 | NA | 25 | 0 | 16 | 0 | 33 | 16 | NA | 0 | 0 |
| 129 | Chr7 | 24103867 | 24103908 | 0 | 7,75 | NA | 6 | NA | 8,125 | 9,375 | 15,375 | 20,75 | 16,25 | 24,625 |
| 130 | Chr7 | 24107273 | 24107318 | 40 | NA | 16 | NA | 22 | 14 | 14 | 28 | 14 | 16 | 40 |
| 131 | Chr7 | 24495589 | 24495816 | 9,76923 | 3,92308 | 9 | 23,68421 | 18,16 | 30,69231 | 20 | 16,38462 | 26,53846 | 34,42857 | 36,23077 |
| 132 | Chr7 | 25738766 | 25738789 | 0 | 5,5 | 0 | NA | 0 | 10 | 20 | NA | 18 | 25 | 40 |
| 133 | Chr7 | 27159314 | 27159344 | 0 | 0 | 0 | 11 | 13 | 3,5 | 20 | 15 | 9,25 | 19,25 | NA |

| | | | | | | | | | | | | | | |
|---|---|---|---|---|---|---|---|---|---|---|---|---|---|---|
| 134 | Chr7 | 27365000 | 27365201 | 15,3 | 12,65385 | 5,30769 | 15,08 | 10,76923 | 29,44 | 27,42308 | 20,85714 | 23,84615 | 24,88462 | 14,64 |
| 135 | Chr7 | 31845302 | 31845348 | 20 | NA | NA | 42 | 30 | 80 | 25 | 28 | 11 | 20 | 28 |
| 136 | Chr7 | 33439390 | 33439434 | 29,54545 | 29,71429 | 14,76923 | 21,28571 | 41,46154 | 37,5 | 46,28571 | 25,42857 | 54,78571 | 52,85714 | 53,375 |
| 137 | Scaffold_1 | 4889611 | 4889827 | 11,125 | 17,4375 | 11,13333 | 14,6875 | 27,1875 | 41,125 | 20,5625 | 10 | 18,42857 | 21,7 | 43,93333 |
| 138 | Scaffold_1 | 5424347 | 5424387 | 0 | 1,81818 | 1,09091 | 16,54545 | 15,54545 | 12,54545 | 23,09091 | 22,72727 | 17,18182 | 2,36364 | 2,72727 |
| 139 | Scaffold_1 | 6227902 | 6227997 | 14 | 14 | 40 | 40 | 62 | 33 | 20 | 14 | NA | 33 | 55 |
| 140 | Scaffold_1 | 7989655 | 7989713 | 9,71429 | 7,14286 | 20 | 21,71429 | 2 | 28,85714 | 29 | NA | 5 | 18,85714 | 6,28571 |
| 141 | Scaffold_1 | 19308850 | 19308903 | 10,5 | 13,3 | 8,9 | 5,4 | 8 | 8,1 | 11,1 | 7,42857 | 0 | 0 | 2,7 |
| 142 | Scaffold_10 | 2068190 | 2068247 | 26 | 30,33333 | 36,33333 | 18 | 11,33333 | 26 | 15 | 28,66667 | 90 | 21 | 17,33333 |
| 143 | Scaffold_2 | 1770327 | 1770383 | 14 | 4,66667 | 0 | 10 | 5,8 | 14,16667 | 9,33333 | 6,16667 | 29 | 22,66667 | 19 |

| | | | | | | | | | | | | | | |
|---|---|---|---|---|---|---|---|---|---|---|---|---|---|---|
| 144 | Scaffold_2 | 5285259 | 5285306 | 13 | 0 | 39 | 30 | 10 | 29 | 13,5 | 0 | 17 | 10 | 28 |
| 145 | Scaffold_2 | 5553157 | 5553188 | 14 | 10 | 13,6 | 25,6 | 28,3 | 21,2 | 22,9 | 12,3 | 54,75 | 26,1 | 39,9 |
| 146 | Scaffold_2 | 5857054 | 5857108 | 10,46154 | 18,76923 | 12,92308 | 20,72727 | 25,53846 | 48,46154 | 50,92308 | 21,30769 | 47,61538 | 35,33333 | 46,23077 |
| 147 | Scaffold_2 | 7153416 | 7153726 | 45,69231 | 16 | 33,38462 | 18,38462 | 26,33333 | 10,66667 | 3,33333 | 23,16667 | 20,44444 | 26 | 38,61538 |
| 148 | Scaffold_2 | 7229614 | 7229655 | 2,22222 | 6,6 | 0 | 12 | 10 | 9,84615 | 9,15385 | 3,61538 | 13,5 | 23,53846 | 18,36364 |
| 149 | Scaffold_2 | 7970063 | 7970120 | 10 | 8,85714 | 16 | 16 | 21,71429 | 34 | 9 | 1,42857 | 33,14286 | 30,57143 | 37,57143 |
| 150 | Scaffold_2 | 9109584 | 9109670 | 35,5 | 16,5 | NA | 31 | 22 | 24,5 | NA | 30 | 50 | 42,5 | 30 |
| 151 | Scaffold_2 | 9346256 | 9346299 | 3,125 | 8,25 | NA | 27,375 | 20,5 | 34,25 | 52,5 | 12 | 0 | 13,33333 | 1,75 |
| 152 | Scaffold_2 | 9728827 | 9728889 | 19,53846 | 21,4 | 11,26667 | 0 | 1,2 | 5,09091 | 8,13333 | 9,06667 | 13,2 | 11,11111 | 0,86667 |
| 153 | Scaffold_2 | 9985094 | 9985128 | 42,57143 | 21,21429 | 33,07143 | 60,76923 | 56,85714 | 51,64286 | 44,21429 | 39,42857 | 60,625 | 60,66667 | 76,21429 |

| | | | | | | | | | | | | | | |
|---|---|---|---|---|---|---|---|---|---|---|---|---|---|---|
| 154 | Scaffold_2 | 10220741 | 10220765 | 0 | 11,9 | 13,8 | 18,6 | NA | 25 | 34,1 | 71,1 | 10,5 | 3,6 | 20,8 |
| 155 | Scaffold_2 | 10442117 | 10442168 | 15,16667 | 20,16667 | NA | NA | 9,16667 | 0 | 0 | 0 | 0 | 1,83333 | 0 |
| 156 | Scaffold_2 | 10503249 | 10503378 | 33,22222 | 37,33333 | 47,22222 | 41,22222 | 76,75 | 68 | 64 | 62,5 | 48 | 65,66667 | 49,875 |
| 157 | Scaffold_2 | 11305097 | 11305129 | 11,125 | 3,5 | 0 | 13,71429 | 17,5 | 26,25 | 36,375 | 25,75 | 15,33333 | 11 | 22,5 |
| 158 | Scaffold_2 | 12278561 | 12278598 | 45,57143 | 33,53846 | 36,84615 | 41,33333 | 25,6 | 12 | 21,53846 | 3,2 | 28,92308 | 44,38462 | 15,9 |
| 159 | Scaffold_2 | 12329176 | 12329242 | 0 | 0 | 25 | 7 | 10 | 40 | 0 | 12 | 0 | NA | 11 |
| 160 | Scaffold_2 | 12508532 | 12508590 | 18,23077 | 19,11111 | 17,92308 | 6,61538 | 40 | 34 | 27,07692 | 27,5 | 49,46154 | 17 | 29,61538 |
| 161 | Scaffold_2 | 13579724 | 13579773 | 1,66667 | 9,75 | 4,66667 | 1,91667 | 6,5 | 3,27273 | 4 | 8,44444 | 16 | 36,5 | 26,08333 |
| 162 | Scaffold_2 | 14073739 | 14073784 | 32,75 | 20 | 33,5 | 30,75 | 13,5 | NA | 7,5 | 9,75 | 33,5 | 40,75 | 29,75 |
| 163 | Scaffold_2 | 14204516 | 14204569 | 5,21429 | 3,73333 | 10,2 | 23,4 | 4,8 | 17,53333 | 25,46667 | 27 | 6 | 18,53333 | 11,93333 |

| | | | | | | | | | | | | | | |
|---|---|---|---|---|---|---|---|---|---|---|---|---|---|---|
| 164 | Scaffold_2 | 14722564 | 14722611 | 3,25 | 3,5 | 0 | 10 | 14,875 | 20 | 20,25 | 18,375 | 18,4 | 3,75 | 18,66667 |
| 165 | Scaffold_2 | 14894682 | 14894786 | 2,3125 | 6,125 | 14,5625 | 18,54545 | 15,33333 | 34,06667 | 21,5625 | 23,44444 | 1,07692 | 24,375 | 24,3125 |
| 166 | Scaffold_2 | 16127961 | 16127990 | 28,9 | 36,5 | 43,6 | 3,3 | 2,4 | 14,4 | 20,2 | 45,2 | 27,8 | 22,8 | 11,6 |
| 167 | Scaffold_2 | 17788917 | 17789093 | 17,05882 | 26,70588 | 34,63636 | 4,57143 | 5,45455 | 6,28571 | 3,66667 | 0,88889 | 11,42857 | 10,4 | 8,52381 |
| 168 | Scaffold_2 | 18059522 | 18059617 | 32,66667 | 45,46667 | 51,33333 | 41,06667 | 36,76923 | 33 | 14,06667 | 23,66667 | 44,57143 | 22,23077 | 30,66667 |
| 169 | Scaffold_2 | 18440324 | 18440366 | 0 | 0 | NA | NA | 0 | 9 | 0 | 16 | 0 | 28 | 0 |
| 170 | Scaffold_2 | 19725454 | 19725502 | 3,44444 | 4 | 1,90909 | 8,63636 | 26 | 11 | 18,55556 | 13,75 | 24,09091 | 15 | 33 |
| 171 | Scaffold_3 | 1491386 | 1491412 | 20 | 16,71429 | 30 | 22,57143 | 0 | NA | 3,14286 | 0 | 1,71429 | 1 | 12,28571 |
| 172 | Scaffold_3 | 2404009 | 2404120 | 17,14286 | 6,28571 | 10 | 36,66667 | 25,54545 | 30,14286 | 35,57143 | NA | 13,27273 | 9,85714 | 11,85714 |
| 173 | Scaffold_3 | 5945881 | 5946254 | 31,83333 | 16 | 27,2 | 15,83333 | 11,66667 | NA | 6,33333 | 3 | 14 | 8 | 13,66667 |

| | | | | | | | | | | | | | | |
|---|---|---|---|---|---|---|---|---|---|---|---|---|---|---|
| 174 | Scaffold_3 | 7259646 | 7259693 | 20,5 | 32,7 | 13 | 0 | 28 | NA | 12,4 | 20,6 | 3,7 | 0 | 0 |
| 175 | Scaffold_3 | 10300553 | 10300600 | 45,75 | 40 | 59,75 | 13 | 40 | NA | 40 | 26,25 | 39,75 | 38,75 | 28 |
| 176 | Scaffold_3 | 10566161 | 10566259 | 6,60714 | 13,5 | 13,67857 | 22,85714 | 28,51852 | 12,09091 | 10 | 1,3913 | 27,5625 | 30,80952 | 29,96429 |
| 177 | Scaffold_3 | 11058085 | 11058192 | 10,5 | 6,66667 | 4,16667 | 6,66667 | 35 | 37,83333 | 30,5 | 10 | 34,16667 | 13,16667 | 16,5 |
| 178 | Scaffold_3 | 13064879 | 13064935 | 3,2 | 4,71429 | 0,78571 | 14,42857 | 0 | 8,92857 | 11,92308 | 9 | 14,21429 | 17,5 | 19,57143 |
| 179 | Scaffold_3 | 13865759 | 13865817 | 19 | 37,8 | 14,5 | 8 | 26,6 | 12 | 10,7 | 28,9 | 0 | 1,4 | 0 |
| 180 | Scaffold_3 | 14445319 | 14445375 | NA | 31 | NA | 7 | 20,5 | 4 | 2,75 | 28 | 40,5 | 18,5 | 3,5 |
| 181 | Scaffold_3 | 14873730 | 14873762 | 3,2 | 15,5 | 30 | 39,5 | 30,16667 | 19,33333 | 18 | 20 | 55,83333 | 45 | 39 |
| 182 | Scaffold_3 | 15384359 | 15384381 | 20 | 11 | 14 | 0 | NA | NA | 10 | 25 | 27 | 37 | 0 |
| 183 | Scaffold_4 | 2350931 | 2351012 | 32,90909 | 28,86364 | 33,04545 | 42,59091 | 47,5 | 55,63636 | 57,95455 | 54,27273 | 55,40909 | 57 | 30,77273 |

| | | | | | | | | | | | | | | |
|---|---|---|---|---|---|---|---|---|---|---|---|---|---|---|
| 184 | Scaffold_4 | 2539376 | 2539412 | 6,83333 | 27,91667 | NA | 0 | 8,16667 | 0 | 0,83333 | 2 | 16,58333 | 18,77778 | 5,5 |
| 185 | Scaffold_4 | 2735252 | 2735323 | 19,16667 | 18,83333 | 25,44444 | 7,27273 | 9 | 6,16667 | 9 | 11,25 | 0 | 6 | 4,91667 |
| 186 | Scaffold_4 | 3525019 | 3525042 | 10 | 18 | 42,25 | 16 | 0 | 21,5 | 32,75 | 55,25 | 45 | 48 | 46,25 |
| 187 | Scaffold_4 | 6020012 | 6020138 | 0 | 13,14286 | 12,33333 | 19 | 11,42857 | NA | 40 | 17,71429 | 2,28571 | 19 | 18,57143 |
| 188 | Scaffold_4 | 8372545 | 8372587 | 20,5 | 35,25 | 31 | 51,5 | 35,25 | 52,5 | 53,33333 | 46,25 | 11,25 | 50 | 30,25 |
| 189 | Scaffold_4 | 9727674 | 9727706 | 6,11111 | 9,11111 | 14,66667 | 44,66667 | 3,11111 | 21,66667 | 27,11111 | 0 | 30,5 | 32,22222 | 33,44444 |
| 190 | Scaffold_4 | 10056304 | 10056457 | 0 | 0 | 0 | 0 | 0 | 0 | 0 | 11 | 33 | NA | 25 |
| 191 | Scaffold_4 | 14340979 | 14341045 | 3 | 2,1 | 6 | 5,63636 | 26 | 7,45455 | 3,81818 | 20,45455 | 16,63636 | 20,27273 | 34,27273 |
| 192 | Scaffold_4 | 16040322 | 16040426 | 61,54545 | 58,81818 | 64,09091 | 68,5 | 45 | 27,72727 | 71,09091 | 69,36364 | 28,63636 | 44,36364 | 42,09091 |
| 193 | Scaffold_5 | 1242940 | 1242969 | 61,33333 | 41,66667 | 53,5 | 39 | 34,5 | 24,5 | 18,83333 | 19,16667 | 22,16667 | 10,66667 | 23,83333 |

| | | | | | | | | | | | | | | |
|---|---|---|---|---|---|---|---|---|---|---|---|---|---|---|
| 194 | Scaffold_5 | 7839195 | 7839261 | 11,15385 | 18,15385 | NA | 3,53846 | 0 | 0 | 0 | 0 | 0 | 15 | 0 |
| 195 | Scaffold_5 | 8204798 | 8204860 | 0 | 0 | 0 | 5 | 0 | 17 | 20,875 | 12,5 | 0 | 1,375 | 13,5 |
| 196 | Scaffold_5 | 10043911 | 10043976 | 2,10526 | 13,05263 | 3,15789 | 2,31579 | 22,36364 | 22,63158 | 21,47368 | 17,78947 | 21,31579 | 32,4375 | 24,63158 |
| 197 | Scaffold_5 | 12540557 | 12540619 | 0 | 5,63636 | 5,54545 | 17,66667 | 21,33333 | 24,83333 | 41 | 26,16667 | 29,08333 | 19 | 15 |
| 198 | Scaffold_5 | 13653572 | 13653721 | 19,78571 | 12,8125 | 16,71429 | 32,84615 | 26,875 | 2,25 | 8 | 16,16667 | 42,64286 | 32 | 29,6875 |
| 199 | Scaffold_5 | 14897565 | 14897661 | 2,75 | 4,875 | 2,33333 | 10 | 13 | 0 | 20 | 22,625 | 13,625 | 27,375 | 39,625 |
| 200 | Scaffold_6 | 231368 | 231440 | 1,46154 | 0 | 2,66667 | 18,4 | 13,42857 | 0,71429 | 7,28571 | 3,14286 | 4 | 0 | 1,42857 |
| 201 | Scaffold_6 | 252650 | 252697 | 0 | 16 | 28 | 0 | 16 | 40 | NA | 0 | 0 | 0 | 0 |
| 202 | Scaffold_6 | 1688179 | 1688255 | 2,90909 | 4,25 | 11,91667 | 21,83333 | 16,25 | 16,5 | 24,91667 | 12,27273 | 18,55556 | 17,41667 | 32,5 |
| 203 | Scaffold_6 | 2061247 | 2061278 | 15,66667 | 4,75 | 12 | 15,5 | 22,66667 | 43,16667 | 34,08333 | 43,54545 | 14,16667 | 8,83333 | 5,91667 |

| | | | | | | | | | | | | | | |
|---|---|---|---|---|---|---|---|---|---|---|---|---|---|---|
| 204 | Scaffold_6 | 2399582 | 2399696 | 10,06667 | 22,92857 | 17,5 | 32,92308 | 26,06667 | 28,8 | 26,46154 | 30,93333 | 48,14286 | 32,53333 | 42,6 |
| 205 | Scaffold_6 | 2643979 | 2644046 | 0,8 | 0 | 0 | 12,6 | 9,6 | 8 | 11 | 12,125 | 10 | 15,1 | 16,7 |
| 206 | Scaffold_6 | 2763973 | 2764037 | 22,54545 | NA | 23,54545 | 36,90909 | 29,18182 | 29,27273 | 32,45455 | 34,09091 | 6,2 | 12,45455 | 11,81818 |
| 207 | Scaffold_6 | 3761344 | 3761386 | 0 | 4,6 | 4,6 | 4 | 16,6 | 22,8 | 15,6 | 23,2 | 0 | 2,4 | 4,8 |
| 208 | Scaffold_6 | 4357936 | 4357965 | 0 | 0 | NA | 0 | 0 | 0 | 0 | NA | 0 | 0 | 0 |
| 209 | Scaffold_6 | 5099024 | 5099061 | 10 | 4,66667 | 19,33333 | 0 | 0 | 6,66667 | 3 | 6,66667 | 0 | 0 | 8,33333 |
| 210 | Scaffold_6 | 7212429 | 7212466 | 34,81818 | 16,90909 | 24,18182 | 29,27273 | 61,45455 | 46,25 | 31,18182 | 34,63636 | 48,90909 | 80 | 56,45455 |
| 211 | Scaffold_6 | 11753382 | 11753464 | 11,44444 | 5,44444 | 14,11111 | 21,66667 | 28 | 26,22222 | 6,22222 | 13,25 | 32,4 | 30 | 35,88889 |
| 212 | Scaffold_7 | 1026456 | 1026510 | 0 | 0,84615 | 1,81818 | 0 | 10 | 3 | 20 | 3,53846 | 22,92308 | 14,69231 | 10,84615 |
| 213 | Scaffold_7 | 1556796 | 1556844 | 43,93333 | 58,71429 | 18,2 | 23,26667 | 35 | 12,4 | 1,33333 | 24,46667 | 20,66667 | 7,86667 | 12,53333 |

| | | | | | | | | | | | | | | |
|---|---|---|---|---|---|---|---|---|---|---|---|---|---|---|
| 214 | Scaffold_7 | 1690185 | 1690223 | 40,7 | 33,1 | 33,85714 | 14,2 | 46,3 | 20,9 | 21,8 | 42,16667 | 0 | 3,7 | 19,14286 |
| 215 | Scaffold_7 | 3203229 | 3203261 | 65,3 | 55,4 | NA | 33,8 | 46,6 | 30,8 | 41 | 57,88889 | 33,33333 | 34,9 | 42,1 |
| 216 | Scaffold_7 | 5780801 | 5780862 | 31,76923 | 28,15385 | 47 | 4,92308 | 8,72727 | 19,46154 | 52,92308 | 48,15385 | 23,27273 | 25,83333 | 22,69231 |
| 217 | Scaffold_7 | 7283096 | 7283142 | 35 | 42,5 | 71 | NA | 33,5 | NA | 10 | 57,5 | 21 | 23,5 | 31 |
| 218 | Scaffold_7 | 9158630 | 9158664 | 20,25 | NA | 0 | 38,5 | 35 | 46,5 | 34,75 | 60,5 | 62 | NA | 0 |
| 219 | Scaffold_7 | 9590225 | 9590253 | 7,16667 | 3,75 | 1,16667 | 6,83333 | 18,66667 | 6 | 7,16667 | 9,91667 | 26,83333 | 14,16667 | 38,25 |
| 220 | Scaffold_7 | 13306863 | 13306925 | 6 | 1,07692 | 8,46154 | 5,30769 | 20,46154 | 16,46154 | 12,33333 | 10,75 | 32,30769 | 29,38462 | 30,84615 |
| 221 | Scaffold_8 | 385728 | 385791 | 0 | 8,4 | 11,6 | 29,8 | 31,2 | 18,2 | 25,2 | 38 | 0 | NA | 30,2 |
| 222 | Scaffold_8 | 1570243 | 1570301 | 46,7 | 32,1 | NA | 9,9 | 6,4 | 10,1 | 5,6 | 0 | 7 | 7,77778 | 40 |
| 223 | Scaffold_9 | 6345343 | 6345437 | 54,92857 | 50 | 41,64286 | 42,07143 | 25,21429 | 23,42857 | 18,35714 | 16,66667 | 44,78571 | 44,35714 | 40,78571 |

| | | | | | | | | | | | | | | |
|---|---|---|---|---|---|---|---|---|---|---|---|---|---|---|
| 224 | Scaffold_9 | 6553226 | 6553322 | 33,125 | 12,71429 | 29,53571 | 5,5 | 6,96429 | 26,53571 | 23,19231 | 20,82143 | 15,21429 | 17,17857 | 21,25 |
| 225 | Scaffold_9 | 6728792 | 6728820 | 19,5 | 21,9 | 13,77778 | 14 | 14,2 | 4,8 | 17,9 | 1,7 | 3,3 | 0 | 0 |
| 226 | Scaffold_9 | 7763266 | 7763379 | 2,72727 | 3,90909 | 0,90909 | 5,27273 | 7,90909 | 5,5 | 3,5 | 36,77778 | 10,22727 | 21,23077 | 17,06667 |

**Supplemental Table 4.** List of DMRs in roots that overlap with TEs.

| Chr | start | end | TE family |
|---|---|---|---|
| Chr1 | 4854138 | 4854191 | Mutator |
| Chr1 | 5087593 | 5087615 | PIF-Harbinger |
| Chr1 | 6382770 | 6382807 | hAT |
| Chr1 | 31432950 | 31433006 | Helitron |
| Chr1 | 31529382 | 31529448 | Helitron |
| Chr1 | 33667677 | 33667797 | Copia |
| Chr1 | 49690319 | 49690391 | Gypsy |
| Chr2 | 28626401 | 28626444 | L1 |
| Chr2 | 32699289 | 32699352 | PIF-Harbinger |
| Chr2 | 33139150 | 33139230 | Mutator |
| Chr2 | 33417120 | 33417165 | Helitron |
| Chr2 | 37243732 | 37243832 | PIF-Harbinger |
| Chr2 | 37840431 | 37840489 | Copia |
| Chr2 | 44438131 | 44438243 | CACTA |
| Chr3 | 19303811 | 19303889 | Gypsy |
| Chr3 | 24082052 | 24082086 | Helitron |
| Chr3 | 28715386 | 28715499 | Gypsy |
| Chr4 | 1065082 | 1065113 | |
| Chr4 | 12421385 | 12421524 | hAT |
| Chr4 | 31745840 | 31745891 | Gypsy |
| Chr5 | 9122774 | 9122819 | Helitron |
| Chr6 | 3599850 | 3599909 | PIF-Harbinger |
| Chr6 | 9047413 | 9047450 | Gypsy |
| Chr7 | 23001451 | 23001483 | Gypsy |
| Chr7 | 30087674 | 30087721 | Gypsy |
| Scaffold_2 | 8360251 | 8360311 | hAT |
| Scaffold_2 | 10204190 | 10204242 | Gypsy |
| Scaffold_2 | 12836466 | 12836516 | Mutator |
| Scaffold_2 | 14254645 | 14254733 | R2 |
| Scaffold_2 | 16165117 | 16165200 | Mutator |
| Scaffold_3 | 741710 | 741752 | Helitron |
| Scaffold_3 | 914678 | 914738 | Helitron |
| Scaffold_3 | 1879031 | 1879100 | PIF-Harbinger |
| Scaffold_3 | 4840118 | 4840221 | hAT |
| Scaffold_3 | 7592880 | 7593001 | PIF-Harbinger |
| Scaffold_3 | 8813968 | 8814009 | Copia |
| Scaffold_3 | 9663043 | 9663100 | hAT |
| Scaffold_4 | 7281145 | 7281242 | Gypsy |
| Scaffold_4 | 11076506 | 11076536 | Gypsy |

| | | | |
|---|---|---|---|
| Scaffold_6 | 6746469 | 6746555 | Copia |
| Scaffold_6 | 10685303 | 10685367 | Copia |
| Scaffold_7 | 1552024 | 1552169 | Copia |
| Scaffold_7 | 1799126 | 1799255 | Helitron |
| Scaffold_7 | 5351025 | 5351052 | Gypsy |
| Scaffold_7 | 6060781 | 6060823 | Gypsy |
| Scaffold_7 | 10142836 | 10142852 | L1 |
| Scaffold_7 | 13240135 | 13240180 | Copia |
| Scaffold_9 | 6945791 | 6945830 | Mutator |

# LIST OF ACRONYMS

**2-ODD** 2-oxoglutarate-dependent dioxygenase

**5HIONG** Indoline-2-one-5-O-*β*-D-glucopyranoside

**AGO** argonaute protein

**AMPO** 2-amino-7-methoxy-phenoxazin-3-one

**ANOVA** analysis of variance

**APO** 2-amino-phenoxazin-3-one

**ATP** Adenosine triphosphate

**BER** excision repair pathway

**BOA** 2-benzoxazolinone

**Bor-4** borky-4

**BX** benzoxazinoids

**Cal-Y BP** calibrated years before present

**CDKA** Cyclin-dependent kinase A

**CMT2** CHROMOMETHYLASE 2

**CMT3** CHROMOMETHYLASE 3

**Col-0** columbia-0

**CRISPR-Cas** clustered regularly interspaced short palindromic repeats

**CSS** Chinese Spring Survey

**CTAB** cetyl trimethylammonium bromide

**DDM1** DECREASE IN DNA METHYLATION 1

**DIBOA** 2,4-dihydroxy-1,4-benzoxazin-3-one

**DIMBOA** 2,4-dihydroxy-7-methoxy-1,4-benzoxazin-3-one

**DIMBOA-Glc** 2,4-dihydroxy-7-methoxy-1,4-benzoxazin-3-one glucoside

**DMR** differentially methylated region

**DMSO** Dimethylsulfoxid

**DNA** deoxyribonucleic acid

**DRM2** DOMAINS REARRANGED METHYLTRANSFERASE 2

**DRM2** DOMAINS REARRANGED METHYLTRANSFERASE 2

**EMS** ethyl methanesulfonate

**epiRILs** epigenetic recombinant inbred lines

**ERD7** EARLY RESPONSIVE TO DEHYDRATION 7

**FAO** food and agriculture organization of the united nations

**FDR** false discovery rate

**gbM** gene body methylation

**GLU** glycosyltransferases

**GMO** genetically modified organism

**HDMBOA-Glc** 2-hydroxy-4,7-dimethoxy-1,4-benzoxazin-3-one glucoside

**HMW** high molecular weight

**HMW** high molecular weight

**IAEA** international atomic energy agency

**JA** jasmonic acid

**KASP** Kompetitive Allele Specific PCR

**KYP** H3K9 histone methyltransferase KRYPTONITE/SUVH4

**LC50** half lethal dose

**LC-HRMS** liquid chromatography–high-resolution mass spectrometry

**MBOA** 6-Methoxy-2-benzoxazolinone

**mC** 5-cytosine methylation

**MET1** DNA METHYLTRANSFERASE 1

**MSAP** methylation-sensitive amplification polymorphism

**MYA** million years ago

**NASC** Nottingham Arabidopsis Stock Centre

**OMT** *O*-methyltransferase

**PCA** principal component analysis

**PCR** polymerase chain reaction

**PPNB** Pre-Pottery Neolithic B

**PSF** plant soil feedback

**PTM** post-translational chemical modification

**Rak-2** raksice-2

**RdDM** RNA-directed DNA methylation

**RNA** ribonucleic acid

**SA** salicylic acid

***Sc*** *Secale cereale*

**SCN** cyst nematode

**siRNAs** small interfering RNA

**SNP** single nucleotide polymorphism

**SUVH5** H3K9 histone methyltransferase 5

**SUVH6** H3K9 histone methyltransferase 6

***Ta*** *Triticum aestivum*

**TE** transposable element

**TF** transcription factor

**TILLING** targeting induced local lesions in genomes

**TRIMBOA-Glc** 2,4,7-trihydroxy-8-methoxy-1,4-benzoxazin-3-one glucoside

**DIM$_2$BOA-Glc** 2,4-dihydroxy-7,8-dimethoxy-1,4-benzoxazin-3-one glucoside

**HDM$_2$BOA-Glc** 2,4-dihydroxy-7,8-dimethoxy-1,4-benzoxazin-3-one glucoside

**TSA** tryptophan synthase

**UGT** UDP-glucosyltransferase

**WGBS** whole genome bisulfite sequencing

**WT** wild type

***Zm*** *Zea mays*

# REFERENCES


1. Kruse, Strandberg, Strandberg. Ecological effects of allelopathic plants. A review, Department of Terrestrial Ecology.

2. Hickman DT, Rasmussen A, Ritz K, Birkett MA, Neve P. Review: Allelochemicals as multi-kingdom plant defence compounds: towards an integrated approach. Pest Manag Sci. 2021;77: 1121–1131.

3. Rizvi SJH, Haque H, Singh VK, Rizvi V. A discipline called allelopathy. In: Rizvi SJH, Rizvi V, editors. Allelopathy: Basic and applied aspects. Dordrecht: Springer Netherlands; 1992. pp. 1–10.

4. Molisch H. Einfluss einer pflanze auf die andere, allelopathie. [cited 10 Jun 2022]. Available: https://agris.fao.org/agris-search/search.do?recordID=US201300388394

5. Cheng F, Cheng Z. Research Progress on the use of Plant Allelopathy in Agriculture and the Physiological and Ecological Mechanisms of Allelopathy. Front Plant Sci. 2015;6: 1020.

6. McCall AC, Fordyce JA. Can optimal defence theory be used to predict the distribution of plant chemical defences? J Ecol. 2010;98: 985–992.

7. Gomaa NH, Hassan MO, Fahmy GM, González L, Hammouda O, Atteya AM. Allelopathic effects of Sonchus oleraceus L. on the germination and seedling growth of crop and weed species. Acta Bot Brasilica. 2014;28: 408–416.

8. Prati D, Bossdorf O. Allelopathic inhibition of germination by Alliaria petiolata (Brassicaceae). Am J Bot. 2004;91: 285–288.

9. Thorpe AS, Thelen GC, Diaconu A, Callaway RM. Root Exudate Is Allelopathic in Invaded Community but Not in Native Community: Field Evidence for the Novel Weapons Hypothesis. J Ecol. 2009;97: 641–645.

10. Qasem JR, Foy CL. Weed Allelopathy, Its Ecological Impacts and Future Prospects. J Crop Prod. 2001;4: 43–119.

11. Weston LA, Duke SO. Weed and Crop Allelopathy. CRC Crit Rev Plant Sci. 2003;22: 367–389.

12. Belz RG. Allelopathy in crop/weed interactions--an update. Pest Manag Sci. 2007;63: 308–326.

13. Weston LA. Utilization of allelopathy for weed management in agroecosystems. Agron J. 1996;88: 860–866.

14. Wu H, Pratley J, Ma W, Haig T. Quantitative trait loci and molecular markers associated with wheat allelopathy. Theor Appl Genet. 2003;107: 1477–1481.

15. Weston LA, Alsaadawi IS, Baerson SR. Sorghum allelopathy--from ecosystem to molecule. J Chem Ecol. 2013;39: 142–153.

16. Kato-Noguchi H, Peters RJ. The role of momilactones in rice allelopathy. J Chem Ecol.

2013;39: 175–185.

17. Cartwright DW, Langcake P, Pryce RJ, Leworthy DP, Ride JP. Isolation and characterization of two phytoalexins from rice as momilactones A and B. Phytochemistry. 1981;20: 535–537.

18. Frey M, Chomet P, Glawischnig E, Stettner C, Grün S, Winklmair A, et al. Analysis of a chemical plant defense mechanism in grasses. Science. 1997;277: 696–699.

19. Schulz M, Marocco A, Tabaglio V, Macias FA, Molinillo JMG. Benzoxazinoids in rye allelopathy - from discovery to application in sustainable weed control and organic farming. J Chem Ecol. 2013;39: 154–174.

20. Kong C-H, Zhang S-Z, Li Y-H, Xia Z-C, Yang X-F, Meiners SJ, et al. Plant neighbor detection and allelochemical response are driven by root-secreted signaling chemicals. Nat Commun. 2018;9: 3867.

21. Zhang S-Z, Li Y-H, Kong C-H, Xu X-H. Interference of allelopathic wheat with different weeds. Pest Manag Sci. 2016;72: 172–178.

22. Li Y-H, Xia Z-C, Kong C-H. Allelobiosis in the interference of allelopathic wheat with weeds. Pest Manag Sci. 2016;72: 2146–2153.

23. Hu L, Robert CAM, Cadot S, Zhang X, Ye M, Li B, et al. Root exudate metabolites drive plant-soil feedbacks on growth and defense by shaping the rhizosphere microbiota. Nat Commun. 2018;9: 2738.

24. Kudjordjie EN, Sapkota R, Steffensen SK, Fomsgaard IS, Nicolaisen M. Maize synthesized benzoxazinoids affect the host associated microbiome. Microbiome. 2019;7: 59.

25. Cotton TEA, Pétriacq P, Cameron DD, Meselmani MA, Schwarzenbacher R, Rolfe SA, et al. Metabolic regulation of the maize rhizobiome by benzoxazinoids. ISME J. 2019;13: 1647–1658.

26. Cadot S, Guan H, Bigalke M, Walser J-C, Jander G, Erb M, et al. Specific and conserved patterns of microbiota-structuring by maize benzoxazinoids in the field. Microbiome. 2021;9: 103.

27. Cadot S, Gfeller V, Hu L, Singh N, Sánchez-Vallet A, Glauser G, et al. Soil composition and plant genotype determine benzoxazinoid-mediated plant-soil feedbacks in cereals. Plant Cell Environ. 2021;44: 3502–3514.

28. Neal AL, Ahmad S, Gordon-Weeks R, Ton J. Benzoxazinoids in root exudates of maize attract Pseudomonas putida to the rhizosphere. PLoS One. 2012;7: e35498.

29. Macías FA, Oliveros-Bastidas A, Marín D, Castellano D, Simonet AM, Molinillo JMG. Degradation Studies on Benzoxazinoids. Soil Degradation Dynamics of (2*R*)-2-*O*-β-d-Glucopyranosyl-4-hydroxy-(2*H*)- 1,4-benzoxazin-3(4*H*)-one (DIBOA-Glc) and Its Degradation Products, Phytotoxic Allelochemicals from Gramineae. Journal of Agricultural and Food Chemistry. 2005. pp. 554–561. doi:10.1021/jf048702l

30. Makowska B, Bakera B, Rakoczy-Trojanowska M. The genetic background of benzoxazinoid biosynthesis in cereals. Acta Physiol Plant. 2015;37: 176.

31. Wolf RB, Spencer GF, Plattner RD. Benzoxazolinone, 2,4-Dihydroxy-1,4-benzoxazin-3-one, and Its Glucoside from Acanthus mollis Seeds

Inhibit Velvetleaf Germination and Growth. J Nat Prod. 1985;48: 59–63.

32. Baumeler A, Hesse M, Werner C. Benzoxazinoids-cyclic hydroxamic acids, lactams and their corresponding glucosides in the genus Aphelandra (Acanthaceae). Phytochemistry. 2000;53: 213–222.

33. Sicker D, Frey M, Schulz M, Gierl A. Role of natural benzoxazinones in the survival strategy of plants. International Review of Cytology. Academic Press; 2000. pp. 319–346.

34. Chiu-Ming C, Ming-Tyan C. 6-methoxybenzoxazolinone and triterpenoids from roots of Scoparia dulcis. Phytochemistry. 1976;15: 1997–1999.

35. Perez FJ. Allelopathic effect of hydroxamic acids from cereals on Avena sativa and A. Fatua. Phytochemistry. 1990;29: 773–776.

36. Niemeyer HM. Hydroxamic acids (4-hydroxy-1,4-benzoxazin-3-ones), defence chemicals in the gramineae. Phytochemistry. 1988. pp. 3349–3358. doi:10.1016/0031-9422(88)80731-3

37. Grün S, Frey M, Gierl A. Evolution of the indole alkaloid biosynthesis in the genus Hordeum: distribution of gramine and DIBOA and isolation of the benzoxazinoid biosynthesis genes from Hordeum lechleri. Phytochemistry. 2005;66: 1264–1272.

38. Venturelli S, Petersen S, Langenecker T, Weigel D, Lauer UM, Becker C. Allelochemicals of the phenoxazinone class act at physiologically relevant concentrations. Plant Signal Behav. 2016;11: e1176818.

39. Frey M, Schullehner K, Dick R, Fiesselmann A, Gierl A. Benzoxazinoid biosynthesis, a model for evolution of secondary metabolic pathways in plants. Phytochemistry. 2009;70: 1645–1651.

40. Schullehner K, Dick R, Vitzthum F, Schwab W, Brandt W, Frey M, et al. Benzoxazinoid biosynthesis in dicot plants. Phytochemistry. 2008;69: 2668–2677.

41. Ebisui K, Ishihara A, Hirai N, Iwamura H. Occurrence of 2,4-Dihydroxy-7-methoxy-1,4-benzoxazin-3-one (DIMBOA) and a β-Glucosidase Specific for Its Glucoside in Maize Seedlings. Zeitschrift für Naturforschung C. 1998;53: 793–798.

42. Nomura T, Ishihara A, Yanagita RC, Endo TR, Iwamura H. Three genomes differentially contribute to the biosynthesis of benzoxazinones in hexaploid wheat. Proc Natl Acad Sci U S A. 2005;102: 16490–16495.

43. Niemeyer HM. Hydroxamic acids derived from 2-hydroxy-2H-1,4-benzoxazin-3(4H)-one: key defense chemicals of cereals. J Agric Food Chem. 2009;57: 1677–1696.

44. Ahmad S, Veyrat N, Gordon-Weeks R, Zhang Y, Martin J, Smart L, et al. Benzoxazinoid metabolites regulate innate immunity against aphids and fungi in maize. Plant Physiol. 2011;157: 317–327.

45. Hanhineva K, Rogachev I, Aura A-M, Aharoni A, Poutanen K, Mykkänen H. Qualitative characterization of benzoxazinoid derivatives in whole grain rye and wheat by LC-MS metabolite profiling. J Agric Food Chem. 2011;59: 921–927.

46. Friebe A, Roth U, Kück P, Schnabl H, Schulz M. Effects of 2,4-dihydroxy-1,4-benzoxazin-3-ones on the activity of plasma membrane H+-ATPase.

Phytochemistry. 1997;44: 979–983.

47. Hashimoto Y, Shudo K. Chemistry of biologically active benzoxazinoids. Phytochemistry. 1996;43: 551–559.

48. Köhler A, Maag D, Veyrat N, Glauser G, Wolfender J-L, Turlings TCJ, et al. Within-plant distribution of 1,4-benzoxazin-3-ones contributes to herbivore niche differentiation in maize. Plant Cell Environ. 2015;38: 1081–1093.

49. Li B, Förster C, Robert CAM, Züst T, Hu L, Machado RAR, et al. Convergent evolution of a metabolic switch between aphid and caterpillar resistance in cereals. Sci Adv. 2018;4: eaat6797.

50. Maag D, Köhler A, Robert CAM, Frey M, Wolfender J-L, Turlings TCJ, et al. Highly localized and persistent induction of Bx1-dependent herbivore resistance factors in maize. Plant J. 2016;88: 976–991.

51. Guo J, Guo J, He K, Bai S, Zhang T, Zhao J, et al. Physiological Responses Induced by Ostrinia furnacalis (Lepidoptera: Crambidae) Feeding in Maize and Their Effects on O. furnacalis Performance. J Econ Entomol. 2017;110: 739–747.

52. Tzin V, Hojo Y, Strickler SR, Bartsch LJ, Archer CM, Ahern KR, et al. Rapid defense responses in maize leaves induced by Spodoptera exigua caterpillar feeding. J Exp Bot. 2017;68: 4709–4723.

53. Yan F, Liang X, Zhu X. The role of DIMBOA on the feeding of Asian corn borer, Ostrinia furnacalis (Guenée) (Lep., Pyralidae). J Appl Entomol. 1999;123: 49–53.

54. Dafoe NJ, Huffaker A, Vaughan MM, Duehl AJ, Teal PE, Schmelz EA. Rapidly induced chemical defenses in maize stems and their effects on short-term growth of Ostrinia nubilalis. J Chem Ecol. 2011;37: 984–991.

55. Klun JA, Tipton CL, Brindley TA. 2,4-Dihydroxy-7-methoxy-1,4-benzoxazin-3-one (DIMBOA), an Active Agent in the Resistance of Maize to the European Corn Borer. J Econ Entomol. 1967;60: 1529–1533.

56. Glauser G, Marti G, Villard N, Doyen GA, Wolfender J-L, Turlings TCJ, et al. Induction and detoxification of maize 1,4-benzoxazin-3-ones by insect herbivores. Plant J. 2011;68: 901–911.

57. Shavit R, Batyrshina ZS, Dotan N, Tzin V. Cereal aphids differently affect benzoxazinoid levels in durum wheat. PLoS One. 2018;13: e0208103.

58. Meihls LN, Handrick V, Glauser G, Barbier H, Kaur H, Haribal MM, et al. Natural variation in maize aphid resistance is associated with 2,4-dihydroxy-7-methoxy-1,4-benzoxazin-3-one glucoside methyltransferase activity. Plant Cell. 2013;25: 2341–2355.

59. Betsiashvili M, Ahern KR, Jander G. Additive effects of two quantitative trait loci that confer Rhopalosiphum maidis (corn leaf aphid) resistance in maize inbred line Mo17. J Exp Bot. 2015;66: 571–578.

60. Song J, Liu H, Zhuang H, Zhao C, Xu Y, Wu S, et al. Transcriptomics and Alternative Splicing Analyses Reveal Large Differences between Maize Lines B73 and Mo17 in Response to Aphid Rhopalosiphum padi Infestation. Front Plant Sci. 2017;8: 1738.

61. Robert CAM, Veyrat N, Glauser G, Marti G, Doyen GR, Villard N, et al. A specialist root

herbivore exploits defensive metabolites to locate nutritious tissues. Ecol Lett. 2012;15: 55–64.

62. Robert CA, Zhang X, Machado RA, Schirmer S, Lori M, Mateo P, et al. Sequestration and activation of plant toxins protect the western corn rootworm from enemies at multiple trophic levels. Elife. 2017;6. doi:10.7554/eLife.29307

63. Sasai H, Ishida M, Murakami K, Tadokoro N, Ishihara A, Nishida R, et al. Species-specific glucosylation of DIMBOA in larvae of the rice Armyworm. Biosci Biotechnol Biochem. 2009;73: 1333–1338.

64. Gianoli E, Niemeyer HM. DIBOA in wild Poaceae: Sources of resistance to the Russian wheat aphid (Diuraphis noxia) and the greenbug (Schizaphis graminum). Euphytica. 1998;102: 317–321.

65. Meyer SLF, Rice CP, Zasada IA. DIBOA: Fate in soil and effects on root-knot nematode egg numbers. Soil Biol Biochem. 2009;41: 1555–1560.

66. Oikawa A, Ishihara A, Tanaka C, Mori N, Tsuda M, Iwamura H. Accumulation of HDMBOA-Glc is induced by biotic stresses prior to the release of MBOA in maize leaves. Phytochemistry. 2004;65: 2995–3001.

67. Virtanen AI, Hietala PK. 2 (3)-Benzoxazolinone, an anti-Fusarium factor in rye seedlings. Acta Chemica Scandinavica. MUNKSGAARD INT PUBL LTD 35 NORRE SOGADE, PO BOX 2148, DK-1016 COPENHAGEN …; 1955. pp. 1543–1544.

68. Glenn AE, Bacon CW. FDB2 encodes a member of the arylamine N-acetyltransferase family and is necessary for biotransformation of benzoxazolinones by Fusarium verticillioides. J Appl Microbiol. 2009;107: 657–671.

69. Glenn AE, Hinton DM, Yates IE, Bacon CW. Detoxification of corn antimicrobial compounds as the basis for isolating Fusarium verticillioides and some other Fusarium species from corn. Appl Environ Microbiol. 2001;67: 2973–2981.

70. Etzerodt T, Maeda K, Nakajima Y, Laursen B, Fomsgaard IS, Kimura M. 2,4-dihydroxy-7-methoxy-2H-1,4-benzoxazin-3(4H)-one (DIMBOA) inhibits trichothecene production by Fusarium graminearum through suppression of Tri6 expression. Int J Food Microbiol. 2015;214: 123–128.

71. Gleńsk M, Gajda B, Franiczek R, Krzyżanowska B, Biskup I, Włodarczyk M. In vitro evaluation of the antioxidant and antimicrobial activity of DIMBOA [2,4-dihydroxy-7-methoxy-2H-1,4-benzoxazin-3(4H)-one]. Nat Prod Res. 2016;30: 1305–1308.

72. Bravo HR, Lazo W. Antialgal and Antifungal Activity of Natural Hydroxamic Acids and Related Compounds. J Agric Food Chem. 1996;44: 1569–1571.

73. Bravo HR, Copaja SV, Lazo W. Antimicrobial Activity of Natural 2-Benzoxazolinones and Related Derivatives. J Agric Food Chem. 1997;45: 3255–3257.

74. Neal A, Ton J. Systemic defense priming by*Pseudomonas putida*KT2440 in maize depends on benzoxazinoid exudation from the roots. Plant Signaling & Behavior. 2013. p. e22655. doi:10.4161/psb.22655

75. Whitney NJ, Mortimore CG. Effect of 6-Methoxybenzoxazolinone on the Growth of Xanthomonas stewartii (Erw. Smith) Dowson and its Presence in Sweet Corn (Zea mays

var. saccharata Bailey). Nature. 1961;189: 596–597.

76. Corcuera LJ, Woodward MD, Helgeson JP, Kelman A, Upper CD. 2,4-Dihydroxy-7-methoxy-2H-1,4-benzoxazin-3(4H)-one, an Inhibitor from Zea mays with Differential Activity against Soft Rotting Erwinia Species. Plant Physiol. 1978;61: 791–795.

77. Corn metabolites affect growth and virulence of Agrobacterium tumefaciens. In: PNAS [Internet]. [cited 16 May 2022]. Available: https://www.pnas.org/doi/abs/10.1073/pnas.87.10.3879

78. Putnam AR, DeFrank J. Use of phytotoxic plant residues for selective weed control. Crop Prot. 1983;2: 173–181.

79. Belz RG, Hurle K. Differential exudation of two benzoxazinoids--one of the determining factors for seedling allelopathy of Triticeae species. J Agric Food Chem. 2005;53: 250–261.

80. Baerson SR, Sánchez-Moreiras A, Pedrol-Bonjoch N, Schulz M, Kagan IA, Agarwal AK, et al. Detoxification and transcriptome response in Arabidopsis seedlings exposed to the allelochemical benzoxazolin-2(3H)-one. J Biol Chem. 2005;280: 21867–21881.

81. von Rad U, Hüttl R, Lottspeich F, Gierl A, Frey M. Two glucosyltransferases are involved in detoxification of benzoxazinoids in maize. Plant J. 2001;28: 633–642.

82. Venturelli S, Belz RG, Kämper A, Berger A, von Horn K, Wegner A, et al. Plants Release Precursors of Histone Deacetylase Inhibitors to Suppress Growth of Competitors. Plant Cell. 2015;27: 3175–3189.

83. Macías FA, Marín D, Oliveros-Bastidas A, Castellano D, Simonet AM, Molinillo JMG. Structure-activity relationship (SAR) studies of benzoxazinones, their degradation products, and analogues. Phytotoxicity on problematic weeds Avena fatua L. and Lolium rigidum Gaud. J Agric Food Chem. 2006;54: 1040–1048.

84. Quader M, Daggard G, Barrow R, Walker S, Sutherland MW. Allelopathy, DIMBOA production and genetic variability in accessions of Triticum speltoides. J Chem Ecol. 2001;27: 747–760.

85. Lu CH, Liu XG, Xu J, Dong FS, Zhang CP, Tian YY, et al. Enhanced Exudation of DIMBOA and MBOA by Wheat Seedlings Alone and in Proximity to Wild Oat (Avena fatua) and Flixweed (Descurainia sophia). Weed Sci. 2012;60: 360–365.

86. Hussain MI, Vieites-Álvarez Y, Otero P, Prieto MA, Simal-Gandara J, Reigosa MJ, et al. Weed pressure determines the chemical profile of wheat (Triticum aestivum L.) and its allelochemicals potential. Pest Manag Sci. 2022;78: 1605–1619.

87. Tabaglio V, Marocco A, Schulz M. Allelopathic cover crop of rye for integrated weed control in sustainable agroecosystems. Ital J Agronomy. 2013;8: e5–e5.

88. Rakoczy-Trojanowska M, Święcicka M, Bakera B, Kowalczyk M, Stochmal A, Bolibok L. Cocultivating rye with berseem clover affects benzoxazinoid production and expression of related genes. Crop Sci. 2020;60: 3228–3246.

89. Turner TR, James EK, Poole PS. The plant microbiome. Genome Biol. 2013;14: 209.

90. Sasse J, Martinoia E, Northen T. Feed Your Friends: Do Plant Exudates Shape the Root Microbiome? Trends Plant Sci. 2018;23: 25–41.

91. Pieterse CMJ, Zamioudis C, Berendsen RL, Weller DM, Van Wees SCM, Bakker PAHM. Induced systemic resistance by beneficial microbes. Annu Rev Phytopathol. 2014;52: 347–375.

92. Martyniuk S, Stochmal A, Macías FA, Marín D, Oleszek W. Effects of some benzoxazinoids on in vitro growth of Cephalosporium gramineum and other fungi pathogenic to cereals and on Cephalosporium stripe of winter wheat. J Agric Food Chem. 2006;54: 1036–1039.

93. Schalchli H, Pardo F, Hormazábal E, Palma R, Guerrero J, Bensch E. Antifungal activity of wheat root exudate extracts on Gaeumannomyces graminis var. Tritici growth. J Soil Sci Plant Nutr. 2012;12: 329–337.

94. Maresh J, Zhang J, Lynn DG. The innate immunity of maize and the dynamic chemical strategies regulating two-component signal transduction in Agrobacterium tumefaciens. ACS Chem Biol. 2006;1: 165–175.

95. Putten WH van der, van der Putten WH, Bardgett RD, Bever JD, Martijn Bezemer T, Casper BB, et al. Plant-soil feedbacks: the past, the present and future challenges. Journal of Ecology. 2013. pp. 265–276. doi:10.1111/1365-2745.12054

96. Poveda J, Eugui D, Velasco P. Natural control of plant pathogens through glucosinolates: an effective strategy against fungi and oomycetes. Phytochem Rev. 2020;19: 1045–1059.

97. Brennan RJB, Glaze-Corcoran S, Wick R, Hashemi M. Biofumigation: An alternative strategy for the control of plant parasitic nematodes. J Integr Agric. 2020;19: 1680–1690.

98. Nomura T, Ishihara A, Imaishi H, Endo TR, Ohkawa H, Iwamura H. Molecular characterization and chromosomal localization of cytochrome P450 genes involved in the biosynthesis of cyclic hydroxamic acids in hexaploid wheat. Mol Genet Genomics. 2002;267: 210–217.

99. Tanwir F, Dionisio G, Adhikari KB, Fomsgaard IS, Gregersen PL. Biosynthesis and chemical transformation of benzoxazinoids in rye during seed germination and the identification of a rye Bx6-like gene. Phytochemistry. 2017;140: 95–107.

100. Niculaes C, Abramov A, Hannemann L, Frey M. Plant Protection by Benzoxazinoids—Recent Insights into Biosynthesis and Function. Agronomy. 2018;8: 143.

101. Kriechbaumer V, Weigang L, Fiesselmann A, Letzel T, Frey M, Gierl A, et al. Characterisation of the tryptophan synthase alpha subunit in maize. BMC Plant Biol. 2008;8: 44.

102. Jonczyk R, Schmidt H, Osterrieder A, Fiesselmann A, Schullehner K, Haslbeck M, et al. Elucidation of the final reactions of DIMBOA-glucoside biosynthesis in maize: characterization of Bx6 and Bx7. Plant Physiol. 2008;146: 1053–1063.

103. Handrick V, Robert CAM, Ahern KR, Zhou S, Machado RAR, Maag D, et al. Biosynthesis of 8-O-Methylated Benzoxazinoid Defense Compounds in Maize. Plant Cell. 2016;28: 1682–1700.

104. Zhou S, Richter A, Jander G. Beyond Defense: Multiple Functions of Benzoxazinoids in Maize Metabolism. Plant Cell Physiol. 2018;59: 1528–1537.

105. Malook S ul, Qi J, Hettenhausen C, Xu Y, Zhang C, Zhang J, et al. The oriental armyworm (Mythimna separata) feeding induces systemic defence responses within and between maize leaves. Philos Trans R Soc Lond B Biol Sci. 2019;374: 20180307.

106. Zhou P, Li Z, Magnusson E, Gomez Cano F, Crisp PA, Noshay JM, et al. Meta Gene Regulatory Networks in Maize Highlight Functionally Relevant Regulatory Interactions. Plant Cell. 2020;32: 1377–1396.

107. Gao L, Shen G, Zhang L, Qi J, Zhang C, Ma C, et al. An efficient system composed of maize protoplast transfection and HPLC-MS for studying the biosynthesis and regulation of maize benzoxazinoids. Plant Methods. 2019;15: 144.

108. Batyrshina ZS, Shavit R, Yaakov B, Bocobza S, Tzin V. The transcription factor TaMYB31 regulates the benzoxazinoid biosynthetic pathway in wheat. J Exp Bot. 2022;73: 5634–5649.

109. Wegel E, Koumproglou R, Shaw P, Osbourn A. Cell type-specific chromatin decondensation of a metabolic gene cluster in oats. Plant Cell. 2009;21: 3926–3936.

110. Zheng L, McMullen MD, Bauer E, Schön C-C, Gierl A, Frey M. Prolonged expression of the BX1 signature enzyme is associated with a recombination hotspot in the benzoxazinoid gene cluster in Zea mays. J Exp Bot. 2015;66: 3917–3930.

111. Oka R, Zicola J, Weber B, Anderson SN, Hodgman C, Gent JI, et al. Genome-wide mapping of transcriptional enhancer candidates using DNA and chromatin features in maize. Genome Biol. 2017;18: 137.

112. Sue M, Nakamura C, Nomura T. Dispersed benzoxazinone gene cluster: molecular characterization and chromosomal localization of glucosyltransferase and glucosidase genes in wheat and rye. Plant Physiol. 2011;157: 985–997.

113. Bakera B, Makowska B, Groszyk J, Niziołek M, Orczyk W, Bolibok-Brągoszewska H, et al. Structural characteristics of ScBx genes controlling the biosynthesis of hydroxamic acids in rye (Secale cereale L.). J Appl Genet. 2015;56: 287–298.

114. Salse J, Bolot S, Throude M, Jouffe V, Piegu B, Quraishi UM, et al. Identification and characterization of shared duplications between rice and wheat provide new insight into grass genome evolution. Plant Cell. 2008;20: 11–24.

115. Nomura T, Ishihara A, Imaishi H, Ohkawa H, Endo TR, Iwamura H. Rearrangement of the genes for the biosynthesis of benzoxazinones in the evolution of Triticeae species. Planta. 2003;217: 776–782.

116. Dick R, Rattei T, Haslbeck M, Schwab W, Gierl A, Frey M. Comparative analysis of benzoxazinoid biosynthesis in monocots and dicots: independent recruitment of stabilization and activation functions. Plant Cell. 2012;24: 915–928.

117. Hannemann L, Lucaciu CR, Sharma S, Rattei T, Mayer KFX, Gierl A, et al. A promiscuous beta-glucosidase is involved in benzoxazinoid deglycosylation in Lamium galeobdolon. Phytochemistry. 2018;156: 224–233.

118. Dubcovsky J, Dvorak J. Genome plasticity a key factor in the success of polyploid wheat under domestication. Science. 2007;316: 1862–1866.

119. Levy AA, Feldman M. Evolution and origin of bread wheat. Plant Cell. 2022. doi:10.1093/plcell/koac130

120. Heun M, Schäfer-Pregl R, Klawan D, Castagna R, Accerbi M, Borghi B, et al. Site of Einkorn Wheat Domestication Identified by DNA Fingerprinting. Science. 1997;278: 1312–1314.

121. Luo M-C, Yang Z-L, You FM, Kawahara T, Waines JG, Dvorak J. The structure of wild and domesticated emmer wheat populations, gene flow between them, and the site of emmer domestication. Theor Appl Genet. 2007;114: 947–959.

122. Nave M, Avni R, Çakır E, Portnoy V, Sela H, Pourkheirandish M, et al. Wheat domestication in light of haplotype analyses of the Brittle rachis 1 genes (BTR1-A and BTR1-B). Plant Sci. 2019;285: 193–199.

123. Kislev ME. Emergence of wheat agriculture. Paléorient. 1984;10: 61–70.

124. Nalam VJ, Vales MI, Watson CJW, Kianian SF, Riera-Lizarazu O. Map-based analysis of genes affecting the brittle rachis character in tetraploid wheat (Triticum turgidum L.). Theor Appl Genet. 2006;112: 373–381.

125. Dvorak J, Luo M-C, Yang Z-L, Zhang H-B. The structure of the Aegilops tauschii genepool and the evolution of hexaploid wheat. Theor Appl Genet. 1998;97: 657–670.

126. Delorean E, Gao L, Lopez JFC, Open Wild Wheat Consortium, Wulff BBH, Ibba MI, et al. High molecular weight glutenin gene diversity in Aegilops tauschii demonstrates unique origin of superior wheat quality. Commun Biol. 2021;4: 1242.

127. Salamini F, Ozkan H, Brandolini A, Schäfer-Pregl R, Martin W. Genetics and geography of wild cereal domestication in the near east. Nat Rev Genet. 2002;3: 429–441.

128. Jantasuriyarat C, Vales MI, Watson CJW, Riera-Lizarazu O. Identification and mapping of genetic loci affecting the free-threshing habit and spike compactness in wheat (Triticum aestivum L.). Theor Appl Genet. 2004;108: 261–273.

129. Simons KJ, Fellers JP, Trick HN, Zhang Z, Tai Y-S, Gill BS, et al. Molecular Characterization of the Major Wheat Domestication Gene Q. Genetics. 2006;172: 547–555.

130. Uauy C, Distelfeld A, Fahima T, Blechl A, Dubcovsky J. A NAC Gene regulating senescence improves grain protein, zinc, and iron content in wheat. Science. 2006;314: 1298–1301.

131. McFADDEN ES, Sears ER. The origin of Triticum spelta and its free-threshing hexaploid relatives. J Hered. 1946;37: 81 107.

132. Feldman M, Levy AA. Allopolyploidy – a shaping force in the evolution of wheat genomes. Cytogenetic and Genome Research. 2005. pp. 250–258. doi:10.1159/000082407

133. Li L-F, Zhang Z-B, Wang Z-H, Li N, Sha Y, Wang X-F, et al. Genome sequences of five Sitopsis species of Aegilops and the origin of polyploid wheat B subgenome. Mol Plant. 2022;15: 488–503.

134. Marcussen T, Sandve SR, Heier L, Spannagl M, Pfeifer M, International Wheat Genome Sequencing Consortium, et al. Ancient hybridizations among the ancestral genomes of bread wheat. Science. 2014;345: 1250092.

135. Glémin S, Scornavacca C, Dainat J, Burgarella C, Viader V, Ardisson M, et al.

Pervasive hybridizations in the history of wheat relatives. Sci Adv. 2019;5: eaav9188.

136. Avni R, Lux T, Minz-Dub A, Millet E, Sela H, Distelfeld A, et al. Genome sequences of three Aegilops species of the section Sitopsis reveal phylogenetic relationships and provide resources for wheat improvement. Plant J. 2022;110: 179–192.

137. Bottley A, Xia GM, Koebner RMD. Homoeologous gene silencing in hexaploid wheat. Plant J. 2006;47: 897–906.

138. Shitsukawa N, Tahira C, Kassai K-I, Hirabayashi C, Shimizu T, Takumi S, et al. Genetic and epigenetic alteration among three homoeologous genes of a class E MADS box gene in hexaploid wheat. Plant Cell. 2007;19: 1723–1737.

139. Akhunova AR, Matniyazov RT, Liang H, Akhunov ED. Homoeolog-specific transcriptional bias in allopolyploid wheat. BMC Genomics. 2010;11: 505.

140. Chen L, Hao L, Parry MAJ, Phillips AL, Hu Y-G. Progress in TILLING as a tool for functional genomics and improvement of crops. J Integr Plant Biol. 2014;56: 425–443.

141. Gilchrist E, Haughn G. Reverse genetics techniques: engineering loss and gain of gene function in plants. Brief Funct Genomics. 2010;9: 103–110.

142. Parry MAJ, Madgwick PJ, Bayon C, Tearall K, Hernandez-Lopez A, Baudo M, et al. Mutation discovery for crop improvement. J Exp Bot. 2009;60: 2817–2825.

143. Shama Rao HK, Sears ER. Chemical mutagenesis in Triticum aestivum. Mutat Res/Fundam Mol Mech Mutag. 1964;1: 387–399.

144. McCallum CM, Comai L, Greene EA, Henikoff S. Targeted screening for induced mutations. Nat Biotechnol. 2000;18: 455–457.

145. Jung C, Till B. Mutagenesis and genome editing in crop improvement: perspectives for the global regulatory landscape. Trends Plant Sci. 2021;26: 1258–1269.

146. Uauy C, Wulff BBH, Dubcovsky J. Combining Traditional Mutagenesis with New High-Throughput Sequencing and Genome Editing to Reveal Hidden Variation in Polyploid Wheat. Annu Rev Genet. 2017;51: 435–454.

147. Tsai H, Missirian V, Ngo KJ, Tran RK, Chan SR, Sundaresan V, et al. Production of a high-efficiency TILLING population through polyploidization. Plant Physiol. 2013;161: 1604–1614.

148. Krasileva KV, Vasquez-Gross HA, Howell T, Bailey P, Paraiso F, Clissold L, et al. Uncovering hidden variation in polyploid wheat. Proc Natl Acad Sci U S A. 2017;114: E913–E921.

149. Adamski NM, Borrill P, Brinton J, Harrington SA, Marchal C, Bentley AR, et al. A roadmap for gene functional characterisation in crops with large genomes: Lessons from polyploid wheat. Elife. 2020;9. doi:10.7554/eLife.55646

150. Kashtwari M, Wani AA, Rather RN. TILLING: an alternative path for crop improvement. J Crop Improv. 2019;33: 83–109.

151. Acevedo-Garcia J, Spencer D, Thieron H, Reinstädler A, Hammond-Kosack K, Phillips AL, et al. mlo-based powdery mildew resistance in hexaploid bread wheat generated by a non-transgenic TILLING approach. Plant Biotechnol J. 2017;15: 367–378.

152. Sestili F, Palombieri S, Botticella E, Mantovani P, Bovina R, Lafiandra D. TILLING mutants of durum wheat result in a high amylose phenotype and provide information on alternative splicing mechanisms. Plant Sci. 2015;233: 127–133.

153. Doğan ES, Liu C. Three-dimensional chromatin packing and positioning of plant genomes. Nat Plants. 2018;4: 521–529.

154. Luger K, Mäder AW, Richmond RK, Sargent DF, Richmond TJ. Crystal structure of the nucleosome core particle at 2.8 A resolution. Nature. 1997;389: 251–260.

155. Zhang H, Lang Z, Zhu J-K. Dynamics and function of DNA methylation in plants. Nat Rev Mol Cell Biol. 2018;19: 489–506.

156. Lämke J, Bäurle I. Epigenetic and chromatin-based mechanisms in environmental stress adaptation and stress memory in plants. Genome Biol. 2017;18: 124.

157. Law JA, Jacobsen SE. Establishing, maintaining and modifying DNA methylation patterns in plants and animals. Nat Rev Genet. 2010;11: 204–220.

158. Beaulaurier J, Schadt EE, Fang G. Deciphering bacterial epigenomes using modern sequencing technologies. Nat Rev Genet. 2019;20: 157–172.

159. Liang Z, Geng Y, Gu X. Adenine Methylation: New Epigenetic Marker of DNA and mRNA. Mol Plant. 2018;11: 1219–1221.

160. Liang Z, Shen L, Cui X, Bao S, Geng Y, Yu G, et al. DNA N6-Adenine Methylation in Arabidopsis thaliana. Dev Cell. 2018;45: 406–416.e3.

161. Zhang Q, Liang Z, Cui X, Ji C, Li Y, Zhang P, et al. N6-Methyladenine DNA Methylation in Japonica and Indica Rice Genomes and Its Association with Gene Expression, Plant Development, and Stress Responses. Mol Plant. 2018;11: 1492–1508.

162. Zhou C, Wang C, Liu H, Zhou Q, Liu Q, Guo Y, et al. Identification and analysis of adenine N6-methylation sites in the rice genome. Nat Plants. 2018;4: 554–563.

163. Zhang X, Yazaki J, Sundaresan A, Cokus S, Chan SW-L, Chen H, et al. Genome-wide high-resolution mapping and functional analysis of DNA methylation in arabidopsis. Cell. 2006;126: 1189–1201.

164. Finnegan EJ, Peacock WJ, Dennis ES. Reduced DNA methylation in Arabidopsis thaliana results in abnormal plant development. Proc Natl Acad Sci U S A. 1996;93: 8449–8454.

165. Saze H, Mittelsten Scheid O, Paszkowski J. Maintenance of CpG methylation is essential for epigenetic inheritance during plant gametogenesis. Nat Genet. 2003;34: 65–69.

166. Lindroth AM, Cao X, Jackson JP, Zilberman D, McCallum CM, Henikoff S, et al. Requirement of CHROMOMETHYLASE3 for maintenance of CpXpG methylation. Science. 2001;292: 2077–2080.

167. Bartee L, Malagnac F, Bender J. Arabidopsis cmt3 chromomethylase mutations block non-CG methylation and silencing of an endogenous gene. Genes Dev. 2001;15: 1753–1758.

168. Jackson JP, Lindroth AM, Cao X, Jacobsen SE. Control of CpNpG DNA methylation

by the KRYPTONITE histone H3 methyltransferase. Nature. 2002;416: 556–560.

169. Du J, Johnson LM, Groth M, Feng S, Hale CJ, Li S, et al. Mechanism of DNA methylation-directed histone methylation by KRYPTONITE. Mol Cell. 2014;55: 495–504.

170. Stroud H, Do T, Du J, Zhong X, Feng S, Johnson L, et al. Non-CG methylation patterns shape the epigenetic landscape in Arabidopsis. Nat Struct Mol Biol. 2014;21: 64–72.

171. Cao X, Jacobsen SE. Role of the arabidopsis DRM methyltransferases in de novo DNA methylation and gene silencing. Curr Biol. 2002;12: 1138–1144.

172. Gong Z, Morales-Ruiz T, Ariza RR, Roldán-Arjona T, David L, Zhu JK. ROS1, a repressor of transcriptional gene silencing in Arabidopsis, encodes a DNA glycosylase/lyase. Cell. 2002;111: 803–814.

173. Cokus SJ, Feng S, Zhang X, Chen Z, Merriman B, Haudenschild CD, et al. Shotgun bisulphite sequencing of the Arabidopsis genome reveals DNA methylation patterning. Nature. 2008;452: 215–219.

174. Takuno S, Gaut BS. Gene body methylation is conserved between plant orthologs and is of evolutionary consequence. Proc Natl Acad Sci U S A. 2013;110: 1797–1802.

175. Niederhuth CE, Bewick AJ, Ji L, Alabady MS, Kim KD, Li Q, et al. Widespread natural variation of DNA methylation within angiosperms. Genome Biol. 2016;17: 194.

176. Matzke MA, Mosher RA. RNA-directed DNA methylation: an epigenetic pathway of increasing complexity. Nat Rev Genet. 2014;15: 394–408.

177. Takuno S, Ran J-H, Gaut BS. Evolutionary patterns of genic DNA methylation vary across land plants. Nat Plants. 2016;2: 15222.

178. Lang Z, Wang Y, Tang K, Tang D, Datsenka T, Cheng J, et al. Critical roles of DNA demethylation in the activation of ripening-induced genes and inhibition of ripening-repressed genes in tomato fruit. Proc Natl Acad Sci U S A. 2017;114: E4511–E4519.

179. Alleman M, Sidorenko L, McGinnis K, Seshadri V, Dorweiler JE, White J, et al. An RNA-dependent RNA polymerase is required for paramutation in maize. Nature. 2006;442: 295–298.

180. Erhard KF Jr, Stonaker JL, Parkinson SE, Lim JP, Hale CJ, Hollick JB. RNA polymerase IV functions in paramutation in Zea mays. Science. 2009;323: 1201–1205.

181. Wei L, Gu L, Song X, Cui X, Lu Z, Zhou M, et al. Dicer-like 3 produces transposable element-associated 24-nt siRNAs that control agricultural traits in rice. Proc Natl Acad Sci U S A. 2014;111: 3877–3882.

182. Liu R, How-Kit A, Stammitti L, Teyssier E, Rolin D, Mortain-Bertrand A, et al. A DEMETER-like DNA demethylase governs tomato fruit ripening. Proc Natl Acad Sci U S A. 2015;112: 10804–10809.

183. Berr A, Shafiq S, Shen W-H. Histone modifications in transcriptional activation during plant development. Biochim Biophys Acta. 2011;1809: 567–576.

184. Strahl BD, Allis CD. The language of covalent histone modifications. Nature. 2000;403: 41–45.

185. Ramos-Cruz D, Troyee AN, Becker C. Epigenetics in plant organismic interactions. Curr Opin Plant Biol. 2021;61: 102060.

186. Zhang Y-Y, Fischer M, Colot V, Bossdorf O. Epigenetic variation creates potential for evolution of plant phenotypic plasticity. New Phytol. 2013;197: 314–322.

187. Liu J, He Z. Small DNA Methylation, Big Player in Plant Abiotic Stress Responses and Memory. Front Plant Sci. 2020;11: 595603.

188. Chang Y-N, Zhu C, Jiang J, Zhang H, Zhu J-K, Duan C-G. Epigenetic regulation in plant abiotic stress responses. J Integr Plant Biol. 2020;62: 563–580.

189. Alonso C, Ramos-Cruz D, Becker C. The role of plant epigenetics in biotic interactions. New Phytol. 2019;221: 731–737.

190. Ma Y, Min L, Wang M, Wang C, Zhao Y, Li Y, et al. Disrupted Genome Methylation in Response to High Temperature Has Distinct Affects on Microspore Abortion and Anther Indehiscence. Plant Cell. 2018;30: 1387–1403.

191. Shen X, De Jonge J, Forsberg SKG, Pettersson ME, Sheng Z, Hennig L, et al. Natural CMT2 variation is associated with genome-wide methylation changes and temperature seasonality. PLoS Genet. 2014;10: e1004842.

192. Lai Y-S, Zhang X, Zhang W, Shen D, Wang H, Xia Y, et al. The association of changes in DNA methylation with temperature-dependent sex determination in cucumber. J Exp Bot. 2017;68: 2899–2912.

193. Xu J, Zhou S, Gong X, Song Y, van Nocker S, Ma F, et al. Single-base methylome analysis reveals dynamic epigenomic differences associated with water deficit in apple. Plant Biotechnol J. 2018;16: 672–687.

194. López M-E, Roquis D, Becker C, Denoyes B, Bucher E. DNA methylation dynamics during stress response in woodland strawberry (Fragaria vesca). Hortic Res. 2022; uhac174.

195. González RM, Ricardi MM, Iusem ND. Epigenetic marks in an adaptive water stress-responsive gene in tomato roots under normal and drought conditions. Epigenetics. 2013;8: 864–872.

196. Ma N, Chen W, Fan T, Tian Y, Zhang S, Zeng D, et al. Low temperature-induced DNA hypermethylation attenuates expression of RhAG, an AGAMOUS homolog, and increases petal number in rose (Rosa hybrida). BMC Plant Biol. 2015;15: 237.

197. Iwasaki M, Hyvärinen L, Piskurewicz U, Lopez-Molina L. Non-canonical RNA-directed DNA methylation participates in maternal and environmental control of seed dormancy. Elife. 2019. Available: https://elifesciences.org/articles/37434

198. Liu T, Li Y, Duan W, Huang F, Hou X. Cold acclimation alters DNA methylation patterns and confers tolerance to heat and increases growth rate in Brassica rapa. J Exp Bot. 2017;68: 1213–1224.

199. Hewezi T, Pantalone V, Bennett M, Neal Stewart C Jr, Burch-Smith TM. Phytopathogen-induced changes to plant methylomes. Plant Cell Rep. 2018;37: 17–23.

200. Troyee AN, Medrano M, Müller C, Alonso C. Variation in DNA methylation and response to short-term herbivory in Thlaspi arvense. Flora. 2022;293: 152106.

201. Dowen RH, Pelizzola M, Schmitz RJ, Lister R, Dowen JM, Nery JR, et al. Widespread dynamic DNA methylation in response to biotic stress. Proc Natl Acad Sci U S A. 2012;109: E2183–91.

202. Yu A, Lepère G, Jay F, Wang J, Bapaume L, Wang Y, et al. Dynamics and biological relevance of DNA demethylation in Arabidopsis antibacterial defense. Proc Natl Acad Sci U S A. 2013;110: 2389–2394.

203. Geng S, Kong X, Song G, Jia M, Guan J, Wang F, et al. DNA methylation dynamics during the interaction of wheat progenitor Aegilops tauschii with the obligate biotrophic fungus Blumeria graminis f. sp. tritici. New Phytol. 2019;221: 1023–1035.

204. Rambani A, Rice JH, Liu J, Lane T, Ranjan P, Mazarei M, et al. The Methylome of Soybean Roots during the Compatible Interaction with the Soybean Cyst Nematode. Plant Physiol. 2015;168: 1364–1377.

205. Hewezi T, Lane T, Piya S, Rambani A, Rice JH, Staton M. Cyst Nematode Parasitism Induces Dynamic Changes in the Root Epigenome. Plant Physiol. 2017;174: 405–420.

206. Reinders J, Wulff BBH, Mirouze M, Marí-Ordóñez A, Dapp M, Rozhon W, et al. Compromised stability of DNA methylation and transposon immobilization in mosaic Arabidopsis epigenomes. Genes Dev. 2009;23: 939–950.

207. Johannes F, Porcher E, Teixeira FK, Saliba-Colombani V, Simon M, Agier N, et al. Assessing the Impact of Transgenerational Epigenetic Variation on Complex Traits. PLoS Genet. 2009;5: e1000530.

208. Popova OV, Dinh HQ, Aufsatz W, Jonak C. The RdDM pathway is required for basal heat tolerance in Arabidopsis. Mol Plant. 2013;6: 396–410.

209. Xie H, Sun Y, Cheng B, Xue S, Cheng D, Liu L, et al. Variation in ICE1 Methylation Primarily Determines Phenotypic Variation in Freezing Tolerance in Arabidopsis thaliana. Plant Cell Physiol. 2019;60: 152–165.

210. Conde D, Le Gac A-L, Perales M, Dervinis C, Kirst M, Maury S, et al. Chilling-responsive DEMETER-LIKE DNA demethylase mediates in poplar bud break. Plant Cell Environ. 2017;40: 2236–2249.

211. Conde D, Moreno-Cortés A, Dervinis C, Ramos-Sánchez JM, Kirst M, Perales M, et al. Overexpression of DEMETER, a DNA demethylase, promotes early apical bud maturation in poplar. Plant Cell Environ. 2017;40: 2806–2819.

212. López Sánchez A, Stassen JHM, Furci L, Smith LM, Ton J. The role of DNA (de)methylation in immune responsiveness of Arabidopsis. Plant J. 2016;88: 361–374.

213. Espinas NA, Saze H, Saijo Y. Epigenetic Control of Defense Signaling and Priming in Plants. Front Plant Sci. 2016;7: 1201.

214. Latzel V, Allan E, Bortolini Silveira A, Colot V, Fischer M, Bossdorf O. Epigenetic diversity increases the productivity and stability of plant populations. Nat Commun. 2013;4: 2875.

215. Niyikiza D, Piya S, Routray P, Miao L, Kim W-S, Burch-Smith T, et al. Interactions of gene expression, alternative splicing, and DNA methylation in determining nodule identity. Plant J. 2020;103: 1744–1766.

216. Nagymihály M, Veluchamy A, Györgypál Z, Ariel F, Jégu T, Benhamed M, et al.

Ploidy-dependent changes in the epigenome of symbiotic cells correlate with specific patterns of gene expression. Proc Natl Acad Sci U S A. 2017;114: 4543–4548.

217. Satgé C, Moreau S, Sallet E, Lefort G, Auriac M-C, Remblière C, et al. Reprogramming of DNA methylation is critical for nodule development in Medicago truncatula. Nat Plants. 2016;2: 16166.

218. Varga S, Soulsbury CD. Arbuscular mycorrhizal fungi change host plant DNA methylation systemically. Plant Biol . 2019;21: 278–283.

219. Varga S, Soulsbury CD. Paternal arbuscular mycorrhizal fungal status affects DNA methylation in seeds. Biol Lett. 2017;13. doi:10.1098/rsbl.2017.0407

220. Wilkinson SW, Ton J. Methylation moulds microbiomes. Nature plants. 2020. pp. 910–911.

221. Vílchez JI, Yang Y, He D, Zi H, Peng L, Lv S, et al. DNA demethylases are required for myo-inositol-mediated mutualism between plants and beneficial rhizobacteria. Nat Plants. 2020;6: 983–995.

222. Kellenberger RT, Schlüter PM, Schiestl FP. Herbivore-Induced DNA Demethylation Changes Floral Signalling and Attractiveness to Pollinators in Brassica rapa. PLoS One. 2016;11: e0166646.

223. Marfil CF, Camadro EL, Masuelli RW. Phenotypic instability and epigenetic variability in a diploid potato of hybrid origin, Solanum ruiz-lealii. BMC Plant Biol. 2009;9: 21.

224. Conrath U, Beckers GJM, Langenbach CJG, Jaskiewicz MR. Priming for enhanced defense. Annu Rev Phytopathol. 2015;53: 97–119.

225. Hilker M, Schwachtje J, Baier M, Balazadeh S, Bäurle I, Geiselhardt S, et al. Priming and memory of stress responses in organisms lacking a nervous system. Biol Rev Camb Philos Soc. 2016;91: 1118–1133.

226. D'Urso A, Brickner JH. Mechanisms of epigenetic memory. Trends Genet. 2014;30: 230–236.

227. Light WH, Brickner JH. Nuclear pore proteins regulate chromatin structure and transcriptional memory by a conserved mechanism. Nucleus. 2013;4: 357–360.

228. Ptashne M. Transcription: a mechanism for short-term memory. Current biology: CB. 2008. pp. R25–7.

229. Paszkowski J, Grossniklaus U. Selected aspects of transgenerational epigenetic inheritance and resetting in plants. Curr Opin Plant Biol. 2011;14: 195–203.

230. Uller T, English S, Pen I. When is incomplete epigenetic resetting in germ cells favoured by natural selection? Proc Biol Sci. 2015;282. doi:10.1098/rspb.2015.0682

231. Jaskiewicz M, Conrath U, Peterhänsel C. Chromatin modification acts as a memory for systemic acquired resistance in the plant stress response. EMBO Rep. 2011;12: 50–55.

232. Wibowo A, Becker C, Marconi G, Durr J, Price J, Hagmann J, et al. Hyperosmotic stress memory in Arabidopsis is mediated by distinct epigenetically labile sites in the genome and is restricted in the male germline by DNA glycosylase activity. Elife. 2016;5. doi:10.7554/eLife.13546

233. Murgia I, Giacometti S, Balestrazzi A, Paparella S, Pagliano C, Morandini P. Analysis of the transgenerational iron deficiency stress memory in Arabidopsis thaliana plants. Front Plant Sci. 2015;6: 745.

234. Luna E, Bruce TJA, Roberts MR, Flors V, Ton J. Next-generation systemic acquired resistance. Plant Physiol. 2012;158: 844–853.

235. Slaughter A, Daniel X, Flors V, Luna E, Hohn B, Mauch-Mani B. Descendants of primed Arabidopsis plants exhibit resistance to biotic stress. Plant Physiol. 2012;158: 835–843.

236. Rasmann S, De Vos M, Casteel CL, Tian D, Halitschke R, Sun JY, et al. Herbivory in the previous generation primes plants for enhanced insect resistance. Plant Physiol. 2012;158: 854–863.

237. Geng Y, Chang N, Zhao Y, Qin X, Lu S, Crabbe MJC, et al. Increased epigenetic diversity and transient epigenetic memory in response to salinity stress in Thlaspi arvense. Ecol Evol. 2020;10: 11622–11630.

238. Warwick SI, Francis A, Susko DJ. The biology of Canadian weeds. 9. *Thlaspi arvense* L. (updated). Canadian Journal of Plant Science. 2002. pp. 803–823. doi:10.4141/p01-159

239. Moser BR, Knothe G, Vaughn SF, Isbell TA. Production and Evaluation of Biodiesel from Field Pennycress (Thlaspi arvense L.) Oil. Energy Fuels. 2009;23: 4149–4155.

240. Moser BR. Biodiesel from alternative oilseed feedstocks: camelina and field pennycress. Biofuels. 2012;3: 193–209.

241. Fan J, Shonnard DR, Kalnes TN, Johnsen PB, Rao S. A life cycle assessment of pennycress (Thlaspi arvense L.) -derived jet fuel and diesel. Biomass Bioenergy. 2013;55: 87–100.

242. Sedbrook JC, Phippen WB, Marks MD. New approaches to facilitate rapid domestication of a wild plant to an oilseed crop: example pennycress (Thlaspi arvense L.). Plant Sci. 2014;227: 122–132.

243. McGinn M, Phippen WB, Chopra R, Bansal S, Jarvis BA, Phippen ME, et al. Molecular tools enabling pennycress (Thlaspi arvense) as a model plant and oilseed cash cover crop. Plant Biotechnol J. 2019;17: 776–788.

244. Johnson GA, Kantar MB, Betts KJ, Wyse DL. Field pennycress production and weed control in a double crop system with soybean in Minnesota. Agron J. 2015;107: 532–540.

245. Ott MA, Eberle CA, Thom MD, Archer DW, Forcella F, Gesch RW, et al. Economics and agronomics of relay-cropping pennycress and Camelina with soybean in Minnesota. Agron J. 2019;111: 1281–1292.

246. Phippen WB, Phippen ME. Soybean seed yield and quality as a response to field pennycress residue. Crop Sci. 2012;52: 2767–2773.

247. Chopra R, Johnson EB, Daniels E, McGinn M, Dorn KM, Esfahanian M, et al. Translational genomics using Arabidopsis as a model enables the characterization of pennycress genes through forward and reverse genetics. Plant J. 2018;96: 1093–1105.

248. Nunn A, Rodríguez-Arévalo I, Tandukar Z, Frels K, Contreras-Garrido A,

Carbonell-Bejerano P, et al. Chromosome-level Thlaspi arvense genome provides new tools for translational research and for a newly domesticated cash cover crop of the cooler climates. Plant Biotechnol J. 2022;20: 944–963.

249. Geng Y, Guan Y, Qiong L, Lu S, An M, Crabbe MJC, et al. Genomic analysis of field pennycress (Thlaspi arvense) provides insights into mechanisms of adaptation to high elevation. BMC Biol. 2021;19: 143.

250. Galanti D, Ramos-Cruz D, Nunn A, Rodríguez-Arévalo I, Scheepens JF, Becker C, et al. Genetic and environmental drivers of large-scale epigenetic variation in Thlaspi arvense. PLoS Genet. 2022;18: e1010452.

251. Doyle JJ, Doyle JL. A rapid DNA isolation procedure for small quantities of fresh leaf tissue. 1987. Report No.: RESEARCH. Available: https://worldveg.tind.io/record/33886/

252. Doppler M, Kluger B, Bueschl C, Steiner B, Buerstmayr H, Lemmens M, et al. Stable Isotope-Assisted Plant Metabolomics: Investigation of Phenylalanine-Related Metabolic Response in Wheat Upon Treatment With the Fusarium Virulence Factor Deoxynivalenol. Front Plant Sci. 2019;10: 1137.

253. Wickham H. ggplot2: Elegant Graphics for Data Analysis 2016 New York Springer-Verlag 10.1007. Google Scholar Google Scholar Cross Ref Cross Ref.

254. Hoagland DR. The water-culture method for growing plants without soil. Berkeley, Calif: College of Agriculture, University of California; 1950. Available: https://openlibrary.org/books/OL25240089M.opds

255. Schindelin J, Arganda-Carreras I, Frise E, Kaynig V, Longair M, Pietzsch T, et al. Fiji: an open-source platform for biological-image analysis. Nat Methods. 2012;9: 676–682.

256. Delventhal R, Falter C, Strugala R, Zellerhoff N, Schaffrath U. Ectoparasitic growth of Magnaporthe on barley triggers expression of the putative barley wax biosynthesis gene CYP96B22 which is involved in penetration resistance. BMC Plant Biol. 2014;14: 26.

257. Kuck KH, Reisener HJ. In vitro sporulation of race 32 of Puccinia graminis Pers. f.sp. tritici Erikss. & Henn. Physiological Plant Pathology. 1985;27: 259–268.

258. Marticke KH, Reisener HJ, Fischer R, Hippe-Sanwald S. In situ detection of a fungal glycoprotein-elicitor in stem rust-infected susceptible and resistant wheat using immunogold electron microscopy. Eur J Cell Biol. 1998;76: 265–273.

259. Ritz C, Streibig JC. Bioassay Analysis Using R. J Stat Softw. 2005;12: 1–22.

260. Nunn A, Can SN, Otto C, Fasold M, Díez Rodríguez B, Fernández-Pozo N, et al. EpiDiverse Toolkit: a pipeline suite for the analysis of bisulfite sequencing data in ecological plant epigenetics. NAR Genom Bioinform. 2021;3: lqab106.

261. Fojtová M, Kovarík A, Matyásek R. Cytosine methylation of plastid genome in higher plants. Fact or artefact? Plant Sci. 2001;160: 585–593.

262. Quinlan AR, Hall IM. BEDTools: a flexible suite of utilities for comparing genomic features. Bioinformatics. 2010;26: 841–842.

263. Hussain MI, Iftikhar Hussain M, Araniti F, Schulz M, Baerson S, Vieites-Álvarez Y, et al. Benzoxazinoids in wheat allelopathy – From discovery to application for sustainable weed management. Environmental and Experimental Botany. 2022. p. 104997. doi:10.1016/j.envexpbot.2022.104997

264. Du J, Johnson LM, Jacobsen SE, Patel DJ. DNA methylation pathways and their crosstalk with histone methylation. Nat Rev Mol Cell Biol. 2015;16: 519–532.

265. Wendte JM, Pikaard CS. The RNAs of RNA-directed DNA methylation. Biochim Biophys Acta Gene Regul Mech. 2017;1860: 140–148.

266. Aufsatz W, Mette MF, van der Winden J, Matzke M, Matzke AJM. HDA6, a putative histone deacetylase needed to enhance DNA methylation induced by double-stranded RNA. EMBO J. 2002;21: 6832–6841.

267. Aufsatz W, Stoiber T, Rakic B, Naumann K. Arabidopsis histone deacetylase 6: a green link to RNA silencing. Oncogene. 2007;26: 5477–5488.

268. To TK, Kim J-M, Matsui A, Kurihara Y, Morosawa T, Ishida J, et al. Arabidopsis HDA6 regulates locus-directed heterochromatin silencing in cooperation with MET1. PLoS Genet. 2011;7: e1002055.

269. Bewick AJ, Ji L, Niederhuth CE, Willing E-M, Hofmeister BT, Shi X, et al. On the origin and evolutionary consequences of gene body DNA methylation. Proc Natl Acad Sci U S A. 2016;113: 9111–9116.

270. Seymour DK, Koenig D, Hagmann J, Becker C, Weigel D. Evolution of DNA methylation patterns in the Brassicaceae is driven by differences in genome organization. PLoS Genet. 2014;10: e1004785.

271. Widman N, Feng S, Jacobsen SE, Pellegrini M. Epigenetic differences between shoots and roots in Arabidopsis reveals tissue-specific regulation. Epigenetics. 2014;9: 236–242.

272. Bartels A, Han Q, Nair P, Stacey L, Gaynier H, Mosley M, et al. Dynamic DNA Methylation in Plant Growth and Development. Int J Mol Sci. 2018;19. doi:10.3390/ijms19072144

273. Stroud H, Ding B, Simon SA, Feng S, Bellizzi M, Pellegrini M, et al. Plants regenerated from tissue culture contain stable epigenome changes in rice. Elife. 2013;2: e00354.

274. Wibowo A, Becker C, Durr J, Price J, Spaepen S, Hilton S, et al. Partial maintenance of organ-specific epigenetic marks during plant asexual reproduction leads to heritable phenotypic variation. Proc Natl Acad Sci U S A. 2018;115: E9145–E9152.

275. Vandepoele K, Raes J, De Veylder L, Rouzé P, Rombauts S, Inzé D. Genome-wide analysis of core cell cycle genes in Arabidopsis. Plant Cell. 2002;14: 903–916.

276. Van Leene J, Hollunder J, Eeckhout D, Persiau G, Van De Slijke E, Stals H, et al. Targeted interactomics reveals a complex core cell cycle machinery in Arabidopsis thaliana. Mol Syst Biol. 2010;6: 397.

277. Sofroni K, Takatsuka H, Yang C, Dissmeyer N, Komaki S, Hamamura Y, et al. CDKD-dependent activation of CDKA;1 controls microtubule dynamics and cytokinesis during meiosis. J Cell Biol. 2020;219. doi:10.1083/jcb.201907016

278. Zhang X, Wu J, Yu Q, Liu R, Wang Z-Y, Sun Y. AtOFPs regulate cell elongation by modulating microtubule orientation via direct interaction with TONNEAU2. Plant Sci. 2020;292: 110405.

279. Spinner L, Gadeyne A, Belcram K, Goussot M, Moison M, Duroc Y, et al. A protein

phosphatase 2A complex spatially controls plant cell division. Nat Commun. 2013;4: 1863.

280. Wright AJ, Gallagher K, Smith LG. discordia1 and alternative discordia1 function redundantly at the cortical division site to promote preprophase band formation and orient division planes in maize. Plant Cell. 2009;21: 234–247.

281. Camilleri C, Azimzadeh J, Pastuglia M, Bellini C, Grandjean O, Bouchez D. The Arabidopsis TONNEAU2 gene encodes a putative novel protein phosphatase 2A regulatory subunit essential for the control of the cortical cytoskeleton. Plant Cell. 2002;14: 833–845.

282. Bechtold U, Richard O, Zamboni A, Gapper C, Geisler M, Pogson B, et al. Impact of chloroplastic- and extracellular-sourced ROS on high light-responsive gene expression in Arabidopsis. J Exp Bot. 2008;59: 121–133.

283. Zsigmond L, Rigó G, Szarka A, Székely G, Otvös K, Darula Z, et al. Arabidopsis PPR40 connects abiotic stress responses to mitochondrial electron transport. Plant Physiol. 2008;146: 1721–1737.

284. Doner NM, Seay D, Mehling M, Sun S, Gidda SK, Schmitt K, et al. Arabidopsis thaliana EARLY RESPONSIVE TO DEHYDRATION 7 Localizes to Lipid Droplets via Its Senescence Domain. Front Plant Sci. 2021;12: 658961.

285. Barajas-Lopez J de D, Tiwari A, Zarza X, Shaw MW, Pascual JS, Punkkinen M, et al. EARLY RESPONSE TO DEHYDRATION 7 Remodels Cell Membrane Lipid Composition during Cold Stress in Arabidopsis. Plant Cell Physiol. 2021;62: 80–91.

286. Sharma N, Cram D, Huebert T, Zhou N, Parkin IAP. Exploiting the wild crucifer Thlaspi arvense to identify conserved and novel genes expressed during a plant's response to cold stress. Plant Mol Biol. 2007;63: 171–184.

287. Sattler MC, Carvalho CR, Clarindo WR. The polyploidy and its key role in plant breeding. Planta. 2016;243: 281–296.

288. Dong C, Dalton-Morgan J, Vincent K, Sharp P. A modified TILLING method for wheat breeding. Plant Genome. 2009;2: 39–47.

289. Chen L, Huang L, Min D, Phillips A, Wang S, Madgwick PJ, et al. Development and characterization of a new TILLING population of common bread wheat (Triticum aestivum L.). PLoS One. 2012;7: e41570.

290. Rawat N, Sehgal SK, Joshi A, Rothe N, Wilson DL, McGraw N, et al. A diploid wheat TILLING resource for wheat functional genomics. BMC Plant Biol. 2012;12: 205.

291. Zhu H, Li C, Gao C. Applications of CRISPR–Cas in agriculture and plant biotechnology. Nat Rev Mol Cell Biol. 2020;21: 661–677.

292. Schaart JG, van de Wiel CCM, Smulders MJM. Genome editing of polyploid crops: prospects, achievements and bottlenecks. Transgenic Res. 2021;30: 337–351.

293. Schulman AH, Oksman-Caldentey K-M, Teeri TH. European Court of Justice delivers no justice to Europe on genome-edited crops. Plant Biotechnol J. 2020;18: 8–10.

294. Slade AJ, Fuerstenberg SI, Loeffler D, Steine MN, Facciotti D. A reverse genetic, nontransgenic approach to wheat crop improvement by TILLING. Nat Biotechnol. 2005;23: 75–81.

295. Ishihara A, Matsuda F, Miyagawa H, Wakasa K. Metabolomics for metabolically manipulated plants: effects of tryptophan overproduction. Metabolomics. 2007;3: 319–334.

296. Abramov A, Hoffmann T, Stark TD, Zheng L, Lenk S, Hammerl R, et al. Engineering of benzoxazinoid biosynthesis in Arabidopsis thaliana: Metabolic and physiological challenges. Phytochemistry. 2021;192: 112947.

297. Wakasa K, Hasegawa H, Nemoto H, Matsuda F, Miyazawa H, Tozawa Y, et al. High-level tryptophan accumulation in seeds of transgenic rice and its limited effects on agronomic traits and seed metabolite profile. J Exp Bot. 2006;57: 3069–3078.

298. Matsuda F, Ishihara A, Takanashi K, Morino K, Miyazawa H, Wakasa K, et al. Metabolic profiling analysis of genetically modified rice seedlings that overproduce tryptophan reveals the occurrence of its inter-tissue translocation. Plant Biotechnol. 2010;27: 17–27.

299. Yamada T, Tozawa Y, Hasegawa H, Terakawa T, Ohkawa Y, Wakasa K. Use of a feedback-insensitive α subunit of anthranilate synthase as a selectable marker for transformation of rice and potato. Mol Breed. 2005;14: 363–373.

300. Inaba Y, Brotherton JE, Ulanov A, Widholm JM. Expression of a feedback insensitive anthranilate synthase gene from tobacco increases free tryptophan in soybean plants. Plant Cell Rep. 2007;26: 1763–1771.

301. Hanafy MS, Rahman SM, Khalafalla MM, El-Shemy HA, Nakamoto Y, Ishimoto M, et al. Accumulation of free tryptophan in azuki bean (Vigna angularis) induced by expression of a gene (OASA1D) for a modified α-subunit of rice anthranilate synthase. Plant Sci. 2006;171: 670–676.

302. Ishihara A, Asada Y, Takahashi Y, Yabe N, Komeda Y, Nishioka T, et al. Metabolic changes in Arabidopsis thaliana expressing the feedback-resistant anthranilate synthase alpha subunit gene OASA1D. Phytochemistry. 2006;67: 2349–2362.

303. Friebe A. Role of Benzoxazinones in Cereals. J Crop Prod. 2001;4: 379–400.

304. Elnaghy MA, Shaw M. Correlation between Resistance to Stem Rust and the Concentration of a Glucoside in Wheat. Nature. 1966;210: 417–418.

305. Bücker C, Grambow HJ. Alterations in 1,4-Benzoxazinone Levels Following Inoculation with Stem Rust in Wheat Leaves Carrying Various Alleles for Resistance and Their Possible Role as Phytoalexins in Moderately Resistant Leaves. Zeitschrift für Naturforschung C. 1990;45: 1151–1155.

306. Elnaghy MA, Linko P. The Role of 4-O-Glueosyl-2,4-dihydroxy-7-methoxy-l,4-benzoxazin-3-one Resistance of Wheat to Stem Rust. Physiol Plant. 1962;15: 764–771.

307. Mogensen BB, Krongaard T, Mathiassen SK, Kudsk P. Quantification of benzoxazinone derivatives in wheat (Triticum aestivum) varieties grown under contrasting conditions in Denmark. J Agric Food Chem. 2006;54: 1023–1030.

308. Wu H, Haig T, Pratley J, Lemerle D, An M. Distribution and Exudation of Allelochemicals in Wheat Triticum aestivum. J Chem Ecol. 2000;26: 2141–2154.

309. Copaja SV, Nicol D, Wratten SD. Accumulation of hydroxamic acids during wheat germination. Phytochemistry. 1999;50: 17–24.

310. Weibull J, Niemeyer HM. Changes in dihydroxymethoxybenzoxazinone glycoside content in wheat plants infected by three plant pathogenic fungi. Physiol Mol Plant Pathol. 1995;47: 201–212.

311. Friebe A, Vilich V V, Hennig L, Kluge M, Sicker D. Detoxification of Benzoxazolinone Allelochemicals from Wheat by Gaeumannomyces graminis var. tritici, G. graminis var. graminis, G. graminis var. avenae, and Fusarium culmorum. Appl Environ Microbiol. 1998;64: 2386–2391.

312. Glenn AE, Davis CB, Gao M, Gold SE, Mitchell TR, Proctor RH, et al. Two Horizontally Transferred Xenobiotic Resistance Gene Clusters Associated with Detoxification of Benzoxazolinones by Fusarium Species. PLoS One. 2016;11: e0147486.

313. Schandry N, Becker C. Allelopathic Plants: Models for Studying Plant–Interkingdom Interactions. Trends Plant Sci. 2020;25: 176–185.

314. Wu H, Haig T, Pratley J, Lemerle D, An M. Allelochemicals in wheat (Triticum aestivum L.): production and exudation of 2,4-dihydroxy-7-methoxy-1,4-benzoxazin-3-one. J Chem Ecol. 2001;27: 1691–1700.

315. Mwendwa JM, Weston PA, Weidenhamer JD, Fomsgaard IS, Wu H, Gurusinghe S, et al. Metabolic profiling of benzoxazinoids in the roots and rhizosphere of commercial winter wheat genotypes. Plant Soil. 2021;466: 467–489.

316. Inderjit, Callaway RM. Experimental designs for the study of allelopathy. Plant Soil. 2003;256: 1–11.

317. Uesugi A, Johnson R, Kessler A. Context‐dependent induction of allelopathy in plants under competition. Oikos. 2019;128: 1492–1502.

318. Chen K-J, Zheng Y-Q, Kong C-H, Zhang S-Z, Li J, Liu X-G. 2,4-Dihydroxy-7-methoxy-1,4-benzoxazin-3-one (DIMBOA) and 6-methoxy-benzoxazolin-2-one (MBOA) levels in the wheat rhizosphere and their effect on the soil microbial community structure. J Agric Food Chem. 2010;58: 12710–12716.

319. Schütz V, Bigler L, Girel S, Laschke L, Sicker D, Schulz M. Conversions of Benzoxazinoids and Downstream Metabolites by Soil Microorganisms. Frontiers in Ecology and Evolution. 2019;7. doi:10.3389/fevo.2019.00238

320. Blair AC, Hanson BD, Brunk GR, Marrs RA, Westra P, Nissen SJ, et al. New techniques and findings in the study of a candidate allelochemical implicated in invasion success. Ecol Lett. 2005;8: 1039–1047.

321. Knoch E, Kovács J, Deiber S, Tomita K, Shanmuganathan R, Serra Serra N, et al. Transcriptional response of a target plant to benzoxazinoid and diterpene allelochemicals highlights commonalities in detoxification. BMC Plant Biol. 2022;22: 402.

322. Weidenhamer JD, Hartnett DC, Romeo JT. Density-Dependent Phytotoxicity: Distinguishing Resource Competition and Allelopathic Interference in Plants. J Appl Ecol. 1989;26: 613–624.

323. Weidenhamer JD. Distinguishing resource competition and chemical interference: Overcoming the methodological impasse. Agron J. 1996;88: 866–875.

324. Inderjit, von Dahl CC, Baldwin IT. Use of silenced plants in allelopathy bioassays: a novel approach. Planta. 2009;229: 569–575.

325. Zilberman D, Gehring M, Tran RK, Ballinger T, Henikoff S. Genome-wide analysis of Arabidopsis thaliana DNA methylation uncovers an interdependence between methylation and transcription. Nat Genet. 2007;39: 61–69.

326. Kraft E, Bostick M, Jacobsen SE, Callis J. ORTH/VIM proteins that regulate DNA methylation are functional ubiquitin E3 ligases. Plant J. 2008;56: 704–715.

327. Kim J, Kim JH, Richards EJ, Chung KM, Woo HR. Arabidopsis VIM proteins regulate epigenetic silencing by modulating DNA methylation and histone modification in cooperation with MET1. Mol Plant. 2014;7: 1470–1485.

328. Chwialkowska K, Nowakowska U, Mroziewicz A, Szarejko I, Kwasniewski M. Water-deficiency conditions differently modulate the methylome of roots and leaves in barley (Hordeum vulgare L.). J Exp Bot. 2016;67: 1109–1121.

329. Ferreira LJ, Azevedo V, Maroco J, Oliveira MM, Santos AP. Salt Tolerant and Sensitive Rice Varieties Display Differential Methylome Flexibility under Salt Stress. PLoS One. 2015;10: e0124060.

330. Kenchanmane Raju SK, Ritter EJ, Niederhuth CE. Establishment, maintenance, and biological roles of non-CG methylation in plants. Essays Biochem. 2019;63: 743–755.

331. Li R, Hu F, Li B, Zhang Y, Chen M, Fan T, et al. Whole genome bisulfite sequencing methylome analysis of mulberry (Morus alba) reveals epigenome modifications in response to drought stress. Sci Rep. 2020;10: 8013.

332. Stanišić M, Ćosić T, Savić J, Krstić-Milošević D, Mišić D, Smigocki A, et al. Hairy root culture as a valuable tool for allelopathic studies in apple. Tree Physiol. 2019;39: 888–905.

333. Golisz A, Sugano M, Fujii Y. Microarray expression profiling of Arabidopsis thaliana L. in response to allelochemicals identified in buckwheat. J Exp Bot. 2008;59: 3099–3109.

334. Chang S, Pikaard CS. Transcript Profiling in Arabidopsis Reveals Complex Responses to Global Inhibition of DNA Methylation and Histone Deacetylation*[boxs]. J Biol Chem. 2005;280: 796–804.

335. Wang Y, Zhang W-Z, Song L-F, Zou J-J, Su Z, Wu W-H. Transcriptome analyses show changes in gene expression to accompany pollen germination and tube growth in Arabidopsis. Plant Physiol. 2008;148: 1201–1211.

336. Meinke DW. Genome-wide identification of EMBRYO-DEFECTIVE (EMB) genes required for growth and development in Arabidopsis. New Phytol. 2020;226: 306–325.

337. Dorn KM, Fankhauser JD, Wyse DL, Marks MD. De novo assembly of the pennycress (Thlaspi arvense) transcriptome provides tools for the development of a winter cover crop and biodiesel feedstock. Plant J. 2013;75: 1028–1038.

338. Dorn KM, Fankhauser JD, Wyse DL, Marks MD. A draft genome of field pennycress (Thlaspi arvense) provides tools for the domestication of a new winter biofuel crop. DNA Res. 2015;22: 121–131.